6-23-2014

Characterization of the Bacterial Metallothionein, PmtA in the Human Pathogen Pseudomonas aeruginosa

Kathryn M. Pietrosimone
University of Connecticut - Storrs, kathryn.pietrosimone@gmail.com

Characterization of the Bacterial Metallothionein, PmtA, from the Human Pathogen *Pseudomonas aeruginosa*

Kathryn M. Pietrosimone, Ph.D.

University of Connecticut, 2014

Small, cysteine-rich proteins called metallothioneins (MTs) bind essential divalent heavy metal cations, such as zinc and copper, as well as toxic heavy metals, such as cadmium and mercury. Stressful conditions such as exposure to heavy metals or reactive oxygen species (ROS) increase the expression of MTs. The numerous cysteine residues in MTs allow the protein to neutralize toxic effects of ROS, bind heavy metals, influence immune cell movement and proliferation. The bacteria *Pseudomonas aeruginosa* expresses an MT, PmtA, that is similar in structure the eukaryotic MTs. Evidence presented in these suggests that PmtA is an immunomodulatory protein, similar to the eukaryotic counterpart. Jurkat T cells pre-incubated with PmtA and subsequently exposed to a gradient of SDF-1α, lost the ability to move in a persistent direction, while Jurkat T cells pre-incubated with GST did respond to the SDF-1α gradient. Incubation with PmtA also decreased SDF-1α-induced internalization of the receptor CXCR4 on Jurkat T cells. *P. aeruginosa* strain PW4670 lacks PmtA expression, and is also more sensitive to oxidant exposure than the parent strain PA01. PW4670 also fails to produce pyocyanin, a secondary metabolite that produces ROS that can disrupts the immune response to *P. aeruginosa*. Due to the lack of pyocyanin by PW4670, PAO1 supernatant is more likely to kill macrophage cells *in vitro* and *Galleria mellonella* larvae *in vivo*, that PW4670 supernatant. Taken together, these results suggest that the expression of PmtA influences the virulence of *P. aeruginosa*, and may be a novel target for therapeutic intervention.

Characterization of the Bacterial Metallothionein, PmtA in the Human Pathogen

Pseudomonas aeruginosa

Kathryn M. Pietrosimone

B.A. Assumption College, 2008

A Dissertation

Submitted in Partial Fulfillment of the

Requirements of the Degree of Doctor of Philosophy

at the

University of Connecticut

2014

APPROVAL PAGE

Doctor of Philosophy Dissertation

Characterization of the Bacterial Metallothionein, PmtA, in the Human Pathogen

Pseudomonas aeruginosa

Presented by
Kathryn M. Pietrosimone

Major Advisor: _____

Michael A. Lynes, Ph.D.

Associate Advisor: _____

Lawrence K. Silbart, Ph.D.

Associate Advisor: _____

Joerg Graf, Ph.D.

Examiner: _____

David Benson, Ph.D.

Examiner: _____

Adam Zweifach, Ph.D.

University of Connecticut, 2014

ACKNOWLEDGEMENTS

As a young scientific investigator, I have quickly learned that it is always in your best interest to acknowledge your funding sources. Therefore, first and foremost, I would like to acknowledge my largest source of funding, my parents, Frank and Patricia Pietrosimone. Without this funding, I would not have been able to perform any of the experiments discussed in this dissertation. The sacrifices my parents have made to insure I could achieve my goals are immense and deeply appreciated. Their selfless dedication to my success consistently drives me to work harder than I did the day before to achieve everything within my reach. As a result of their sacrifice, there is much within my reach. My family always encourages me to work hard and never settle for 'good enough'. The ever-encouraging voice of my older brother, Brian, constantly rings in my ear and recites, "Second place is first loser". Thank you for all of your support, I promise to always strive for first place.

I owe my decision to pursue a career in science to my high school chemistry teacher, Dr. Elizabeth Christophy, Ph.D. I remember sitting through honors convocation my sophomore year in high school wondering why I had been invited to the ceremony. As my name was called for the Excellence in Chemistry award, I was stunned. That moment was a turning point in my academic career. Someone had acknowledged my interest in science and thought I was good enough to pursue it. From that moment forward, I knew I would be a scientist. The opportunity to experience real scientific research at my high school, Sacred Heart Academy, was second to none, and solidified my decision to pursue science. For this, I owe many thanks to Sr. Mary Jane Paolella for her dedication to the science curriculum at SHA.

I would also like to thank my advisor at Assumption College, Dr. David Crowley Ph.D., for his support of my undergraduate research. I appreciate all the times he pretended not to notice when I screwed up an experiment and let me learn to fix it myself. Thank you.

All of the support I mentioned led me to pursue my Ph.D. at the University of Connecticut. I could not have completed this degree without the guidance and support from my mentor, Dr. Michael A. Lynes. Dr. Lynes

allowed me to tackle a new and exciting project in his lab, and always acquired the resources I needed for these experiments. From day one, Dr. Lynes was committed to my success in graduate school. He consistently provided me with many opportunities to advance my career, such as publishing book chapters, presenting at conferences, and applying for fellowships. I am very grateful for these opportunities and know that his commitment to my success will not end when I leave UConn.

I also appreciate the guidance of my committee members, Dr. Lawrence K. Silbart Ph.D. and Dr. Joerg Graf Ph.D. My unique project crossed over a few disciplines and really required the expert experience of Dr. Silbart and Dr. Graf to focus my approaches and ensure my questions were addressed in the appropriate manner. My committee always met when I needed direction, answered my questions and, more often than not, came up with even more questions. Thank you for your commitment to my project.

Over the years I have benefitted from the collaborative nature of our department and have worked with many people in the process. I would like to acknowledge Dr. David A. Knecht Ph.D., Dr. Adam Zweifach Ph.D., and Dr. Victoria Robinson Ph.D. for their assistance with experimental techniques over the years. I could not appropriately write an acknowledgement section without mentioning Dr. Carol Norris Ph.D. for the massive amount of time and energy she spent training me in flow cytometry and microscopy.

The journey of a graduate student requires support from faculty as well as the day-by-day support of your lab mates. My journey through graduate school, both professionally and personally, would have been nearly impossible without our research technician, Clare Melchiorre. Clare single handedly keeps our lab functioning when the rest of have no clue how to order supplies, when our safety training is due, or how to accomplish any other administrative task. Clare also assisted in the acquisition of some of the data presented in Chapter 4, I would like to thank her for her hard work on this project. For the many other roles she have played in my life the last 6 years – Thank you. Some of the data presented in Chapter 4 was gathered with the assistance of Ph.D. students Amy V. Thees and Kristen E. Dostie. I would like to thank them for their assistance with these experiments. I would also like to thank all of the past and present members of the Lynes Lab (yes, even Peter) who truly made our

lab a pleasant place to work. In addition, I would like to recognize Dr. Renee Gilberti for her guidance throughout my graduate career.

Lastly, I would like to acknowledge a particular former lab mate and current colleague of mine, Andrew Buckley, for his guidance with the *Galleria mellonella* virulence experiments. I would also like to thank him for all his support over the past 8 years.

"Since its detection in 1957 metallothionein and its possible function have provided a splendid source of frustration for the many who have been attracted to this Sphinx and tempted to solve its riddle."

Bert L. Vallee Ph.D.

Table of Contents

CHAPTER 1: BACKGROUND AND SIGNIFICANCE

1 Introduction

Metallothioneins (MTs) are a family of low molecular weight, cysteine-rich proteins. MTs were first identified in mammals due to their metal binding capacity [1]. Extensive research on MTs has revealed that these proteins possess several diverse functions from acting as a reservoir for essential metals to influencing the cellular redox environment and immune cell functions. MTs are not essential to life, as viable MT-knockout mouse models have been constructed, but evidence shows that the expression of MT is advantageous to animals exposed to stressful conditions. The majority of this research focuses on eukaryotic forms of MTs from small mammals such as mice and rabbits. Research that involves MTs from other species is not as extensive as the research in mammalian MTs.

The human pathogen *Pseudomonas aeruginosa* expresses a small molecular weight, cysteine rich MT, referred to as PmtA. Aside from its metal binding capacity, very little research has been done on this protein's functions in *P. aeruginosa*. If PmtA acts similarly to mammalian MT and enhances survival of the organism in stressful conditions through several multifunctional roles, PmtA may influence the progression of infection and overall virulence of the pathogen.

The focus of this study is to determine if PmtA modifies the mammalian immune response in a similar manner as its eukaryotic counterparts, with a focus on the

chemotactic and redox sensitive properties of PmtA. The chemotactic model uses a GST-PmtA purified from *Escherichia coli* expressing the pGEX-6p-*PmtA* plasmid. The movement of Jurkat T cells was measured after exposure to the purified GST-PmtA. PmtA's function in the presence of oxidative stress was determined with a *P. aeruginosa* strain that lacked the expression of a functional PmtA protein. This study determined that PmtA alters the chemotactic response of host immune cell and influences the expression of *P. aeruginosa* virulence factors.

1.1 Stress and Immunity

Exposure to acute or chronic stressors intensify symptoms of many inflammatory disease states such as multiple sclerosis [2, 3], irritable bowel syndrome [4, 5] diabetes [6] and cardiovascular disease [7]. External stressors include elevated temperature, bacterial infection, exposure to toxins, toxicants, metals and reactive oxygen and nitrogen species. Stressors can be psychological, physical, or chemical and impact the other functions of the immune system through the activation of an inflammatory response. This leaves patients susceptible to the aforementioned inflammatory disease states as well as bacterial infection [8].

Psychological stressors impact the overall efficiency of the immune response by altering cytokine and cortisol expression. A change in the cytokine profile of an organism alters its immune response to pathogens and can intensify symptoms of inflammatory disease states. For example, chronic work stress elevates and sustains levels of the pro-inflammatory cytokines interleukin-6 (IL-6) and tumor necrosis factor-

α (TNF-α) [9, 10]. An increase in pro-inflammatory cytokines can disrupt the Th1/Th2 cell balance and worsen inflammatory disease states. The change in cytokine expression associated with psychological stressors such as, anxiety or depression can modify the T cell response to anti-viral vaccines against hepatitis B virus and rubella virus [11, 12]. Change in the cytokine profile of accompanying social stressors can decrease the microbial intestinal diversity in the mice and leave them susceptible to intestinal inflammation [13]. Psychological stressors in mice also alter the kinetics of an antibody response to the influenza virus and the ability of immune cells to traffic to the site of infection [14].

Chemical stressors like ROS alter redox-sensitive signaling in immune cells, which interrupts signal transduction and subsequently changes cytokine expression [15]. ROS production by immune cells is necessary, as it allows immune cells to kill invading pathogens. However, excessive ROS production can cause apoptosis of host cells and alter cytokine profiles of organism in ways that are not advantageous to the host.

Cells attempt to counteract the profound affects of psychological, chemical and biological stressors on the immune response and other cellular functions through the expression of stress response proteins [16].

1.2 Cellular Stress and Stress Response Proteins

In response to the changes in extracellular stimuli brought on though exposure to stress, cells induce a stress response. This response allows the cell to repair damage and adapt to the new environment, or triggers apoptosis and autophagy [17]. In general, the

cellular stress response alters expression of certain proteins to protect against cellular damage.

A well-studied family of stress response proteins is the heat shock proteins (HSPs). The high degree of evolutionary conservation among HSPs highlights importance of these proteins to the survival of cells. As their name would suggest, HSPs were first identified in cells that were exposed to high temperatures, or heat shock. Many other potentially damaging stressors such as ROS, hypoxia, heavy metal stress, glucose deprivation, and microbial infection all induce expression of HSPs [18]. The numerous HSPs expressed in mammals are categorized by molecular weight, therefore HSP70 and HSP90 are 70 and 90 kilodaltons, respectively [19]. In the absence of stress, cells express HSPs at low levels, the onset of stress forces the cell to upregulate expression of these proteins to maintain homeostasis [20].

Expression of HSPs can profoundly affect the immune response to pathogens and tumor cells. Upon increase in HSP expression, HSPs are broken into peptides presented on major histocompatibility complex (MHC) class I. Presentation on MHCI activates cytotoxic T cells (CTLs) [21] and increases CTL-mediated killing of virally infected cells [22]. Through this same mechanism, HSPs can be presented on the MHCI of tumor cells and induce CTL-mediated killing tumor cells [23-25]. In mice, CTL-mediated killing of tumor cells often lyses the cells and subsequently immunizes the animals against the tumor [25-27]. HSPs can also act as chaperone proteins that carry antigenic peptides [23, 28], which can be readily phagocytized by APC's and eventually presented to $CD4^+$ T cells on MHCII [27]. Phagocytosis of these HSP-peptide complexes also induce macrophage expression of proinflammatory cytokines IL-1β, TNFα, IL-12, GM-CSF and

the chemokines MCP-1, MIP-1, RANTES and promotes the inflammatory response against a pathogen [29, 30]. These changes in expression will affect immune cell activation, signaling and chemotaxis [27].

1.3 The Stress Response Protein Metallothionein

The stress response protein metallothionein (MT) is a small molecular weight, cysteine rich protein. MT uses sulfhydryl groups present on cysteine residues to bind toxic and essential heavy metals and to neutralize ROS [31]. In the absence of cellular stress, MT acts as a reservoir for essential heavy metals such as zinc and copper [32]. MT donates these metals to apoenzymes and zinc-finger transcription factors that require these essential metals to function [33]. MT maintains homeostasis of essential heavy metals through the redistribution of the metals to different parts of the cell [34]. MT in a zinc bound state is very stable which makes it an ideal reservoir for intracellular zinc [35].

Under cellular stress from toxic heavy metals, such as cadmium and mercury, the cell increases MT expression. MT releases some essential metals in order to sequester toxic heavy metals and prevent these metals from damaging the cell [36]. MT expression also increases in the presence of ROS. The thiol groups on MT become oxidized to prevent ROS from oxidizing other parts of the cell.

Protection from ROS is vital to cells as the oxidation of cellular components can lead to cellular damage and inflammatory disease. For example, in rheumatoid arthritis (RA) neutrophils, macrophages, and lymphocytes infiltrate the synovium and cause

persistent inflammation [37-39]. Once in the synovium macrophages and neutrophils produce ROS through oxidative bursts. The resulting ROS can oxidize polyunsaturated fatty acids of the membrane lipids, a process called lipid peroxidation [38]. Lipid peroxidation damages the membranes of cells and causes persistent inflammation in the joints [40, 41]. As evidenced from the role of oxidation in the pathogenesis of RA, defenses against cellular oxidation are necessary to maintain redox homeostasis within the cell. In the collagen-induced arthritis murine model of RA injection of MT reduced the severity of the disease [42]. MT may be able to become oxidized and decrease the oxidation of lipids in the arthritic mouse. However, injection of MT also decreases proinflammatory mediators, which in turn can decrease the expansion of proinflammatory, ROS-producing cells in the arthritic mouse [42].

1.3.1 Classes of Metallothioneins

Proteins in several different organisms are classified as MTs due to their extremely high metal and sulfur content. All of these proteins are low molecular weight proteins with a high number of cysteine residues, which are associated with their ability to bind metals [1]. Previously, the classification as an MT did not include any protein with aromatic amino acids, however, more recently bacterial proteins that utilize both cysteine and histidine residues in their metal binding functions have been classified as MTs [1, 43, 44]. Aromatic amino acids can bind metals and influence cellular redox status. Therefore, it is not expected that the presence of aromatic amino acids changes the function of these MTs [45].

In mammals, MTs are categorized into 4 major classes: MT-I, -II, -III, and -IV. In humans these genes map onto chromosome 16 [46], and in mice MT genes are located on chromosome 8 [47]. The MT-III and –IV genes encode for single isoforms of these proteins, while MT-I and MT-II have several different isoforms that tend to be expressed in specific cell types [48]. MT-I and MT-II are expressed in all types of tissues, while MT-III and MT-IV are more, but not exclusively, tissue specific [48].

The functional differences between MT-I and MT-II have not been elucidated because a single knockout mouse model has not been constructed. MT-I and MT-II are highly homologous and difficult to chemically separate. MT murine models consist of MT-I and MT-II double knockouts, as well as MT-I transgenic models [48]. MT-I and MT-II double knockout mice are more susceptible to heavy metal stress and oxidation by ROS. The inflammatory response and immune response to infection also differ in MT-I, -II, double knockout mice when compared to wild type mice [49].

Heavy metals induce expression of MT-I and II, however, that is not the case with MT-III [50]. MT-III first called growth inhibitory factor (GIF), is also a small molecular weight, high cysteine protein that is known to bind both copper and zinc. MT-III was originally defined as GIF because it inhibited the growth of neuronal cells *in vitro.* The genes that encode MT-III are found in the same gene cluster as MT-I and MT-II in both humans and mice and share 65% homology with MT-I genes [50].

The MT-IV gene lies 20kb from the 5' end of the MT-III gene in humans and mice and is highly conserved in both species. Expression of MT-IV is limited to the stratified squamous epithelia [51]. *In situ* experiments that label MT-IV mRNA show

that MT-IV expression dominates in the differentiating spinous layer of the epithelia, while MT-I expression increases in the basal, proliferating layer of epithelium. This suggests that a switch in the MT isoform expression is necessary during the differentiation of epithelia [51].

1.4 MT and immunity

A very interesting aspect of MT is its influence on immune cell function. Tissues vital to the development of an immune response, such as mammalian fetal liver and neonatal thymus, express MT at very high levels [52]. MT can be found on the surface of leukocytes in culture exposed to mitogen or exogenous MT, which suggests that leukocytes may express a receptor for MT [53-55].

Another immunomodulatory function of MT is its effects on the proliferation and function of T and B cells. The combination of MT and Concanvlin A (Con A) stimulates proliferation of T cells more than just Con A alone [53, 56]. Similarly, MT increases proliferation of B cells in the presence of the polyclonal B cell activator, lipopolysaccharide (LPS) [53]. MT also affects the antibody response by B cells to an antigen. MT decreases the anti-ovalbumin production in mice co-immunized with MT and ovalbumin compared to injection with ovalbumin alone. The addition of UC1MT, a monoclonal MT-specific antibody, reverses this immunosuppression [57]. Apo-MT, which lacks association with metals and has a decrease in free thiols due to oxidation, fails to change the anti-ovalbumin level in immunized mice, which indicates the thiols on MT are vital to MT's immunosuppressive effects [57]. MT-I and MT-II double knockout

mice mount a vigorous T-cell dependent humoral response when compared to their wildtype counter parts, which further supports the hypothesis that MT is immunosuppressive [54].

MT affects cells that contribute to the cell-mediated immune response differently than their humoral immune counterparts. The phagocytic capacity of macrophages does not change with exposure to MT, but MT-exposed macrophages do increase the production of ROS. This increase in ROS may contribute to MT-exposed macrophages superior ability to kill *Candida albicans* when compared to macrophages that are not exposed to exogenous MT [55]. MT can be detected on the cell surface of MT-exposed macrophages, which again could suggest the existence of an MT cell surface receptor [55].

MT gene dose impacts the ability of mice to eliminate *Listeria monocytogenes* infections, measured by bacterial burden in both the liver and spleen of infected animals. MT knockout and MT transgenic mice were better able to clear the pathogen 3 days post-inoculation than their wildtype counterparts. However, death of lymphocytes was increased in infected MT knockout mice, perhaps due to the increase in oxidant measured in both knockout and transgenic mice compared to wildtype mice [49]. The effect of MT gene dose on the progression of infection supports the hypothesis that MT is an immunomodulatory protein.

1.5 Reactive Oxygen Species

Reactive oxygen species (ROS) are oxygen species that contain unpaired valence electrons. These valance electrons make ROS highly reactive and able to cause cellular damage. [58]. Normal aerobic metabolic processes can produce ROS in the mitochondria and peroxisomes. Some ROS, such as hydrogen peroxide (H_2O_2), pass through membranes and can cause damage to intracellular components including the nucleus [58]. Cells express stress response proteins that defend against ROS, like MT and the antioxidant enzyme catalase. However, a large amount of endogenous or exogenous ROS can overwhelm antioxidant defenses in the cell and cause oxidative damage. ROS target cellular components such as nucleic acids, proteins and lipids [15, 59, 60]. Oxidative damage to nucleic acids, proteins and lipids can alter the structure and function of these components and disrupt cell signaling. Disruption of cell signaling as a result of ROS-induced damage can lead to the development of several disorders, such as diabetes [61, 62], atherosclerosis [63], rheumatoid arthritis [64, 65], Parkinson's disease [66, 67] and cancer [68].

The production of ROS during aerobic respiration is unavoidable so aerobic organisms have developed antioxidant mechanisms to detoxify ROS. As the most abundant intracellular antioxidant, the peptide glutathione provides cells with protection against ROS. The amino acids cysteine, glutamic acid, and glycine comprise glutathione. Much like MT, the cysteine thiol of glutathione serves as the active group [69].

All mammalian organs and tissues express glutathione. In the absence of oxidative stress, glutathione is mainly in its reduced form, GSH. Under oxidative stress, GSH is oxidized to GSSG. The enzyme glutathione reductase then reduces GSSG back to GSH. [69] The redox environment of the cell can be determined by the ratio of GSH to GSSG [70].

Mammalian cells also contain mechanisms to produce ROS. Professional phagocytic cells, such as antigen presenting cells (APCs), produce ROS in order to damage bacterial cells and thus can eliminate infections. Polymorphonuclear neutrophils (PMNs) and macrophages engulf infiltrating bacteria into intracellular vesicles called phagosomes, which release an oxidative burst [71]. This release of oxygen aims to kill the bacteria contained within the phagosome, but it can also change the overall redox potential of the cell, which affects cell signaling. The cytosolic H_2O_2 that results from an oxidative burst in the phagosome inactivates tyrosine phosphatases and activates tyrosine kinases through oxidation of cysteine thiol groups [72]. The majority of the H_2O_2 in the cytosol is produced by NADPH oxidase.

1.5.1 NADPH oxidase

As a member of the NOX family transmembrane electron transport system, NADPH oxidase is responsible for the generation of extracellular superoxide released from phagocytes as well as intracellular oxidative bursts in phagosomes [73]. It is a membrane-associated enzyme that catalyzes the production of superoxide anion (O_2^-).

NADPH oxidase activates through the phosphorylation of the cytosolic NADPH subunit $p47^{phox}$ and subsequent interaction with the $p22^{phox}$ subunit, which causes membrane translocation of $p47^{phox}$. The membrane translocation of $p47^{phox}$ then allows for the assembly of other cytoplasmic subunits, and the formation of the complete, and active, NADPH complex [74]. The NADPH complex transports electrons from the cytoplasmic portion of NADPH to extracellular oxygen, as well as phagosomal oxygen [75]. This generates superoxide (O_2^-), which serves as a precursor to other ROS, such as singlet oxygen, hypochlorous acid (HOCl) and H_2O_2 [76].

The clearance of pathogens often depends on the production of ROS by NADPH oxidase. In 1957 two patients were identified as suffering from constant infections accompanied by granulomas, swollen lymph nodes and hypergammaglobulinemia [77]. Their condition became known as Chronic Granulomatous Disease (CGD) and the symptoms were attributed to the lack of the protein cytochrome b_{558}, which is essential to the function of NADPH oxidase [78, 79]. The phagocytes of CGD patients fail to produce ROS and cannot successfully clear many microbial infections [80-82].

On the opposite end of the spectrum, over activation of NOX family of NADPH oxidases, such as NOX2, can also cause complications. Activation of NOX2 NADPH oxidases requires signals from protein kinase C (PKC) activators, microbial components, G-protein coupled receptor (GPCR) agonists or chemotactic peptides [83]. However, NOX2 can be chronically active without these signals and causes localized oxidative stress. This localized oxidative stress due to chronic activation of NOX2 has been associated with the inflammation in the joints of RA patients in inflamed tissues [84]. In

RA, over activation of NOX2 overwhelms host antioxidant defenses and causes peroxidation of lipids. This leads to the localized joint inflammation [84].

1.5.2 Superoxide

The initial oxidant produced by NADPH oxidase and released in the oxidative burst is superoxide (O_2^-) [85]. Superoxide reacts with cysteine residues on proteins, oxidizing thiol groups [86]. NADPH oxidase generates superoxide in the following reaction [75]:

$$NADPH + 2O_2 \rightarrow NADP^+ + 2O_2^- + H^+$$

Although superoxide is the initial oxidant produced, it is a relatively weak anti-microbial [87-89], and therefore does not directly kill bacteria. Superoxide dismutase rapidly converts superoxide into H_2O_2, which can then kill bacteria or further react with superoxide to form other ROS, such as singlet oxygen or hydroxyl radicals that are toxic to bacteria [75].

1.5.3.Hydrogen peroxide

Release of superoxide in an oxidative burst quickly lends itself to the production of H_2O_2 in the following reaction:

O_2-+ O_2- +2H+ → H_2O_2 + O_2

[90].

The formation of H_2O_2 can be spontaneous, catalyzed by the enzyme superoxide dismutase, or a produced as a byproduct of mitochondrial respiration [91]. H_2O_2 carries a high reduction potential and serves as a strong oxidizer, which contribute to its strong anti-microbial response.

1.5.4 ROS Signaling

ROS affect cellular signaling through two major mechanisms; the oxidative modification of proteins and the alteration of cellular redox state and [15]. ROS influence cellular signal transduction through the oxidation and subsequent inactivation of enzymes that utilize cysteine residues at their active site, such as, protein tyrosine phosphatase (PTPs) [92-96]. ROS modification renders the protein non-functional and disrupts signaling downstream from the modified protein. In the absence of oxidative stress, the cell maintains the cytosol in a reduced state with the help of intracellular antioxidants, such as GSH. However, if oxidant overwhelms GSH buffering capacity the level of GSH decreases as it is quickly oxidized into GSSG. When GSH buffering capacity is overwhelmed, the redox status begins to affect cell fate. For example, a decrease in GSH can increase proliferation of fibroblasts [97]. The fibroblast mitogen PDGF relies on GSH to regulate its activity, as reduction of PDGF renders the mitogen inactive. A decrease in GSH is associated with an increase in PDGF activity, which may lead to the increase in fibroblast proliferation [97]. An increase in intracellular thiols partially reverses these proliferative effects, which indicates the maintenance of the intracellular redox environment is essential to the regulation of fibroblast proliferation [98]. ROS can also modify critical amino acids of a protein and change the function of the protein.

Oxidation of the –SH group on a cysteine residue of an enzyme can physically alter the activity of an enzyme, and thus its function [15]. The redox status of the cell therefore regulates the functions of thiol-rich proteins. For example, oxidation of HSP33 forces the formation of a disulfide bond. This signals HSP33 to dimerize and function as a chaperone [99, 100]. Regulation of redox sensitive thiol rich proteins requires reduction of these thiol groups by intracellular antioxidants like GSH, thioredoxin and thioredoxin reductase [101, 102].

Release of ROS in a defensive oxidative burst can also affect the signal transduction of the infiltrating bacteria. Oxidation causes the redox-sensitive bacterial transcription factor OxyR to activate and bind DNA through the formation of a disulfide bond within the transcription factor [103, 104]. This induces the expression of various gene products that combat oxidative damage, including *katG*, which encodes a hydrogen peroxidase that neutralizes the harmful effects of H_2O_2 [105]

1.5.5 MT and ROS

Cells increase the expression of MT in the presence of oxidative stress [106]. Under oxidative stress the –SH groups on MT can become oxidized and protect the host cell from damage. Oxidation of MT's thiols also affects the intracellular free zinc concentration [107]. In order for MT to become oxidized, it must have free thiol groups, which means it cannot be saturated by zinc. Under oxidative conditions MT releases bound zinc, and becomes oxidized by ROS [108]. This couples redox signaling and zinc

homeostasis [35]. As oxidized MT reduces, it regains the ability to bind zinc, and once again becomes a reservoir for the essential heavy metal.

1.5.6 Assessing ROS

The assessment of ROS within a cell relies on the measurement of oxidative products. The ratio of GSH to GSSG indicates the level of oxidative stress since GSSG should be continuously regenerated by a NADPH-dependent reductase [109] GSH and GSSG concentrations can be determined biochemically or with HPLC [110].

Measurement of lipid peroxidation is a common assessment of oxidative stress. Free radicals target hydrogen on unsaturated fatty acids to form water and a lipid peroxide [111]. The unstable lipid peroxides then break down to form carbonyl compounds such as malondialdehyde (MDA). In an assay called the TBA assay, thiobarbituric acid (TBA) reacts with MDA and forms a colorimetric change that can be measured at an absorbance of 532nm [60].

Superoxide levels can be estimated through the cytochrome C reduction assay. Superoxide reduces ferricytochrome C to ferrocyrochrome C [109]. Addition of cell lysate containing superoxide to cytochrome C causes the oxidation of iron and a colorimetric change that is monitored kinetically through absorbance readings at wavelength of 550nm. Superoxide dismutase can be added to determine the extent of inhibition, and increases specificity of the assay [109].

Dichlorodihydrofluorescein diacetate (DCFH-DA) assays measures the oxidation of 2'-7'dichlorodihyrofluorescin diacetate (DCFH-DA) to the fluorescent compound 2'-

7'-dichlorofluorescein (DCF). Cells internalize DCFH-DA and it becomes "trapped" intracellularly after cleavage by intracellular esterases and forms the non-fluorescent DCF. Upon oxidation, DCF becomes highly fluorescent. This fluorescence can be measured by flow cytometry or fluorescent microscopy [109, 112].

1.6 Stress, Chemotaxis, And Immunity

An effective immune response relies on efficient, directional movement of immune cells, known as chemotaxis. The elimination of an infection requires efficient chemotaxis of immune cells to the site of infection. The stress of an infection changes the expression of cellular effector molecules, and thus the migration of cells. Dendritic Cells (DCs), PMNs, macrophages and T cells can all recognize microbe-associated molecular patterns (MAMPs), such as fmet-leu-phe (fMLP). This formylated tripeptide is associated with many bacterial infections and is recognized by toll-like receptors (TLRs) on the surface of responding cells. MAMPs stimulate host cells to produce chemokines and can cause an influx of effector immune cells to the point of infection [113]. Cells in the bloodstream must respond to small effector molecules called chemokines, in order to migrate to the location of infection [114]. Cell-adhesion molecules called intercellular adhesion molecules (ICAMs) expressed on the surface of endothelial cells bind with integrins expressed on the surface of leukocytes [115]. Integrins can be in active states, in which they tightly bind ICAMs, or inactive states, in which integrin-ICAM interactions are weak. These states change in response to extracellular stimuli. When integrin-ICAM interaction is strong, leukocytes can attach to the surface of endothelial cells and extravasate through the endothelial barrier. Once in tissues, chemokines direct the leukocytes to infected portion of the tissue. In the mucosal immune response, cells from

the bloodstream must cross the endothelial barrier, as well as the epithelial barrier [115]. Lymphocytes involved in the mucosal immune response express the integrin $\alpha_4\beta_7$, which binds to the addressin MAdCAM-1 [115]. MAdCAM-1 is specifically expressed on endothelial cells of the blood vessels of the mucosa [115]. The binding of MAdCAM-1 to integrin $\alpha_4\beta_7$ signals the lymphocyte to move through the endothelium into the lamina propia. Once in the lamina propia, chemokine receptors on the lymphocytes and chemokines produced specifically by mucosal epithelial cells home the lymphocytes to the mucosal epithelium [115].

An interruption in the regulation of cell movement can cause the development of autoimmune disease. For example, IL-8 over expression causes cellular movement of PMNs during autoimmune disease states such as psoriasis, RA, and ulcerative colitis [116-118]. The movement of PMNs increases the inflammatory response and exacerbates these inflammatory disease states. Chemokine expression can be altered in the presence of stress, which in turn changes the immune response to infection and alters inflammatory disease states.

1.6.1 Chemokine families

Inflammatory chemokines recruit and direct cells during inflammation, infection, tissue injury, wound healing, and developmental processes [113]. During an infection chemokines initially direct the short-lived PMNs to the site of infection first. The clearance of many pathogens depends on the proper migration and activation of PMNs

[113, 119-121]. Chemokines direct mature DCs to lymphoid tissues where they present antigen to T cells and initiate an adaptive immune response [122].

Chemokines are categorized into four chemokine subfamilies defined by the first cysteine motifs: CXC, CC, C, CX_3C [123]. Chemokines that direct cells during hematopoiesis in the bone marrow are called homeostatic chemokines. For example, the chemokine CCL21 works in conjunction with its cognate receptor CCR7 in the development of lymph nodes [124]. Formation of lymph-node structures and the recruitment of T and B cells are dependent on CCL21expression in the pancreas [124]. Other chemokines that recruit effector cells during infection, inflammation, tissue injury, and wound healing are called inflammatory cytokines [113]. Neutrophils are rapidly recruited to the site of infection and can influence the recruitment of other immune cell types, such as dendritic cells (DCs) to the site of infection through the secretion of the chemokine CCL3. A decrease in the functionality of neutrophil-derived CCL3 results in a decrease of the recruitment of DCs and a greater susceptibility to invading pathogens [125]. Some chemokines like SDF-1α are involved in both inflammatory and homeostatic processes through the release of neutrophils from the bone marrow upon infection as well as the homing of inflammatory cells in the bone marrow in the absence of infection [126].

G-protein coupled receptors (GPCRs) expressed on the surface of cells mediate chemokine signaling. Once activated, GPCR stimulate phospholipase C, phosphoinositide-3 kinases and c-src family of tyrosine kinases [123, 127]. Different chemotactic responses rely on the expression of specific GPCRs. For example, PMNs increase expression of CXCR4 as they mature, which direct PMNs back to the bone

marrow [128]. An adaptive immune response relies on the expression of CXCR3 and CXCR5 to guide plasma cells from the spleen to the sites of inflammation [129]. Once activated, a chemokine receptor becomes phosphorylated and internalized, which causes an interruption of responsiveness called desensitization. The receptor can be then be rapidly recycled and re-expressed on the cell surface. If the receptor is degraded upon internalization instead of recycled, the cell does not re-express the receptor and is subsequently desensitized to the signal of the chemokine and will no longer migrate [123].

1.6.2 MT chemotaxis

Chemokine genes map closely to MT genes in both humans and mice [46, 47, 130]. MT induces chemotaxis of splenocytes and leukocytes when measured in the *in vitro* Boyden Chamber and ECIS/Taxis assays. Jurkat T cells respond to MT in a dose dependent fashion, and a monoclonal antibody to MT blocks this response [130]. Cholera and pertussis toxins block GPCR signaling and block MT mediated chemotaxis, which suggests MT signals through a GPCR [130].

1.6.3 *In vitro* Chemotactic assays

The Boyden chamber, or transwell chamber, is the most common *in vitro* measurement of chemotaxis. In this assay, a porous membrane separates chemoattractant from cells. As the cells responded to the chemoattractant, they crawl through the membrane and adhere to the underside of the membrane or drop into the well below

[131]. The membrane is then stained and cells are counted under a microscope. Cells from the wells below can also be collected and counted. In this assay, cells are presented with a steep chemoattractant gradient, which only poorly represents actual biological systems [132]. This assay also can only be configured as an endpoint assay since the chamber must be disassembled to visually count migrated cells.

An alternative to the Boyden Chamber, the under-agarose assay measures cell movement across a thin aqueous film that forms beneath a layer of agarose that covers a substrate [133, 134]. Two troughs are cut in the agarose and cells are placed in one trough opposite the chemoattractant trough. Chemoattractant diffuses through the agarose and creates a shallow gradient through the agarose. This is thought to be a better representation of *in vivo* chemoattractant gradients than the steep gradient formed in the Boyden Chamber [135]. Movement of cells in an under-agarose assay is commonly measured with microscopy. Analysis of this assays allows for the tracking of individual cells through the agarose overtime.

The ECIS/Taxis assay combines the under-agarose approach with electric cell-substrate impedance sensing (ECIS) technology [136, 137]. The agarose matrix configuration is identical to the traditional under-agarose assay, but as cells crawl beneath the agarose toward the chemoattractant they cross an electrode located between the cell and chemoattractant wells. As cells cross the electrode they impede the current flow and resistance at the electrode increases [137]. Chemotaxis is monitored by changes in resistance at that electrode over time. This assay allows for real-time, objective, measurement of cell movement. It also allows for the calculation of cellular speed in response to an established gradient [135, 138-140].

1.7 The Bacterial Stress Response

Bacterial cells also have the ability to adapt to stressful environments. The most studied bacterial stress response, often referred to as the heat-shock response, involves HSPs, similar in structure to mammalian HSPs [141]. Induction of the heat-shock response is not limited to heat stress, but is also induced by exposure to ethanol, heavy metals, high salt concentrations and interaction with eukaryotic cells [141]. Bacterial cells express homologues of mammalian Hsp60 and Hsp70, which are transcribed from the genes *GroE* and *DnaK* [142]. GroE and DnaK are chaperone proteins in bacteria that are induced in the bacterial heat-shock response. The absence of these chaperone systems can leave the cells susceptible to elevated temperatures, oxidant exposure, or osmotic stressors. However, redundancy between the two systems can protect bacteria in the absence of either GroE or DnaK-like chaperone systems [143].

Some bacteria also express MT proteins that are up-regulated these MTs in high concentrations of zinc and other heavy metals. The relationship, if any, to the bacterial heat-shock response is unknown.

1.8 Bacterial Metallothioneins

The literature on bacterial MTs refers to the proteins as BmtAs SmtAs, MyMTs or PmtAs. BmtA describes all bacterial MTs, while SmtA, MyMT, and PmtA define classes of BmtAs. The PmtAs are similar in sequence to the first categorized BmtA, SmtA, from the *Synechococcus* species of bacteria [144-146]. More recently in the literature,

bacterial MTs from other species of have been categorized using letters from their host species. For example, the bacterial MT that is the focus of this dissertation has been referred to as PmtA from *P. aeruginosa* [147]. In this dissertation the *P. aeruginosa* bacteria MT will be referred to as PmtA.

1.8.1 SmtA class of bacterial Metallothioneins

Bacterial MTs were first identified in *Synechococcus* sp. [144], *Synechococcus* PC6301 [148] and *Pseudmonas putida* [149]. As the bacteria were adapted to grow in high concentrations of the heavy metal cadmium, it was found that these bacteria expressed an MT to adapt in high levels of this toxic metal [44]. As a member of the cyanobacteria family, *Synechococcus* is thought to be one of the earliest producers of oxygen, which causes the oxidation of ZnS [150]. It is likely that Cyanobacteria developed MT genes to regulate zinc homeostasis and prevent the oxidation of zinc [147]. The most well categorized bacterial MT, SmtA, from *Synechococcus* can bind zinc, cadmium, copper and mercury [151]. There seems to be evolutionary relationships among BmtA families, such as SmtA-like proteins from several bacterial species, but evolutionary relationships between bacterial MT families are not yet defined [44].

Another family of bacterial MTs, MyMTs, act as a copper-binding protein in the pathogen *Mycobacterium tuberculosis* [152]. Unlike other bacterial MTs, MyMT was found during a drug resistance screen of *M. tuberculosis* [152]. *M. tuberculosis* growth depends on the presence of copper and MyMT binds up to 6 copper molecules per protein. MyMT may allow *M. tuberculosis* to compete with the host for copper [152].

In contrast, high concentrations of copper can be toxic to *M. tuberculosis*. Copper levels present in the phagosomes of macrophages are sufficient to kill *M. tuberculosis*, as the minimal inhibitory concentration of copper for this pathogen is quite low [153]. Copper resistance is therefore essential for the survival and full virulence of this pathogen [153]. This is the first evidence of a pathogen's dependence on MT expression for maximum virulence in an infection.

1.8.2. Structure of Known Bacterial Metallothioneins

SmtA classified from *Synechococcus* contains approximately 70 amino acids, 8 to 9 of which are cysteine residues [154]. Unlike mammalian MTs, SmtA uses histidine residues in addition to cysteine residues to bind metals. A mutation of the histidine residues results in a decreased metal binding capacity [154]. Similar to eukaryotic MT, the arrangements of SmtA's cysteine residues are indicative of the four classes of chemokines. SmtA binds 4 zinc or 4 cadmium molecules, and all cysteine residues participate in this function [155].

PmtA from *P. aeruginosa* binds 3 zinc or 4 cadmium molecules. Unlike *Synechococcus* SmtA, but similar to mammalian MT, zinc bound by PmtA from *P. aeruginosa* can be displaced by cadmium. The PmtA from *P. aeruginosa* is slightly less stable the SmtA from *Synechococcus* PC7942, and is more prone to oxidation and aggregation [147].

1.8.3 Metal Function and Induction

Synechoccoccus species that lack the *smt* locus, the locus responsible for *PmtA* transcription, are viable but are approximately 4 times more sensitive to zinc and cadmium than their wildtype counter parts [156]. This indicates cells use PmtA to maintain essential metal homeostasis and to combat toxic levels of metals.

In *Synechococcus* PC7942, the zinc sensing repressor SmtB induces the transcription of the *PmtA* gene in the presence of high concentrations of zinc. In high concentrations of zinc, SmtB dimer bind zinc and undergoes a conformational change that prevents SmtB from binding the repressor region of the *smt* locus. When zinc levels decrease, SmtB releases zinc and again binds the repressor region of the gene and halt transcription [156].

1.9 The Opportunistic Pathogen *Pseudomonas aeruginosa*

Pseudomonas aeruginosa is a Gram-negative opportunistic human pathogen that uses O_2, and nitrate, under anaerobic conditions, as a terminal electron acceptors [157], and is a member of the γ-proteobacteria class of bacteria [158]. As a γ-proteobacteria, *P. aeruginosa* can catabolize an array of low molecular weight organic compounds, such as aromatics and halogenated compounds, which can be useful in biodegradation and soil remediation, and also allows the bacteria to survive in many different environmental niches [159].

In an individual with a healthy immune response, the immune system deprives *P. aeruginosa* of the ability colonize in the host. In order for the bacteria to colonize there

must be a disruption of the epithelial or mucosal barriers, which is often a result of burn, trauma, or the insertion of a ventilator [160]. In addition, *P. aeruginosa* commonly infects Cystic Fibrosis (CF) patients through colonization of the airway epithelium and causes massive damage to the lung tissue. After several acute infections, *P. aeruginosa* extensively damages the airway epithelium to a point that progenitor cells cannot adequately respire the damage, which allows the pathogen to establish a chronic infection. CF patients often succumb to the massive infections caused by *P. aeruginosa.*

P. aeruginosa expresses the bacterial MT, PmtA. PmtA shares many structural characteristics with the mammalian MTs, such as a small size, high cysteine content, and presence of CXC cysteine motif. Current research on PmtA focuses on its metal binding capacity, but lacks any information on its interactions with host immune cells. The characterization of eukaryotic MT as immunomodulatory protein suggests a bacterial MT could also possess immunomodulatory functions. If PmtA modifies immune cell movement or the redox environment during infection, similar to its eukaryotic counterpart, it could impact the course of an *P. aeruginosa* infection.

1.9.1 ROS and *P. aeruginosa* infection

During a *P. aeruginosa* infection, phagocytic cells, such as, macrophages and neutrophils, are the first immune cells to encounter the pathogen once it has breached the epithelial barrier. A major function of these phagocytes is to produce antimicrobial intermediates, such as superoxide and hydrogen peroxide, and initiate signaling that induces an immune response to the pathogen [161, 162]. The production of ROS in an oxidative burst provides antimicrobial intermediates and alters cellular signals.

Mice that lack the NADPH oxidase component $p47^{phox}$ and are exposed to *P. aeruginosa* cannot clear the pathogen as well as their wildtype counterparts [163]. Without a functional NADPH oxidase the immune cell cannot produce the microbiocidal intermediates through an oxidative burst, and also have dysfunctional redox signaling. Upon infection, mice that lack $p47^{phox}$ express less cytokines that depend on NF-κB signaling, such as TNFα [163]. In individuals with an uncompromised immune response *P. aeruginosa* increases neutrophils and inflammatory cytokines at the site of *P. aeruginosa* entry, and adequately combat the bacteria primarily through phagocytosis and the generation of ROS. The host cells involved in the infection show a threefold increase in intracellular GSH and no change in indicators of oxidative stress. This indicates that healthy individuals can manage oxidative stress produced by phagocytes and adequately eliminate *P. aeruginosa*. Immune compromised individuals experience deregulation of many cellular processes. This can increase oxidative stress and disrupt the oxidant buffering capacity of GSH [164].

P. aeruginosa also contributes to the production of ROS through a redox-active compound called pyocyanin. NADH or NADPH can transfer electrons to pyocyanin and form superoxide and hydrogen peroxide[165]. Exposure of host cells to pyocyanin leads to an increase in intracellular ROS and could alter mitochondrial and cytosolic thiol buffering systems and alter redox sensitive signaling [165].

1.9.2 Immune defenses against *Pseudomonas aeruginosa*

In healthy individuals, airway epithelial cells form tight junctions to prevent bacterial invasion. However, in immunocompromised individuals exposed to *P. aeruginosa*, the bacteria can attach to epithelial cells and destabilize these junctions, which exposes more host cells for colonization. When these cells encounter bacteria, signaling cascades are activated to produce anti-microbial peptides to defend against *P. aeruginosa* [166, 167]. Epithelial cells also produce chemokines that recruit neutrophils to the site of infection [119, 121]. Epithelial cells express Toll-like Receptors (TLRs) that recognize MAMPs, and in turn activate various intracellular cascades involving Ras, Src, ERK1/2 and MAP kinases. Lipopolysaccharide (LPS) on the surface of *P. aeruginosa* is recognized by TLR4 [168], while other lipoproteins are recognized by TLR1 [169]. Expression of pili and flagella by the bacterium are recognized by TLR2 and TLR5, respectively [170, 171]. Once these TLR recognize MAMPs, cascades are activated, which result in the activation of the transcription factors NF-κB and AP-1, which in turn up-regulate inflammatory cytokines [172-174]. In *P. aeruginosa* infection NADPH-dependent redox signaling is essential for full TLR4 activation of NF-κB. HLL mice, deficient in $p47^{phox}$ ($p47^{phox-/-}$) are unable to activate the redox sensitive transcription factor, NF-κB, to the same degree as wildtype HLL mice [163].

As one of the first immune cells recruited to the site of infection in the airway, neutrophils are arguably the most important cell type in combating *P. aeruginosa* infection. In murine models, the genetic or chemical depletion of neutrophils prior to exposure to *P. aeruginosa* leads to mortality of many different mouse strains [121]. Even very low doses of *P. aeruginosa* (~8cfu/ml) lead to infection and death of mice if

neutrophils were not present [175]. The recruitment of neutrophils relies on the production of chemokines from macrophages, epithelial cells, and lymphocytes [121]. CXC chemokines are extremely important to the recruitment of neutrophils. A blocked CXCR2 receptor results in decreased neutrophil influx to the site of infection and to an increase in mortality[121].

In a *P. aeruginosa*-induced pneumonia the bacteria first encounter resident alveolar macrophages that release cytokines and chemokines upon contact with MAMPs [176, 177]. These mediators are essential to the host defense, as they recruit other immune cells, such as neutrophils to the site of infection. Alveolar macrophages generate ROS, which serve as both a microbiocidal agent and a secondary messenger in various signaling cascades [178].

Alveolar macrophages can also phagocytose *P. aeruginosa* mediated by the FcR, complement 1 and 3 receptors, and the macrophage mannose receptor [179]. Despite these functions, the role of alveolar macrophages in acute *P. aeruginosa* infections is not clear and is often debated. Kooguchi et. al., has reported that a decrease in alveolar macrophages results in decreased neutrophils recruitment and chemokine production, which results in a decreased bacterial clearance in 48 hours [180]. However, Cheung et. al., found that a 78%-88% depletion of alveolar macrophages did not affect the survival of mice or bacterial clearance [181]. Due to these conflicting reports, the importance of macrophages to either ingest bacteria or produce mediators important to an inflammatory response, remains unclear.

T cells also play an immunomodulatory role during acute or chronic *P. aeruginosa* infections [182]. In mice, a higher interferon gamma (IFN-γ) level, both systemically and at the site of infection, lead to Th1-dominated response, and mice that were more resistant to *P. aeruginosa* than mice with a Th2-dominated response. After day 3 of infection, there was a significant difference in bacterial load, with those mice mounting a Th-1 response fairing better than those with a Th2 dominated response [183]. A Th1-dominated response also provides antibody-independent protection to chronically infected mice. BALB/c mice challenged with *P. aeruginosa* 14 days after initial infection, experienced decreased mortality rates if CD4 cells shifted toward a Th1, rather than a Th2 response, and produced more Interleukin-12 (IL-12). This shift did not affect IgG levels in re-infected mice [184].

Evading or modifying the immune response is essential for the bacterium to cause infection; therefore *P. aeruginosa* possesses many virulence factors, including a type 3 secretion system and pyocyanin, that enable it to escape immune defenses.

1.9.3 PmtA in *P. aeruginosa* infection

Currently, the literature lacks any information on the role of PmtA in the progression of *P. aeruginosa* infection. The structural similarities between PmtA and eukaryotic MT suggest that PmtA also possesses immunomodulatory functions. The high cysteine content of PmtA, although not as high as eukaryotic MT, means the thiols of PmtA may also be oxidized by ROS and protect the bacteria from the harmful ROS. Phagocytes vital to the clearance of *P. aeruginosa*, neutrophils and macrophages, rely on

an oxidative burst to kill the pathogen. If PmtA is oxidized by ROS, it can potentially neutralize the immune response to *P. aeruginosa*. *P. aeruginosa* also produces oxidative metabolites that cripple the host cells and allow the bacteria to colonize the host, such as pyocyanin. The expression of PmtA may allow the bacteria to produce higher amounts of oxidant than a pathogen that lacks PmtA without compromising itself.

Similar to mammalian MT, PmtA cysteine residues are reminiscent of the motifs indicative of chemokines. It is therefore appropriate to suggest that PmtA may influence immune cell function. This could affect the ability of immune cells to get to the site of infection, or influence their motility once at the site of infection.

The similarities in structure of MT and PmtA make it reasonable to hypothesize that PmtA expression by *P. aeruginosa* influences the course of infection. PmtA has potential to influence the effectiveness of the oxidative burst of phagocytes and direct immune cell movement, which could affect the virulence of the pathogen. Knowledge of another potential virulence factor of an increasingly antibiotic resistant human pathogen reveals another avenue for potential therapeutic targets. The study of PmtA is therefore essential to the control of this deadly human pathogen.

CHAPTER 2: MATERIALS AND METHODS

2.1 Tissue Culture

2.1.1 Macrophage Cells

The murine macrophage cell line, RAW264.7 (ATCC #TIB-71), was cultured in 37°C at 5% CO_2 in RPMI 1640 (Cellgro, Cat. #10-040) supplemented with 10% heat inactivated fetal bovine serum (FBS) (Thermo Scientific, Cat. # SH300703), 100µg/mL penicillin/streptomycin (MP Biomedicals Cat. #1670049, 10mM HEPES buffer (MP Biomedicals Cat. # 1688449), and 200mM L-Glutamine (Sigma-Aldrich Cat. #56-58-9).

The murine alveolar macrophage cell line, MH-S (ATCC #CRL-2019) was acquired from the David Knecht Laboratory. MH-S cells were cultured in 37°C at 5% CO_2 in RPMI 1640 (Cellgro, Cat. #10-040) supplemented with 10% heat inactivated fetal bovine serum (FBS) (Thermo Scientific, Cat. # SH300703), 100µg/mL penicillin/streptomycin (MP Biomedicals Cat. #1670049, 10mM HEPES buffer (MP Biomedicals Cat. # 1688449), and 200mM L-Glutamine (Sigma-Aldrich Cat. #56-58-9).

2.1.2 T lymphocytes

The human Jurkat T lymphocyte cell line (ATCC TIB-152), was cultured at 37°C with 5% CO_2 in RPMI 1640 supplemented with 10% heat inactivated FBS, 25mM HEPES buffer, 4mM L-Glutamine, 1% penicillin/streptomycin.

2.1.3 Sterile Technique

Macrophage cells adhere to the bottom of plastic of tissue culture flasks, therefore Raw264.7 cells were scraped from the bottom of a tissue culture flask with a sterile cell scraper. The macrophage cells were then transferred to a new tissue culture flask, at a desired density, in supplemented RPMI 1640 media described in 2.1.1.

Human Jurkat T lymphocyte cells do not adhere to the bottom of plastic tissue culture flasks. Spent media containing cells and cellular debris, was aspirated from the flasks and replaced with fresh supplemented RPMI 1640 media described in 2.1.2. Cells were passed before they reached a concentration of $1x10^6$ cell/ml.

2.1.4 Trypan Blue Exclusion

The survival and percent viability of each cell type were determined through trypan blue exclusion. An equal volume of cell suspension and trypan blue were combined in a single tube. The trypan blue and cell suspension was added to a hemocytometer and viewed under a light microscope. Blue cells were able to take up the trypan blue due to a compromised cell membrane and were not considered viable.

2.2 Bacterial Growth

2.2.1 *E. coli* MC1061 +pGex-6p-PmtA and pGEX-6p-1 in Rich media, expressing Plasmid proteins

Escherichia coli was cultured in a standard YTA media comprised of 1.6% bactotryptone, 1% yeast extract, and 0.5% sodium chloride. Expression of the pGEX-6p-

1 based plasmids in *E. coli* MC1061 required the addition of 100μg/mL ampicillin, and induction of the gene encoded on the plasmid required the addition of 100μM Isopropyl β-D-thiogalactopyranoside (IPTG).

2.2.2 *E. coli* MC1061 + pDual and pDual-*PmtA* in Rich media, expressing Plasmid proteins

E. coli expressing the pDual based plasmids were also cultured in standard YTA media. Expression of the pDual based plasmids in *E. coli* MC1061 required the addition of 100μg/mL kanamycin and induction of the gene encoded on the plasmid required the addition of 100μM IPTG.

2.2.3 Growth of *P. aeruginosa* wildtype strain, PAO1

P. aeruginosa PAO1 was cultured in YTA media. No antibiotic was used for this strain.

2.2.4 Growth of *P. aeruginosa PmtA* knockout strain, PW4670

P. aeruginosa PW4670 was received from the Manoil lab at Washington University on a culture slant. The mutant was streaked out on a YTA plate supplemented with 5μg/ml tetracycline (Tet5) plates. A single colony from the mutant strain was cultured in 5ml YTA media with Tet5 overnight with vigorous shaking at 37°C. The mutant underwent 2 more selections on Tet5 YTA plates and was grown overnight at 37°C in YTA with Tet5 overnight with vigorous shaking at 37°C. It was then frozen in the -80°C freezer in 50% glycerol.

PW4670 was grown for experiments in YTA media supplemented with Tet5 and stored on YTA plus Tet5 plates at 4°C.

2.3 Generation of purified GST or GST-PmtA from E. coli MC1061 Expressing the pGEX-6p-PmtA or the pGEX-6p-1 plasmid

2.3.1 Growth and expression of plasmid PmtA

YTA media containing 100μg/mL ampicillin was inoculated with a single colony of *E. coli* MC1061 expressing either the pGEX-6p-1 plasmid to purify GST or the pGEX-6p-*PmtA* plasmid to purify GST-PmtA, and grown overnight at 37°C with shaking. The overnight culture was diluted 1:100 the following day in 75ml of fresh YTA containing ampicillin. This culture was grown for 48 hours, and induced with 100μM IPTG at 3, 8, 24, 30, 33 and 46 hours after inoculation.

2.3.2 *E. coli* Lysis

The 75mL of *E. coli* was centrifuged at 2,000xg for 15 minutes in 3, 25ml aliquots. The 3 pellets were then combined into a single tube and suspended in 5mL of PBS containing 1% Triton-X-100 and incubated on a rotating platform at 4°C for 4 hours. At this point, the lysate could be frozen at -20°C for later use.

2.3.3 Purification of GST-PmtA or GST

If the lysate was frozen, it was thawed at room temperature. The lysate was centrifuged and the supernatant was exposed to ProCatch Glutathione Resin (Miltenyi Biotech, Auburn CA, Cat. #130-092-186), prepared according to manufacture

instructions, for 2 hours at 4°C. The resin was washed 3 times with PBS before GST-PmtA or GST was eluted from the resin with 50mM Tris-HCl pH 8.0 plus 10mM reduced glutathione. The protein was dialyzed against PBS with a 12,000-14,000 molecular weight cut off dialysis membrane to rid the purified product of free glutathione. The supernatant was then transferred to a fresh microcentrifuge tube, labeled and stored at -20°C for analysis. The resin was suspended again in 1mL elution buffer, and the elution process repeated twice.

2.3.4 Confirmation of purified GST and GST-PmtA (SDS-PAGE and Western Blot)

The presence, and purification of GST-PmtA or GST was confirmed through SDS-PAGE and Western blot analysis. The purified GST-PmtA was added to 6x loading buffer (69.7% 0.5M Tris-Cl, 30% Glycerol, 0.1% SDS, 0.093% dithiothreitol, 0.012% bromophenol blue) and heated for 5 min in a 95°C water bath. The 6x loading buffer was also added the Full Range Rainbow molecular weight marker (GE Healthcare, Piscataway NJ, Cat. #RPN800E). The protein samples and ladder, were loaded into a 12% SDS-PAGE gel and run in a Bio-Rad mini-PROTEAN Tetra Cell electrophoresis system (BioRad, Hercules CA, Cat. #165-8002) at 200 volts until the dye front reached the end of the gel.

The gel was removed from the Bio-Rad mini gel system and placed in coomassie blue stain (2g Coomassie, 10% acetic acid, 25% isopropanol in dH_2O), for 1 hour to stain total protein in the sample. After one hour the gel was removed from the Coomassie stain

and washed with a 45% methanol 10% acetic acid solution, until the background of the gel is clear.

The samples were also analyzed through Western blot analysis. The protein was transferred from a separate 12% SDS-PAGE gel, that was not stained with coomassie blue, to a PVDF membrane (Invitrogen Life Technologies Corp., Grand Island NY, Cat. # IB4010-02) using the Invitrogen iBlot system (Invitrogen Life Technologies Corp., Grand Island NY, Cat. #IB1001) and run under the manufacturer preset program number 3. The PVDF was then removed from the iBlot and placed in block, consisting of 5% dry milk 2% Bovine serum albumin (BSA) in TBST (2.42% Tris-Base, 1.168% NaCl, pH to 7.6, 0.1% Tween) for 1 hour. The primary anti-GST (GE Healthcare, Piscataway NJ, 27-4577) confirmed the presence of GST (24KD) or GST-PmtA (36KD). The primary antibody was diluted TBST 1:1500 in a volume equivalent to the block and added directly to the block, and incubated for 1 hour, with gentle agitation at room temperature. The blot was then washed TBST 3 times for 15 minutes with gentle agitation at room temperature. The secondary antibody, goat anti-mouse IgG, coupled to alkaline phosphatase, (Southern Biotechnology, Birmingham AL Cat. # 1031-04) was used at a dilution of 1:1000 in TBST, and incubated with the blot for 1 hour with gentle agitation at room temperature. The PVDF was then developed in developing buffer (12g Tris base, 0.95g $MgCl_2$, 5.85g NaCl, in 1L, adjust to pH 9.5) with 1mg/mL NBT and 50mg/mL BCIP in DMSO. Distilled water was added to the membrane to stop development.

2.4 Determination of Unknown Protein Concentrations

2.4.1 Bicinchoninic Acid (BCA) Protein Assay

The BCA assay (Thermo Scientific, Rockford, Il, Pierce®, Cat. # 23225) utilizes the biuret reaction, in which a protein in an alkaline medium reduces Cu^{2+} to Cu^{1+}. Cu^{1+} can combine with two molecules of BCA to form a colorimetric product absorbed at 562nm. A standard curve of BSA, ranging from 2,000µg/ml to 25µg/ml was diluted in the same diluent as the unknown protein, and 10µl of the standard, or unknown protein sample, were loaded in triplicate to a clear, flat bottom, NUNC 96-well plate. The working reagent was prepared by combining 1 Part reagent B with 50 parts Reagent A. The working reagent was added to each well at a volume of 200µl, and the plate was incubated at 37°C for 30 min. The absorbance of the plate was then read, at 560nm, on the Molecular Devices, Spectra Max M2 96-well plate reader. The absorbance readings of the unknown protein samples were then interpolated from the standard curve in order to determine the protein concentration.

2.4.2 Micro BCA assay

The micro BCA assay (Thermo Scientific, Rockford, Il, Pierce®, Product # 23235) utilizes the same principles as the BCA assay, but is modified for protein samples between 0.5-20µg/ml. BSA standards were made from 200µg/mL to 0.5µg/ml in the same diluent as the unknown protein sample, and 150µl of the standard, or unknown protein samples, were loaded in triplicate to a clear, flat bottom, NUNC 96-well plate. The working reagent was prepared by combining reagents MA, MB, and MC at a ratio of 25:25:1, and 150µl of the working reagent was added to each well. The plate was then

covered and incubated at 37°C for 2 hours. The absorbance was then read at 560nm, on the Molecular Devices, Spectra Max M2 96-well plate reader. The absorbance readings of the unknown protein samples were than compared to the standard curve in order to determine the protein concentration.

2.4.3 Bradford assay

The Quick Start Bio-Rad Bradford Assay (Bio-Rad Laboratories, Hercules,CA, Cat# 500-0203) was used to determine the concentration of an unknown protein when a reagent used in the preparation of the protein was not compatible with a BCA or microBCA assay. In particular, the Bradford assay was used to determine the concentration of GST or GST-PmtA purified from *E. coli*, because the L-glutathione used to elute the GST tagged protein from the GSH binding resin is not compatible with the BCA assay. A standard of gamma-globulin protein, ranging in concentration from 2,000µg/mL to 125µg/mL, was prepared in the same diluent as the unknown proteins, and 20µl of the standard or samples, was combined with 1mL 2x Dye Reagent in a cuvette. The cuvettes were incubated at room temperature for at least 5 min and then the absorbance was read at 596nm on a spectrophotometer. A standard curve of the absorbance readings vs. protein concentrations of the standards was created and the unknown protein samples were then interpolated from the standard curve to determine the concentrations of the samples.

2.5 Bacterial Cell Assays

2.5.1 Bacterial Growth Curves

2.5.1.1 *E. coli* expressing pGEX-6p-1 and pGEX-6p-*PmtA* plasmids

E. coli expressing pGEX-6p-1 or pGEX-6p-*PmtA* plasmids was grown in YTA media with ampicillin overnight at 37°C with vigorous shaking. The overnight culture was transferred to fresh YTA with ampicillin at a dilution of 1:100 and incubated at 37°C with vigorous shaking. The growth of the bacteria was monitored through OD_{600nm} readings in 96 well NUNC plates. When the culture reached early log phase (OD_{600} ~0.2) IPTG was added to the culture. The OD_{600} readings were used to continue to monitor the growth. In addition to the OD_{600} readings, 100µl of the culture was removed to be diluted and spread on YTA +ampicillin plates. The plates were incubated overnight at 37°C and counted the following day and the cfu/ml was determined for each time point. Data can be shown as OD_{600} vs. cfu/ml.

2.5.1.2 *E. coli* expressing pDual and pDual-*PmtA* plasmids

E. coli expressing pDual or pDual-*PmtA* plasmids were grown in YTA media with kanamycin overnight at 37°C with vigorous shaking. The overnight culture was transferred to fresh YTA with kanamycin at a dilution of 1:100 and incubated at 37°C with vigorous shaking. The growth of the bacteria was monitored through OD_{600nm} readings in 96 well NUNC plates. When the culture reached early log phase (OD_{600} ~0.2) IPTG was added to the culture. The OD_{600} readings were used to continue to monitor the growth. In addition to the OD_{600} readings, 100µl of the culture was removed to be diluted and spread on YTA +kanamycin plates. The plates were incubated

overnight at 37°C and counted the following day and the cfu/ml was determined for each time point. Data can be shown as OD_{600} vs. cfu/ml.

2.5.1.3 *P. aeruginosa* PAO1 and PW4670

P. aeruginosa strains PAO1 and PW4670 were grown overnight in YTA media or YTA media with Tet5, respectively. The overnight culture was transferred to fresh YTA media without antibiotic, for both strains. Growth was monitored for the first 3 hours by transferring 600µl of the culture to a NUNC 96 well plate in triplicate and reading the absorbance at 600nm. After the first 3 hours, *P. aeruginosa* forms aggregates, which makes it difficult to obtain accurate readings. Therefore, the culture was diluted 1:10 in YTA media and the OD_{600nm} was determined. In addition to the OD_{600} readings, 100µl of the culture was removed to be diluted and spread on YTA plates. The plates were incubated overnight at 37°C and counted the following day and the cfu/ml was determined for each time point. Data can be shown as OD_{600} vs. cfu/ml.

2.5.2 *E.coli* and *P. aeruginosa* growth in the presence of oxidant

All cells were grown overnight in the presence of the appropriate antibiotic indicated in 2.2. The next morning, overnight cultures were transferred 1:100 to fresh YTA media with induced with IPTG. *P. aeruginosa* overnight cultures were transferred 1:100 to fresh YTA media without antibiotics.

Bacterial cultured diluted 1:100 were grown to early-log phase (OD_{600nm} ~0.25 - 0.35). Once bacterial cultures reached the proper OD_{600nm}, oxidant diluted in dH_2O was added directly to the cultures. The OD_{600nm} readings were used to monitor the growth of

the cultures after oxidant addition for at least 3 hours. In some experiments, samples were taken and spread on YTA plates to calculate the cfu/ml of the cultures.

2.5.3 Measurement of Pyocyanin production by *P. aeruginosa* strains PAO1 and PW4670

A single colony of *P. aeruginosa* strains PAO1 and PW4670 were grown overnight in 5ml of YTA media or 5ml YTA media with Tet5, respectively, at 37°C with vigorous shaking. Both PAO1 and PW4670 cultures were transferred to 50ml YTA media without antibiotics at a dilution of 1:100 at 37°C with vigorous shaking. To measure pyocyanin, 1ml of the culture was removed and centrifuged form 1 minute at 20,500xg. The supernatant was transferred to a fresh microcentrifuge tube and vortexed vigorously. The supernatant was then placed in a NUNC 96 well plate in triplicate and the absorbance at OD_{691} (the maximum wavelength of pyocyanin [185]) was recorded. The OD_{600} of the bacterial culture was also monitored and data was plotted as OD_{600} vs. OD_{691}. Pyocyanin measurements were taken at various time points over a duration of 30 hours.

2.5.3.1 Addition of L-glutathione (GSH) to PW4670

A single colony of *P. aeruginosa* strains PAO1 and PW4670 were grown overnight in 5ml of YTA media or 5ml YTA media with Tet5, respectively, at 37°C with vigorous shaking. Both PAO1 and PW4670 cultures were transferred to 50ml YTA media without antibiotics at a dilution of 1:100 at 37°C with vigorous shaking. A third flask containing PW4670 was supplemented with 10mM GSH and incubated at 37°C

with vigorous shaking. Pyocyanin and growth was measured according to methods in 2.5.3.

2.5.2 CPM assay

The CPM assay is a technique that uses a thiol-specific fluorochrome (N-[4-(7-diethylamino-4-methy-3-coumarinyl)phenyl]malemide) (CPM) to quantitate cellular or plasma thiols [186]. This assay was used to measure free thiol in PmtA expressing *E.coli*. A standard was created by diluting reduced glutathione (GSH) at a stock concentration of 10mM to 12 concentrations between 10nm to 0.045nm. An overnight culture of expressing either the pGEX-6p-1 or pGEX-6p-*PmtA* plasmids were transferred to fresh YTA media (1:50) and grown to log phase (~0.2 OD_{600}) in the presence of 100μM IPTG and 100μg/ml ampicillin. *P. aeruginosa* wildtype strain PA01 and the *PmtA* knockout strain PW4670 were also cultured 1:50 in YTA and grown to and OD_{600} of 0.2-0.3.

To determine the total free thiol content of the bacteria, the log phase bacterial cells were centrifuged for 4 min at 10,000rpm and washed with 1mL PBS. In order to determine the free thiol content of bacteria in the presence of oxidative stress, log phase bacteria were exposed to 10mM H_2O_2 for one hour at 37°C, and then centrifuged for 4 min at 10,000rpm and washed with 1mL PBS. This centrifugation and wash was repeated twice, for both configurations of the CPM assay. The bacterial cells were suspended to a concentration of $1x10^8$cell/ml and 100 μl of the GSH standards and bacterial cell suspensions were then plated in triplicate in an immunoflour 2 flat-bottom 96-well black plate. PBS was used as a blank for the system. Following the addition of samples, 100μl of CPM working solution (1mM EDTA 0.5% Nonidet P-40, 0.01mg/ml

CPM, in PBS) was added, and the plate was incubated at room temperature in the dark for 1 hour. After incubation the end point fluorescence of each well was measured on a Molecular Devices Spectramax M2 96-well plate reader at an excitation wavelength 387nm and an emission wavelength of 465nm. The GSH standards were graphed on Softmax Pro software, and the nm of free thiol present in the each bacterial sample was calculated by interpolation of the standard curve.

2.5.3 Pyocyanin Extraction

P. aeruginosa strains PAO1 and PW4670 were grown for 30 hours and at least 10mL of cell free supernatant was obtained as described in 2.5.3. In the fume hood, 4.5ml of chloroform was added to 7.5ml of supernatant from each strain. The mixture was then vigorously vortexed for 2 minutes until the chloroform turned blue-green in color. The tubes were centrifuged for 10 minutes at 4°C and 3000xg. At this point, the bottom layer appeared blue and 3ml of this was transferred to a new tube. The absorbance of the blue pyocyanin was measured at 300nm. HCl (1.5ml of 0.2M) was transferred to the blue pyocyanin and vortexed vigorously for 2 minutes. The top blue layer turned pink and samples were centrifuged for 2 min at 4°C and 3000xg. The absorbance of pyocyanin at the pink stage was measured at 520nm.

2.5.4 Biofilm Formation Assay

The biofilm microtiter plate assay was performed as previously described in O'Toole et. al, 2011 with minor adaptations [187]. In brief, fresh YTA media was inoculated at a 1:10 dilution with a stationary phase overnight culture. Cells were grown for 24 hours in 37°C without any shaking. Growth yields were measured with an absorbance reading at 595nm. Media was removed and biofilms were fixed to the side of

the microtiter plate with 90% methanol. Biofilms were stained with 0.1% Crystal violet for 40 minutes and washed with dH_2O. An ethanol:acetone (4:1) suspension was added to each well and incubated for 10 minutes. The liquid was then removed from each well, transferred to a new 96 well microtiter plate, and the amount of crystal violet in each well was determined with an absorbance reading at 595nm. The relative biofilm formation (rbf) for each well was determined by dividing the crystal violet absorbance reading by the growth yield absorbance reading. Any ratios above 1.0 were disregarded in statistical analysis.

2.6 *In Vitro* Chemotaxis Assays

2.6.1 Pre-incubation of Jurkat T cells with GST or GST-PmtA

Jurkat T cells were exposed to 15μM or 5.6 μM of GST or 15μM or 5.6μM GST-PmtA in complete RPMI media for 50 minutes at 37°C in a 5% CO^2, humidity controlled incubator. The cells were then washed with 1ml complete RPMI. Cells that were analyzed for cell motility were then suspended to a concentration of $2x10^6$ cell/ml. Cells that were to undergo cell surface staining were suspended in 1ml FACS buffer (0.09% sodium azide, 0.5% FBS in PBS) and incubated on ice. The cells were then washed and suspended to $1x10^5$cell/condition in FACS buffer.

2.6.2 Boyden Chamber

For the studies analyzing GST-PmtA's ability to induce Jurkat T cell chemotaxis, SDF1-α (25nM), GST-PmtA (14uM), GST (14uM) or RPMI was added to the bottom chamber (30μl), while Jurkat T cells ($2x10^6$cell/ml) were added to the top chamber

(50μl). In the studies that analyzed PmtA's ability to block Jurkat T cell chemotaxis to its natural ligand, SDF-1α, Jurkat T cells ($2x10^6$cell/mL) pre-incubated with GST (14uM) or GST-PmtA (14uM) and were then. Cells were incubated in the Boyden chamber for 4 hours with 5% CO_2 at 37°C. After 4 hours the chamber was disassembled and the side of the polycarbonate membrane that was in contact with the bottom chamber was stained with the Hema-3 Stat pack and cells were counted with a light microscope.

2.6.3 ECIS/Taxis

These assays were performed as described previously, with minor adaptations [140]. The cysteine treated gold ECIS/Taxis electrodes, supplied by Applied Biophysics, Inc. (Troy, NY) were filled with 0.5% agarose made in complete RPMI media. Two wells were cut n the agarose on either side of the target electrode with 14 gauge cannulae approximately 2mm apart. For the studies analyzing GST-PmtA's ability to induce Jurkat T cell chemotaxis, Jurkat T cells ($2x10^6$cell/ml) were added to one well, while the other contained SDF1-α, PmtA, GST, or RMPI control. In the studies that analyzed PmtA's ability to block Jurkat T cell chemotaxis to its natural ligand, SDF-1α, Jurkat T cells ($2x10^6$cell/mL) pre-incubated with GST or GST-PmtA were exposed to SDF-1α (25nM) in the opposing well. The electrodes were connected to the ECIS array holder in a 37°C, humidity controlled, 5% CO_2 incubator. The ECISθ software was used to record the increase in resistance over approximately 35 hours at 4,000hertz.

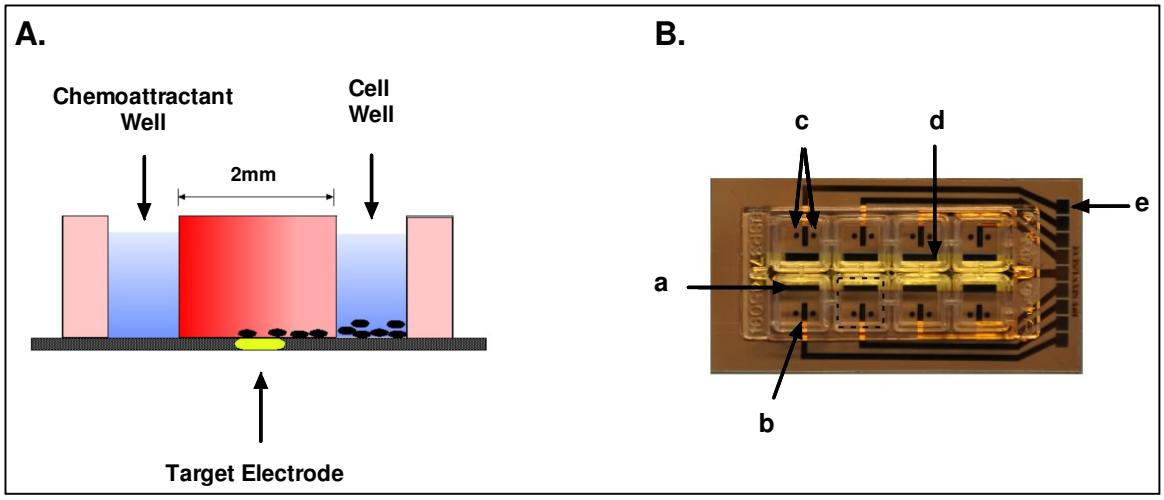

Figure 2.1 ECIS/Taxis System. A.) A Side view of a single chamber in which wells have been cut in the agarose surrounding the target electrode. B.) Top view of an ECIS/Taxis electrode without agarose. Each ECIS/Taxis electrode is comprised of 8 individual chambers. Each chamber shares a large electrode (a), and individual target electrodes (b). Each chamber also has 2 gold circles that serve as aiming points (c), where one well cut in overlaid agarose will contain chemoattractant and the other will contain cell suspension. The gold squares (e) are the contact pads that connect to the pogo pins on the array holder to AC current. The individual target electrodes are each in circuit with larger counter electrode (d).

2.7 *In vitro* Cell Assays

2.7.1 Measurement of Surface Protein Expression

PmtA's ability influence CXCR4 or CD3 surface expression was assessed using flow cytometry and fluorescent microscopy. Some Jurkat T cell cells incubated with

GST or GST-PmtA and suspended to $1x10^5$cell/condition and were subsequently exposed to SDF-1α at 0.75nM for 1 hour at 37°C in a 5% CO_2, humidity controlled incubator. SDF-1α induced CXCR4 internalization was measured in this population of cells. Other Jurkat T cells were not exposed to SDF-1α after GST and GST-PmtA incubation and were stained for CXCR4 and CD3 expression.

The measurement of CXCR4 expression required incubation with 100µl of anti-CXCR4 IgG(R&D Systems, Minneapolis MN, Cat. #MAB172) at a dilution of 1:2000 for 25 minutes at room temperature. The measurement of CD3 expression required incubation with 100µl of anti-CD3 (Thermo Scientific, Cat. #MA5-14524) at a dilution of 1:2000 for 25minutes at room temperature. The cells were washed with 1ml FACS buffer, and suspended in 100µl of fluorescein isothicyanate (FITC)-labeled goat anti-mouse IgG (Southern Biotechnology, Birmingham AL, Cat. #030-02), at a concentration of 1µg/ml for 20 minutes at 25°C. For flow cytometry, the cells were suspended in 0.2ml FACS Buffer in 12x75mm tubes and fixed with 4% paraformaldehyde. The presence of FITC on the cell surface was analyzed via the FACS Calibur, and analyzed suing FlowJo Software. For fluorescent microcopy, the cells were suspended in 10µl FACS buffer and gently spread on a glass slide with 10µl of ProLong Gold Antifade Reagent (Invitrogen Life Technologies, Grand Island, NY P36934). The slide was sealed, and allowed to dry in the dark at 25°C. Cells were viewed with the Zeiss Axiovert 200M inverted microscope equipped with a Plan 100x, 1.30 NA objective. Images were acquired with the Hamamatsu Orca camera controlled by automation routines developed with Openlab

Software (Improvision, Inc.). Quantification of fluorescence was measured with ImageJ Fiji software.

2.7.2 Measurement of ERK Phosphorylation

Cells pre-incubated with GST or GST-PmtA (5.6μM) were exposed to 25nM SDF-1α for 15 min at 37°C and 5% CO_2. The cells were then immediately fixed with 4% paraformaldehyde for 20 minutes at room temperature and subsequently permeablilized with ice-cold methanol for 20 minutes at 4°C. Cells were then incubated with an anti-phospho-p44/p42 MAPK (Erk 1/2) (Thr202/Tyr203) antibody (Cell Signaling, Cat. #9106S) for 20 min, washed and incubated with a secondary goat anti-mouse FITC antibody (Southern Biotechnology Associates, Cat. #1675-OS2). Intracellular ERK phosphorylation was measured via flow cytometry on the FACS Calibur, and analyzed with FlowJo Software.

2.8 Polymerase Chair Reaction for confirmation of PmtA Mutant

PW4670 was acquired from the Manoil Laboratory at the University of Washington. PW4670 was grown from a slant in YTA broth without antibiotic. This culture was then streaked on a YTA plate with 5μg/ml tetracycline for single colony isolation. A single colony on the plate was grown in YTA broth with 5μg/ml tetracycline overnight at 37°C with vigorous shaking. It was then again streaked on a YTA plate with 5μg/ml tetracycline for single colony isolation. This was repeated 3 times.

The insertion of the transposon was confirmed from single colonies on YTA plates with 5μg/ml tetracycline. A single colony was removed from the plate, boiled in 50μl dH_2O for 10 min. The PmtA Forward, PmtA Reverse, and transposon specific primer sequences were obtained from the Manoil Laboratory.

Primer Name	**Sequence (5'-3')**	**Position**
PmtA Forward (54742R.f)	GGTGTCGGTACCGGTGTTC	2355431
PmtA reverse (54742R.r)	GCAGTACAGGATTCCGCAGT	2356262
Hah-138	CGGGTGCAGTAATATCGCCCT	~2356025+108

The transposon was positioned in the PmtA gene in the reverse direction, therefore the PmtA reverse primer and the Hah-138 primers were used to confirm the insertion of the transposon.

A gradient PCR reaction was used to determine the most efficient annealing temperature, which was determined to be 62.5°C. For each cycle the DNA was denatured for 30 seconds at 95°C, the primers annealed for 30 seconds at 62.5°C, and the extension period was 90 seconds at 72°C. This was repeated for 30 consecutive cycles. The PCR reaction was then optimized at this temperature with 15μl reactions and 2xGoTaq Mastermix. The components for each reaction were as follows:

Component	Volume (μl)
2x GoTaq	7.5
F. Primer (or hah)	0.75
R. Primer	0.75
DNA	0.15
Nuclease free water	5.85
Total	**15**

PCR reactions with the wildtype PAO1 DNA as a negative control were conducted in the same manner.

2.9 Virulence studies with *Galleria mellonella*

2.9.1 Virulence of Supernatant

Live *G. mellonella* larvae were purchased (snackworms.com 1000 count), and stored at 4°C before use. Cell-free supernatant from PAO1 and PW4670 was obtained after 30 hours of growth, as described in 2.5.3. Worms were separated into 3 separate groups of 9 worms. One group served as a control and was injected with 5μl of sterile YTA media, and the other two groups were injected with 5μl of either PAO1 supernatant

or PW4670 supernatant. The worms were then incubated at 25°C for 24 hours and survival was assessed at this time.

Worms were injected with YTA or supernatant on ice with a 10µl Hamilton Syringe with 1/4 inch beveled tip needle. Worms were determined healthy enough for injection if they were pale yellow in color and had not yet begun to melonize. Melonization was apparent if the worm was dark yellow, gray, or black in color (Figure 2.2C). Each worm was injected in its left hind pseudopod. If a worm leaked lymph (yellow discharge) upon injection, it was discarded and replaced with another healthy worm. Survival was assessed on by the color of the worm and the movement of worm after stimulation (Figure 2.2D)

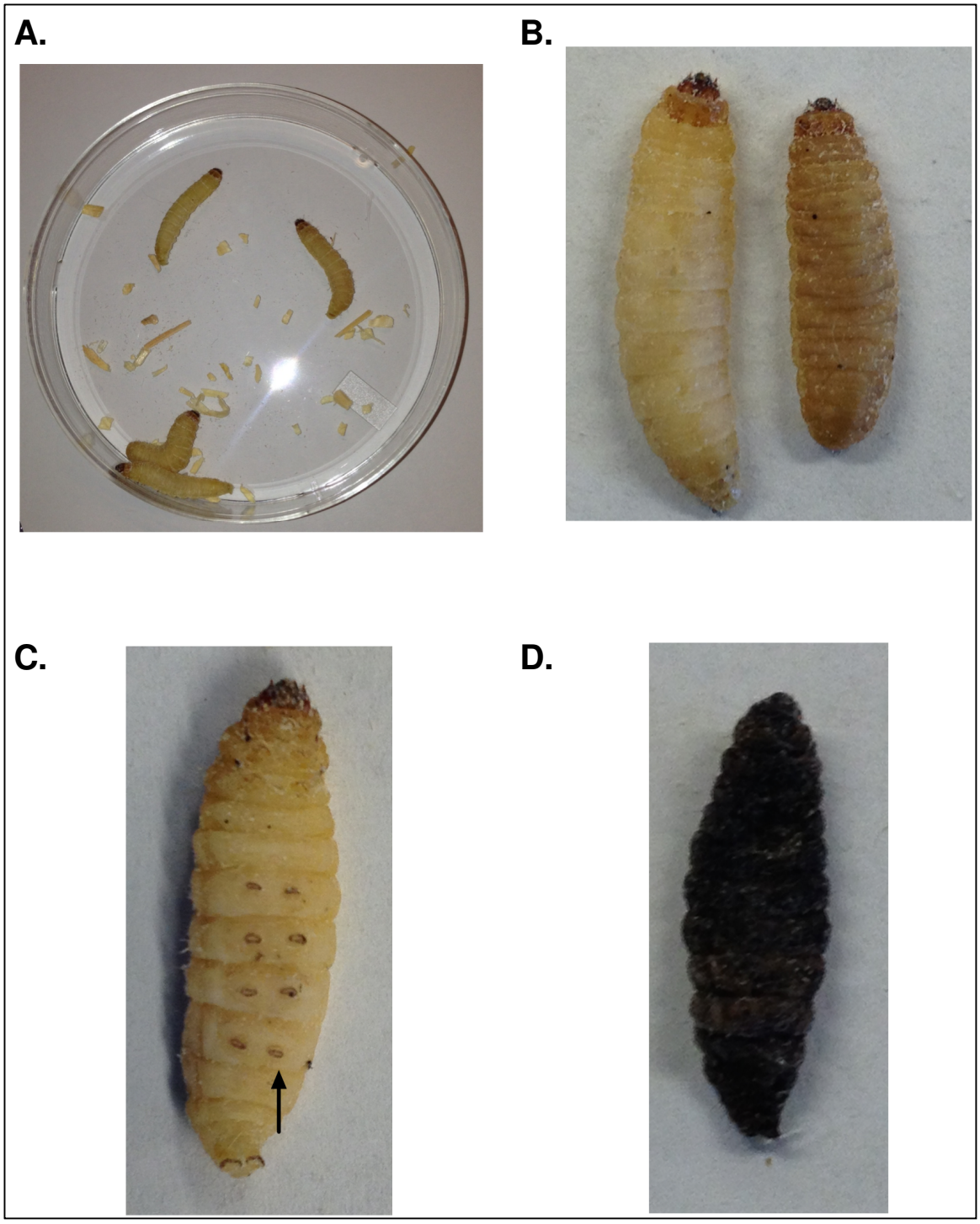

Figure 2.2

Figure 2.2: Galleria mellonella model of virulence. A.) *G. mellonella* experimental groups were placed in petri dishes during injection and incubation at 25°C. Only larvae yellow in color were selected for injection (B, left), while worms that showed any melonization were excluded from the experiments (B, right). B.) Each *G. mellonella* larvae were injected below the left hind pseudopod as indicated by the arrow. Larvae that were turned black, as seen in D.), and did not respond to stimuli were determined to be dead.

CHAPTER 3: PMTA INFLUENCES JURKAT T CELL CHEMOTAXIS

3.1 Introduction

Eukaryotic MT's influence on immune cell function has been extensively studied. However, it is not known if MTs from other species also modulate mammalian immune cell function. In an infection, bacterial MTs contact mammalian immune cells. The similarities between bacterial MTs and eukaryotic MTs suggest bacterial MTs could also modulate the activity of immune cells. Modulation of immune activity by bacterial MTs may influence the progression of infection and the degree of virulence of an MT-expressing bacteria.

The Gram negative opportunistic pathogen *Pseudomonas aeruginosa* expresses a bacterial MT known as PmtA. Similar to eukaryotic MT, PmtA binds zinc molecules and contains cysteine motifs indicative of the 4 classes of chemokines [43, 44, 188]. If PmtA influences the activity of immune cells similar to its eukaryotic counterpart, PmtA might modulate the progression of *P. aeruginosa* infection. As an increasing number of antibiotic-resistant strains of *P. aeruginosa* emerge, the development of new therapeutic regimens to treat the pathogen has become essential. Disruption of any immunomodulatory function of PmtA may present a novel therapeutic approach in the treatment of *P. aeruginosa* infection.

One of eukaryotic MT's many immunomodulatory functions is its ability to induce chemotaxis of lymphocytes. This may operate via one or more G-Protein coupled receptors (GPCR) [130]. The immune response to *P. aeruginosa* relies on the migration of various immune cells, including neutrophils and T cells, to the site of infection. Much of this directed migration relies on the signaling of stromal cell-derived 1α (SDF-1α) and is cognate GPCR CXCR4.

3.1.1 G-Protein Coupled Receptors

G-protein coupled receptors (GPCR) are 7 transmembrane proteins that transduce signals necessary for chemotactic movement of cells. The over 800 human GPCR are divided into 5 families based on the sequence similarity of the transmembrane regions of the protein [189]. The largest of the GPCR families is the rhodopsin family that encompasses 701 human GPCR, while they other four families; adhesion, frizzled/taste, glutamate, and secretin, encompass far fewer receptors [189].

Ligands that associate with GPCR are very structurally diverse. The ligands can be photons, ions, small organic molecules, peptides or proteins. The small organic molecules activate the receptors be binding within the transmembrane segments of the receptor, while peptides and proteins bind the extracellular amino terminus of the receptor [190-192]. Although GPCR bind diverse ligands, the cytoplasmic domains of the receptors are structurally similar. They cytoplasmic domains of GPCR activate the trimeric G-proteins α, β, and γ. When the ligand binds the GPCR, the α G-protein subunit hydrolyzes GDP to GTP. The hydrolysis of GDP to GTP activates the α, β, and γ subunits and allows them to move through the plasma membrane and activate proteins in

membrane. The activation of membrane proteins by the G-protein subunits leads to an increase in the second messenger cyclic AMP (cAMP), which activates many signaling pathways and can affect transcription as well as migration [193]. If the original ligand continues to be bound by the GPCR, then it will continue to hydrolyze GDP to GTP and remain active. They hydrolysis of GTP to GDP renders the GPCR signaling processes inactive. However, with prolonged stimulation, the GPCR will be phosphorylated by a GPCR kinase (GRK) and become desensitized. Phosphorylation by a GRK allows for arrestin to bind and the GPCR is endocytosed. After internalization, the GPCR can either be broken down in lysosomes or recycled to the plasma membrane [193].

3.1.2 Inhibition of GPCR signaling

Small molecules and toxins can interfere with GPCR receptor signaling agonistically or antagonistically. Cholera toxin from the bacterium *Vibrio cholera* is a hexameric protein that interferes with GPCRs. An α subunit of the toxin can breach the eukaryotic cell membrane and cause ADP ribosylation of GTP, which causes constitutive activation of the G-protein subunits and exponentially raises cAMP levels [193]. This deregulated signaling inhibits the chemotaxis of cells exposed to cholera toxin [194]. Another bacterial toxin, pertussis toxin from the bacterium *Bordatella pertussis* also blocks chemotaxis of exposed cells. Pertussis toxin can also penetrate the eukaryotic cell membrane and blocks the release of GDP from G-proteins, which forces the GPCR to remain in an inactivate state [195-197].

Pharmaceutical companies have recently focused on development of chemically synthesized analogs of GPCR ligands. It is estimated that drugs that use GPCR as targets

account for close to 50% of proposed drugs. Since GPCRs are active in essentially every organ the development of one drug that targets a GPCR can potentially be used to treat several disorders [198]. A complete understanding of how these receptors interact with small molecules, peptides, and proteins can assist in the development of these GPCR-targeted pharmaceuticals.

3.1.3 SDF-1α and its cognate receptor CXCR4

The chemokine SDF-1, also known as CXCL12, can be assembled in either of two forms, SDF-1α and SDF-1β, through alternate splicing of the same gene [199, 200]. Both forms are chemotactic, and most *in vitro* research refers to SDF-1α. *In vivo,* many cell types produce SDF-1 including stromal, endothelial, dendritic, epithelial, and macrophage cells [201-203]. SDF-1 signals selectively through the CXCR4 GPCR [204]. SDF-1α signaling through CXCR4 has been studied in the context of organ development, hematopoiesis, HIV infection, and immune cell movement. Developmental processes such B cell lymphopoesis, bone marrow colonization, organogenesis, vascularization and cardiac septum formation all require SDF-1 induced CXCR4 signaling [202, 205, 206]. After development, many tissues constitutively express SDF-1α and CXCR4 including the brain, heart, kidney, liver, lung and spleen [207]. The immune system relies on this signaling during infection and inflammatory disease states, which is evident through the expression of CXCR4 on lymphocytes and monocytes [208, Sanchez-Martin, 2011 #1206].

SDF-1α binds and activates CXCR4 through a two-step process. The receptor first interacts with amino acids 12 to 17 of SDF-1α, which causes a conformational change in the receptor. The conformational change allows the first 8 amino acids of the chemokine to interact with the CXCR4 binding pocket [126]. SDF-1 interaction with the CXCR4 binding pocket causes intracellular phosphorylation of the receptor by G protein coupled receptor kinase (GRK) on the first intracellular loop [209]. As the receptor desensitizes to the SDF-1α signal it becomes internalized [210]. Upon internalization the receptor can either be recycled back to the plasma membrane or degraded in lysosomes [211].

The transcription factors nuclear respirator factor-1 (NRF-1) and specificity protein 1 (SP-1) regulate CXCR4 transcription[212] and SP-1 [213]. Many factors contribute to an increase in transcription of CXCR4 including calcium [214, 215] cyclic AMP [216] and cytokines including IL-2 [217] IL-4 [218] and TGF-1β [219]. Inflammatory cytokines such as TNF-α [216] and interferon-γ and IL-1β decrease the expression of the receptor.

Much of the information known about CXCR4 and SDF-1α signals involves cell development and hematopoiesis. Mice deficient in CXCR4 exhibit serious defects in hematopoietic differentiation and die very soon after birth. CXCR4 deficiency in mice causes a severe reduction in B cell lymphopoiesis and myelopoiesis in fetal liver, and an absence of myelopoiesis in the bone marrow when compared to wild type mice[204]. In contrast, CXCR4 deficiency does not affect T cell lymphopoiesis [204].

Recently, research into CXCR4 and SDF-1α signaling has elucidated roles beyond development and hematopoiesis. CXCR4 plays roles in immune cell recruitment to the sites of infection, cancer, and HIV infection.

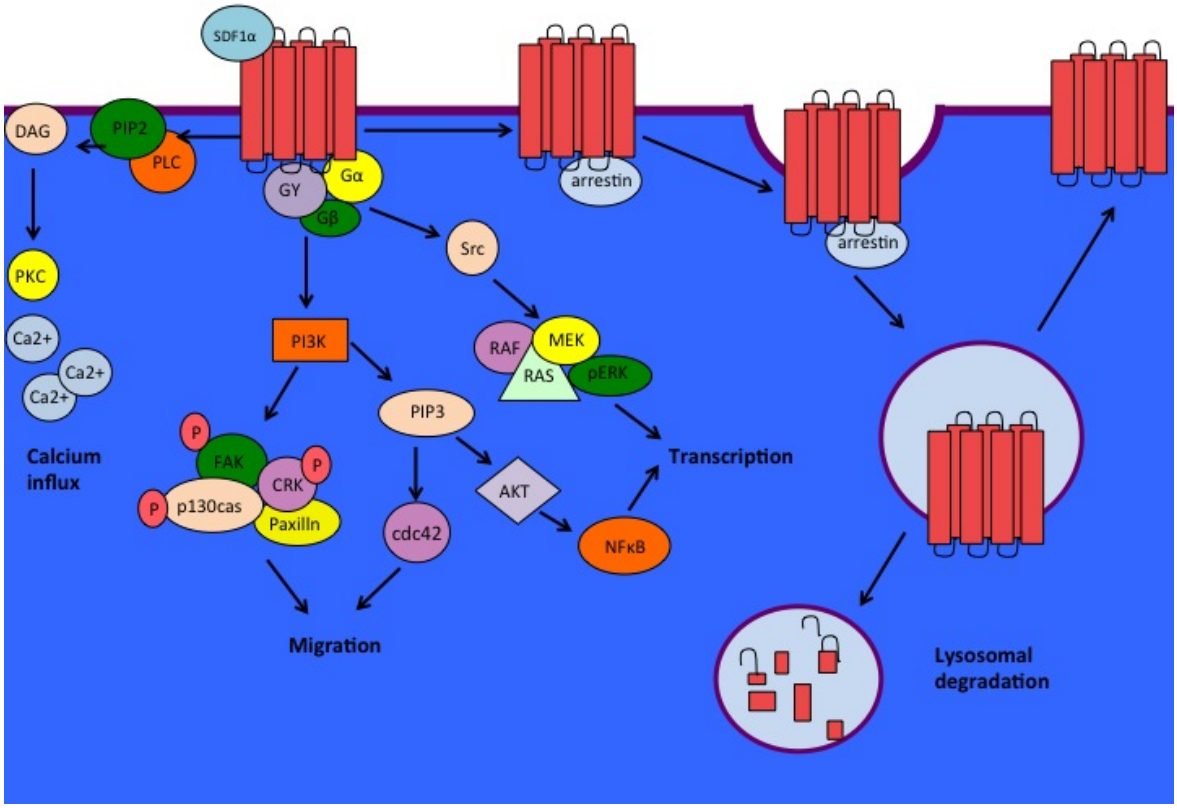

Figure 3.1: CXCR4 and SDF1α Signaling. SDF1α binds to CXCR4, a G-protein coupled receptor. This leads to signaling through various pathways, which leads to an influx in calcium to the cell, migration, transcriptional changes, the phosphorylation of ERK and internalization of CXCR4.

3.1.4 CXCR4 function on Neutrophils

Stromal cells in the bone marrow produce SDF-1α, which causes the retention of CXCR4 expressing neutrophils in the bone marrow. Reduction of SDF-1α-induced signal through CXCR4 causes neutrophils to traffic from the bone marrow to sites of infection [220, 221]. Neutrophils are often the first cell type to the site of infection, but are short lived. CXCR4 expression increases on mature neutrophils and directs these cells either become apoptotic or traffic back to the bone marrow [128]. There is evidence that mature neutrophils traffic back to the bone marrow in a CXCR-4 dependent manner, but there is not yet evidence for the clearance of neutrophils in the bone marrow [222]. Disruption of the CXCR4-regulated neutrophil movement causes neutrophils to migrate uncontrollably and as a consequence fail to arrive at the proper sites[223].

3.1.5 CXCR4 function on B and T lymphocyte

CXCR4 and CCR5 each function as a co-receptor for HIV-1 entry in to $CD4^+$ T cells. More recently, it was discovered that SDF-1α modifies T cell movement [224].

Mechanisms of T cell movement, as well as the physiological conditions necessary for T cells to migrate in response to SDF-lα, remain unclear. It is known that SDF-1α induced CXCR4-mediated chemotaxis in T cells, is enhanced by the presence of CD45 on the surface of T cells [225]. Additionally, SDF-1α induced migration of Jurkat T cells that lack ZAP-70 tyrosine kinase and the adaptor protein Slp-76 decreases when compared to wildtype Jurkat T cells [224]. Downstream from ZAP-70 lies the Tec Family kinase, ITK, [226]. ITK activates rapidly in the presence of SDF-1α, which also

activates Src Kinase and phosphatidylinositol activity (PI3K) [227]. ITK knockout T cells are less able to adhere, polymerize actin and migrate than wildtype a cell, which suggests ITK contributes to T cell migration in response to SDF-1α [227].

SDF-1α induced signaling is vital to pre-B cell proliferation. B cells of OVA immunized mice expressing OVA specific antibodies are responsive to SDF-1α for several days after they migrated from the spleen. This suggests CXCR4-SDF-1α signals regulate the migration of B cells from to the bone marrow and inflamed tissues [129].

3.1.6 Macrophages and CXCR4

Circulating monocytes experience autocrine and paracrine regulation through CXCR4 since these cells both secrete SDF-1 and express CXCR4[207]. These signals assist in the differentiation of monocytes into macrophages that express CD4, CD14 and CD163, as well as the differentiation of dendritic cells. However, dendritic cells that undergo CXCR4 assisted differentiation have a low ability to stimulate an antigen specific T lymphocytes response [207]. Microarray analysis suggests that SDF-1α causes the increase of vascular endothelial growth factor (VEGF) mRNA and the chemokine CCL1 mRNA in primary monocytes. Both of which are pro-angiogenic. SDF-1α also decreases expression of RUNX, a transcription factor responsible for CD4 and CD14 expression on macrophages. This decrease of CD4 and CD14 suppresses the phagocytic capacity of macrophages. Therefore, in macrophages SDF-1α is both immunosuppressive and pro-angiogenic [207].

3.1.7 The Role of CXCR4 in HIV

Functions of CXCR4 and CCR5 have both been studied as HIV-1 co-receptors for the entry of HIV-1 into $CD4^+$ T cells. HIV-1 cannot enter $CD4^+$ T cells without the expression of CCR5. CCR5 expression is vital to viral replication in the earlier stages of HIV-1 infection, CXCR4 has been reported to be essential to viral replication in later stages of infection [228]. Since the virus does not affect macrophages as profoundly as $CD4^+$ T cells, macrophages do act as viral reservoirs for HIV-1 and selectively uses CXCR4 to enter macrophages [229]. This process can be inhibited by the addition of SDF-1α[229].

3.1.8 CXCR4 Signaling in the Tumor Microenvironment

Tumor metastasis relies on the movement of tumor cells and stromal cells in the tumor microenvironment. CXCR4 plays a role in both single and multi cell directed migration in the metastasis of 11 different types of cancers and is known to be very abundant on the surface of many cancer cells [230, 231]. Cancer cells utilize CXCR4 mediated signaling for angiogenesis, invasion, chemotaxis, extravasation, and homing of cells to the tumor microenvironment [231]. Tumor-associate macrophages express high levels of SDF-1 and can recruit bone marrow derived endothelial cells that express CXCR4 to the tumor site [232]. These cells then differentiate into tumor associated vascular endothelial cells [230].

The widespread reliance of cells on CXCR4 for metastasis is exhibited in several different mouse model. Transfection of B16 melanoma cell line with CXCR4 and

subsequent intravenous injection (i.v) into C57BL6 mice causes the formation of pulmonary tumors. Mice infected with CXCR4 expressing B16 mouse melanoma cells accumulated 10 times the number of B16 cells in the lung, compared to $CXCR^-$ B16 cells [233]. This phenotype could be completely blocked with the addition of the CXCR4 antagonist, T22 [233]. Similarly, treatment with a CXCR4 antagonist has been shown to reduce metastasis and primary tumor growth in mouse models of breast cancer [234]. CXCR4 expression also increases SDF-1α-induced adhesion to a fibronectin substrate in the highly invasive BLM melanoma cell line, which increases migration and invasion of these cells [235].

3.1.9 CXCR4 in Lung injury

P. aeruginosa often colonizes the lungs of cystic fibrosis (CF) patients and patients on ventilators. In homeostatic conditions resident progenitor epithelial cells constantly replace epithelial cells of the lung. The colonization of *P. aeruginosa* causes significant injury to the airway epithelial cells and the resident progenitor epithelial cells are no longer able keep pace with the need for replacement of damaged cells. Circulating progenitor epithelial cells must be recruited to the site of injury to combat the infection. This recruitment of epithelial cells relies heavily on CXCR4 interaction with SDF-1α. Interference with this process can slow or abrogate healing. The addition of anti-SDF-1α antibodies blocks SDF-1α mediated signaling through the CXCR4 receptor, and prevents circulating progenitor epithelial cells from reaching the site of injury. [236].

3.1.10 Hypothesis: PmtA will modify Jurkat T cell Chemotaxis

Eukaryotic MT induces chemotaxis of leukocytes through GPCR signaling [130]. The MT produced by *P. aeruginosa,* PmtA, shares structural similarities with the eukaryotic MT and chemokines. The structural similarities between mammalian MT and PmtA provide the basis for the hypothesis that PmtA can affect the chemotaxis of immune cells. Mammalian MT and PmtA are both small proteins. Mammalian MT's are 60 to 68 amino acids in length, while PmtA from *Pseudomonas* species vary in 56 to 79 amino acids in length [1, 43, 44]. The *P. aeruginosa* PmtA, from strain PAO1 contains 79 amino acids. Despite the longer sequence of PmtA, it has only half the number of cysteine residues of mammalian MT, and binds approximately half the amount of zinc [188] (Table 3-1). Unlike mammalian MT, PmtA contains histidine residues. In the *Synechococcus elongatus* PCC7942 SmtA these histidine residues are vital to the metal binding capacity of the protein. Site-directed mutagenesis of the histidine residues decreases the number of zinc molecules bound by PmtA [237].

An analysis of the primary amino acid sequence of PmtA and MT reveals that both contain CXC motifs at the N-termini (Figure 3-1). In chemokines, the N-terminus cysteine motif categorizes the chemokines into the C, CC, CXC, or CX_3C chemokine families. This similarity between MT and PmtA could suggest that PmtA may also have a chemotactic function. Despite the similarities in metal binding capacity, cysteine content, and cysteine motifs, a BLAST comparison between *P. aeruginosa* PAO1 and mammalian MT-1 from humans does not suggest sequence homology (e=6).

The observation that *P. aeruginosa* PmtA displays similarities with both MT and chemokines leads to the hypothesis that PmtA influences cellular chemotaxis. If PmtA

affects immune cell chemotaxis it could disrupt the host response to the infection, and thus act as a virulence factor for the bacterium. If PmtA acts as a chemoattractant, it could disrupt the signals necessary for immune cells traffic to the site of infection. PmtA may also block chemotaxis of immune cells toward chemoattractants by acting directly or indirectly on the receptor.

Jurkat T cells were chosen to address PmtA's effects on CXCR4 mediated migration because of eukaryotic MT's previously established ability to stimulate chemotaxis of Jurkat T cells, and since these cells display a robust chemotactic response to SDF-1α *in vitro* [130, 224]. Jurkat T cells also lack toll-like receptor 4 (TLR-4), which responds to LPS from bacterial cells [238]. Thus the Jurkat T cell model should not be sensitive to any contaminating endotoxin co-purifying with GST-PmtA. Lung infections, like those caused by *P. aeruginosa*, rely on CXCR4 signaling on many cell types to combat the infection and repair damage to epithelial cells. Therefore, the Jurkat T cell model is an appropriate model to determine of PmtA influences CXCR4-mediated immune cell chemotaxis.

	PmtA (*Pseudomonas* species)	**SmtA (*Synechococcus* Species**	**Mammalian MT**
# of Amino Acids	56-79	55-56	60-68
# of Cysteine Residues	8-10	8-10	18-23
# of Bound Zinc	3-4	3-4	7-8

Table 3.1: Comparison of PmtA from *Pseudomonas* species and Mammalian Metallothionein. Mammalian MT contains nearly twice as many cysteine residues as PmtA's, which allows it to bind twice as many bound zinc molecules [188].

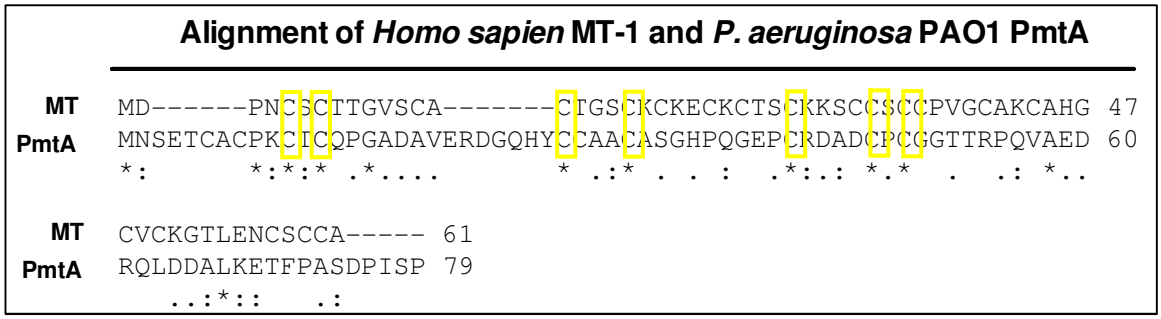

Figure 3.1: Alignment of *P. aeruginosa* PmtA and *Homo Sapien* Metallothionein I.

The MT from *P. aeruginosa* PAO1 contains 79 amino acids, in 10 of which are cysteine residues. This makes it the largest MT from *Pseudomonas* species with the highest number of cysteine residues. Unlike mammalian MT, PAO1 MT contains histidine (H) residues that are necessary for metal binding. Similarly, the first cysteine motif, the motif used to classify chemokines, of both MT's is a CXC motif. A BLAST comparison of both human MTI and PAO1 PmtA reveals there is little homology between the sequences (e=6), but the alignment reveals many of the fully conserved regions (*) are cysteine residues. A (:) indicates conservation of amino acids with strongly similar properties, while (.) indicates conservation of amino acids with weakly similar properties [239-242]. The yellow boxes indicate the conserved cysteine residues in both MT-1 and PmtA.

3.2 Results

3.2.1 Structural Prediction of *P. aeruginosa* PmtA

The structure of *P. aeruginosa* PmtA has yet to be defined by x-ray crystallography. However, the NMR structure of *S. elongates* PC7942 SmtA has been identified, and the structure is available on the NCBI MMDB database [237]. With this information, the structure of *P. aeruginosa* PmtA could be threaded through the *S. elongates* SmtA structure using the I-tasser Protein prediction software. The amino acid sequence of *S. elongates* SmtA is smaller than the *P. aeruginosa* PmtA, at 56 amino acids, but still contains 8 cysteine residues in that short sequence (Figure 3-2 A).

When the 79 amino acid *P. aeruginosa* structure is threaded through the *S. elongates* SmtA (Figure 3-2, B), it is evident that the *P. aeruginosa* PmtA contains a much longer "tail" at the C terminus of the protein (Figure 3-2, C). This is expected based on the primary amino acid sequences of the two proteins. An interesting aspect to this prediction is that the *P. aeruginosa* PmtA seems to form a helical region *S. elongates* PmtA lacks (Figure 3-2, D).

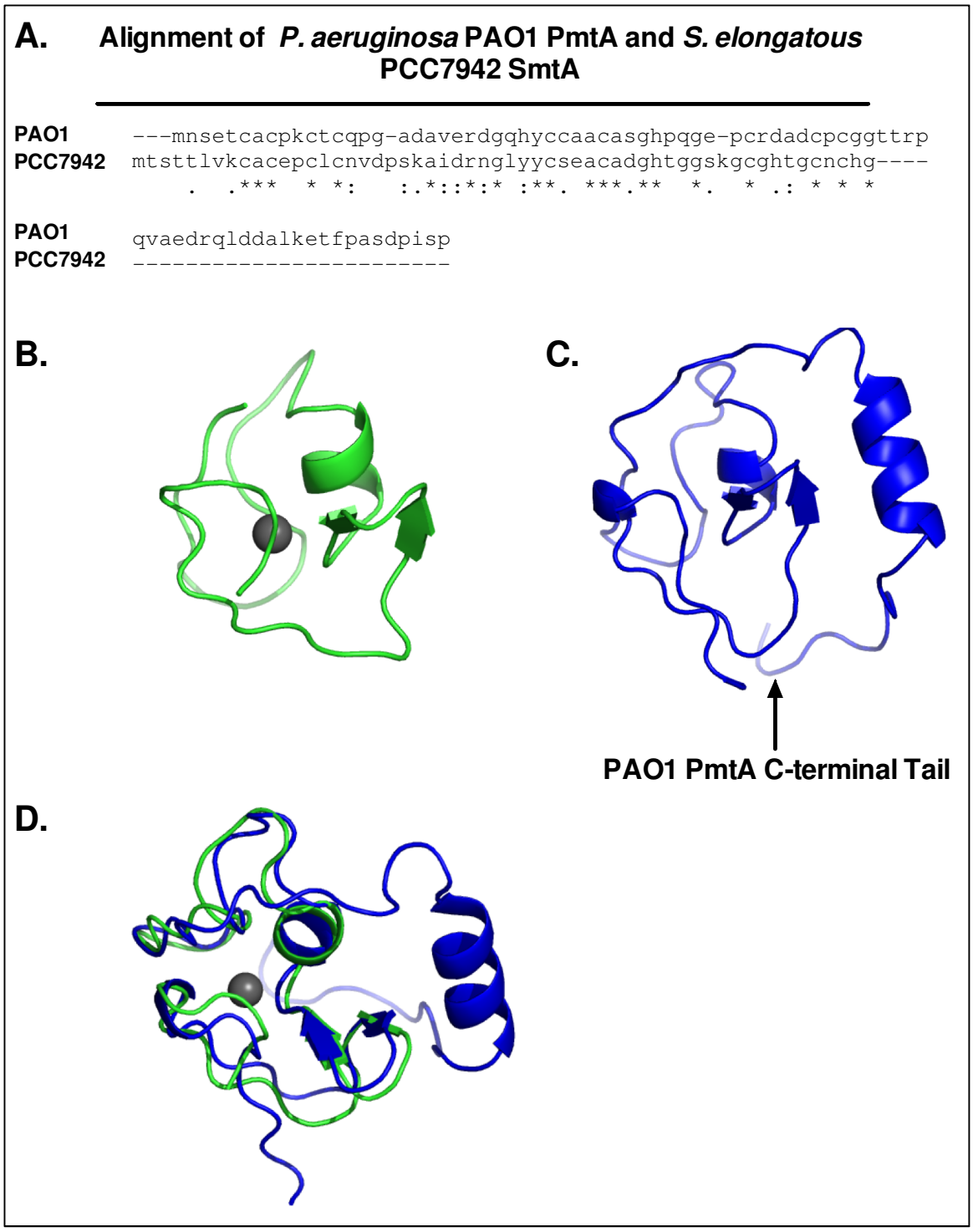
A.
Alignment of P. aeruginosa PAO1 PmtA and S. elongatous PCC7942 SmtA
PAO1 ---mnsetcacpkctcqpg-adaverdgqhyccaacasghpqge-pcrdadcpcggttrp
PCC7942 mtsttlvkcacepclcnvdpskaidrnglyycseacadghtggskgcghtgcnchg----
. .*** * *: :.*::*:* :**. ***.** *. * .: * * *
PAO1 qvaedrqlddalketfpasdpisp
PCC7942 -------------------------
B.
C.
PAO1 PmtA C-terminal Tail
D.

Figure 3.2

Figure 3.2: The Prediction of the *P. aeruginosa* PmtA structure from the *S. elongatus* SmtA Structure. An alignment of *P. aeruginosa* PmtA and *S. elongatus* SmtA reveals the two sequences contain very similar sequences, including conservation of the cysteine residues (A). Fully conserved residues are denoted with an (*). Strongly conserved residues are denoted with (:), and weakly conserved residues are denoted with (.). A BLAST comparison of the two PmtA sequences yields an e value of $e=2x10^{8}$, which indicates a high level of similarity[239-242]. The protein structure of *P. aeruginosa* PmtA has not been defined. The structure of *P.* aeruginosa PAO1 PmtA (C) was predicted with protein threading, and the I-tasser protein prediction software. The sequence of PA01 PmtA was compared to the known sequence and structure of *S. elongatus* SmtA (B) (D.) The superposition of the proteins revealed PmtA PA01 had a helical region not present in SmtA of *S. elongates*.

3.2.2 The effect of *P. aeruginosa* PmtA on Jurkat T cell Chemotaxis

PmtA was expressed in *Escherichia coli* with a GST tag to facilitate purification with GSH-binding resin. Therefore, all experiments using purified PmtA were compared to a GST control. The concentrations of PmtA used in these experiments were chosen based on the concentrations of MT previously shown to produce a chemotactic response in Jurkat T cells [130].

Jurkat T cells were exposed to SDF-1α, a member of the CXC family of chemokines, as a positive control, as well as PmtA and GST. The Jurkat T cells were first exposed to these chemoattractants in the ECIS/Taxis system. In this system, agarose fills a chamber of an ECIS/Taxis electrode, and two wells are cut in the agarose. The cell well contains Jurkat T cells, while the opposite chemoattractant well contains SDF-1α, PmtA or GST. A target electrode that records the resistance at that electrode, separates the two wells. As cells migrate from the cell well towards the chemoattractant, which forms a gradient through the agarose, the resistance at the target electrode increases. This indicates the migration of cells toward chemoattractant [135, 137-140]. In this assay, only Jurkat T cells exposed to SDF-1α migrated across the electrode (Figure 3-4 A). The Boyden Chamber assay was also used to measure chemotaxis of Jurkat T cells. In this assay cells are separated from chemoattractants by a polycarbonate membrane with 5μm pores. Cells that crawl toward the chemoattractant stick to the underside of the membrane and are stained and counted. This assay reconfirmed that Jurkat T cells migrate only in the presence of SDF-1α, and do not chemotax to GST-PmtA or GST (Figure 3-4 B). Although PmtA fails to induce chemotaxis of Jurkat T cells, the similarity to other MTs and chemokines still suggested that PmtA could modify cellular

movement. Thus, we also evaluated PmtA's influence on chemotaxis by incubating Jurkat T cells with PmtA prior to exposure to SDF-1α. Jurkat T cells were incubated with PmtA or GST, and then exposed to SDF-1α in either the ECIS/Taxis system (Figure 3-5, A) or the Boyden chamber (Figure 3-5, B). In each of these assays Jurkat T cells pre-exposed to PmtA, but not GST, were found to lose the ability to migrate in the presence of SDF-1α. Viability of cells after incubation with GST-PmtA or GST was evaluated with trypan blue stain. Incubation with GST-PmtA or GST did not affect the viability of Jurkat T (Figure 3-6). Therefore, the inability to migrate in response to SDF-1α is not due to cell damage or death.

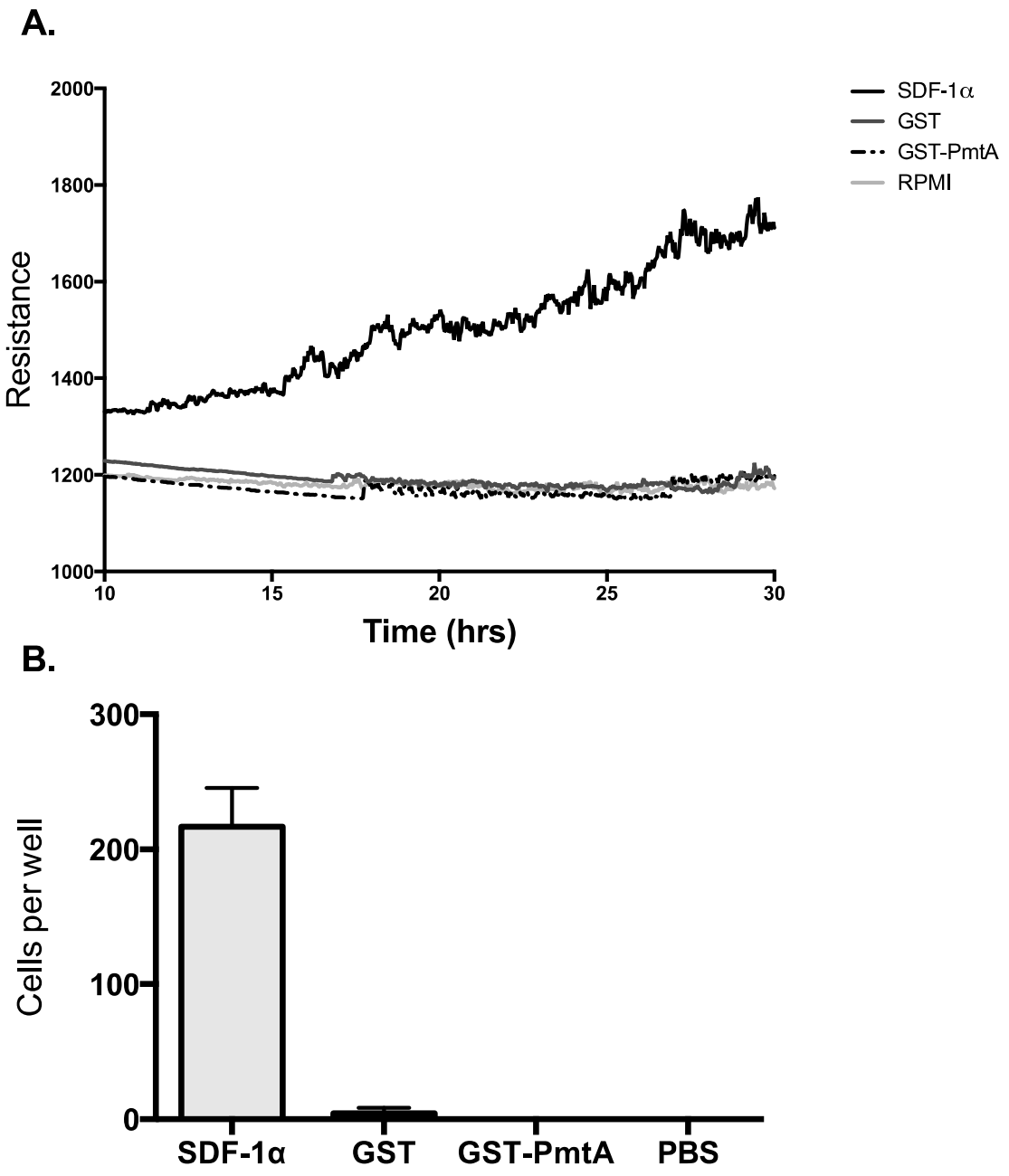
A.
2000
1800
1600
1400
1200
1000
Resistance
10
15
20
25
30
Time (hrs)
SDF-1α
GST
GST-PmtA
RPMI
B.
300
200
100
0
Cells per well
SDF-1α
GST
GST-PmtA
PBS

Figure 3.3

Figure 3.3: PmtA does not cause chemotaxis of Jurkat T cells *in vitro*. A.) Jurkat T cells ($2x10^6$ cell/ml) were exposed to a gradient formed from a well containing either SDF-1α (25nM) GST (14μM) GST-PmtA (14μM) or RPMI in an ECIS/Taxis electrode. The change of resistance at 4000Hz was monitored over a 30 hour period. Jurkat T cells did not migrate in response to either GST or GST-PmtA, but the SDF-1α elicited a robust response. This is a result of triplicate chambers for each condition and is representative of 3 separate experiments. B.) Jurkat T cells ($2x10^6$ cell/ml) were exposed to either SDF-1α (25nM) GST (14μM) GST-PmtA (14 μM) or PBS for 4hr at 37°C in a transwell chamber. Cells that traveled through the 5μm polycarbonate membrane were stained and counted on a microscope. Jurkat T cells did not migrate in response to GST or GST-PmtA, while a large number of cells migrated in response to SDF-1α. This data is a result of 3 replicates and representative of at three separate experiments. (KMP110113)

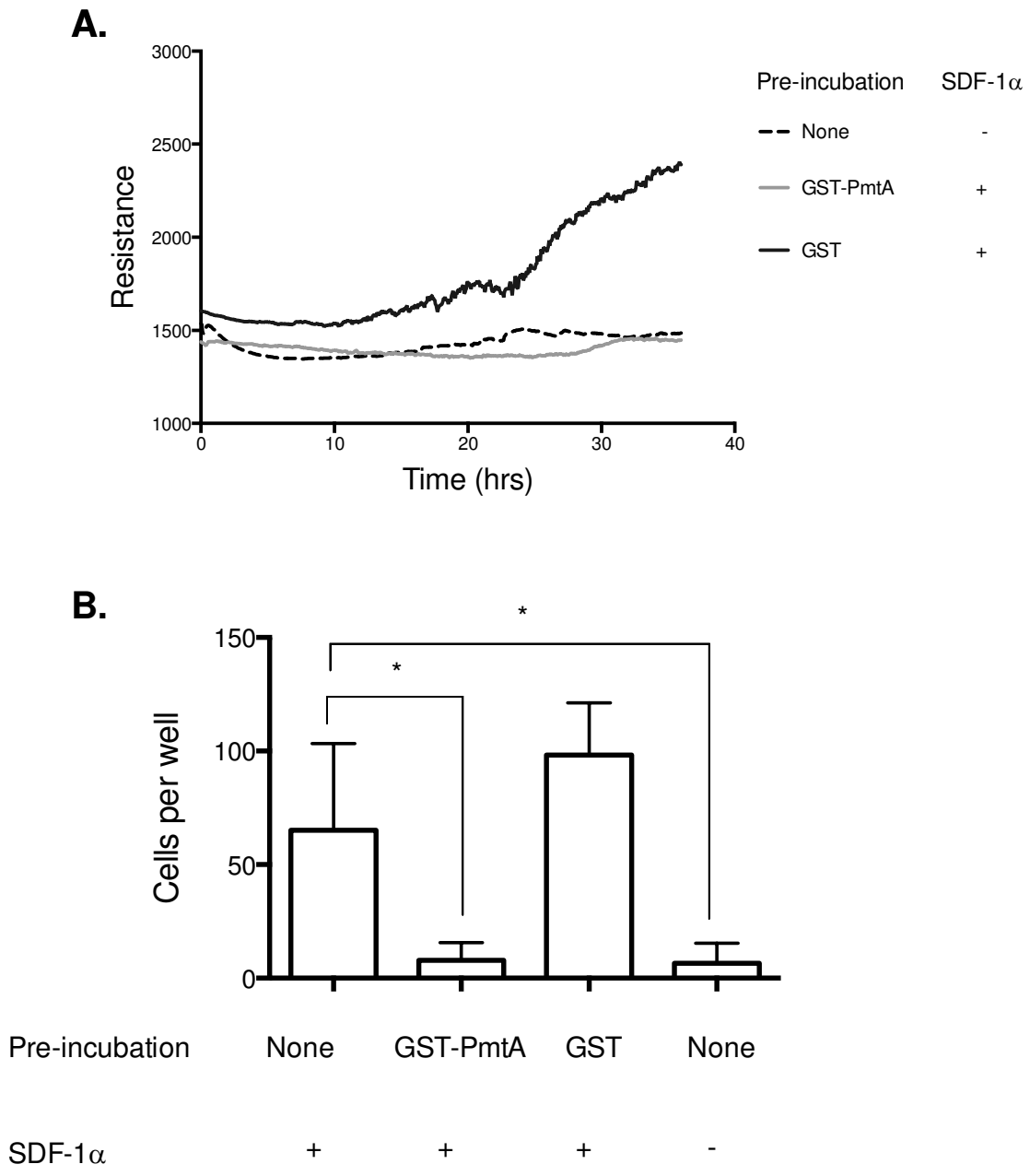

Figure 3.4

Figure 3.4: Jurkat T cells incubated with GST-PmtA lose the ability to respond to SDF-1α. Human Jurkat T cells (A. $2x10^6$ cell/ml B. $4x10^6$ cell/ml) were exposed to

GST-PmtA (14μM), GST (14μM) or RPMI media for 1 hour at 37°C and 5% CO_2. Cells were washed with fresh RPMI media. A.) The cells were exposed to 12.5nM SDF-1α in an ECIS/Taxis electrode at 37°C and 5% CO_2. The change of resistance at 4000Hz was measured over 35 hours. Jurkat T cells pre-exposed to GST-PmtA did not migrate in response to SDF-1α, while those exposed to GST migrated in response to the chemokine. Data is an average of three replicates and representative of 3 separate experiments. B.) Cells were exposed to 12.5nM SDF-1α or RPMI media in a transwell system for 4 hours at 37°C and 5% CO_2. Cells that traveled through the 5μm polycarbonate membrane were stained and counted on a microscope. Cells that were exposed to GST-PmtA prior to exposure to SDF-1α in the transwell system lost the ability to response to SDF-1α. Data is the average of 5 wells and representative of 3 experiments (*=$p<0.05$) . (KMP050112, KMP053112)

A.

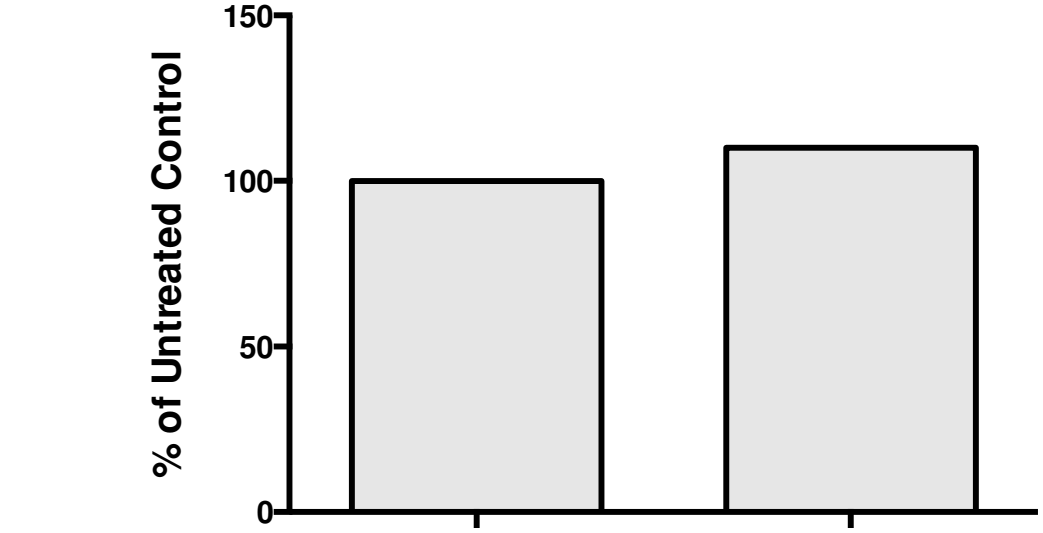

Pre-incubation	5.6μM GST	5.6μM GST-PmtA
SDF-1α	+	+

B.

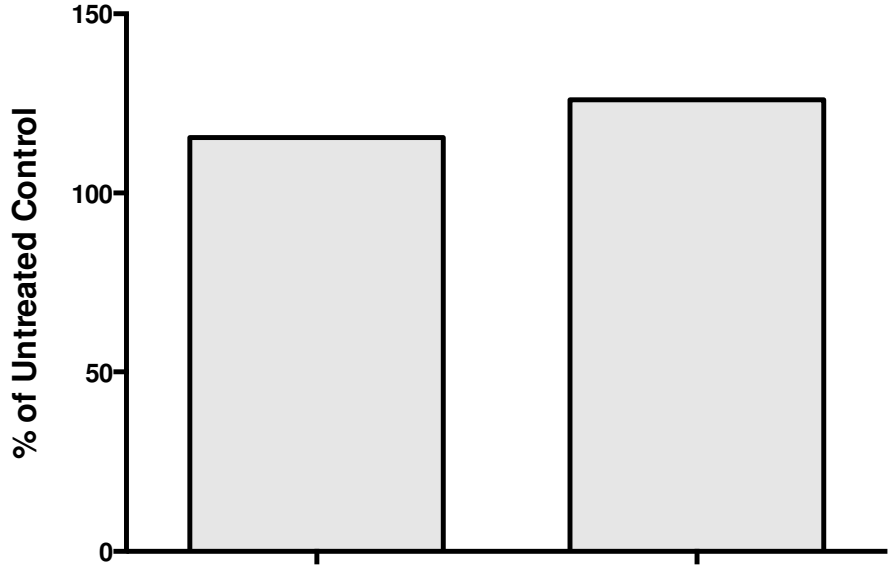

Incubation	5.6μM GST	5.6μM GST-PmtA

Figure 3.5

Figure 3.5: Incubation of Jurkat T cells with GST-PmtA and GST did not affect cell survival. Jurkat T cells ($1x10^5$ cells) were treated with 5.6μM GST or 5.6μM GST-PmtA and subsequently treated with 12.5nM SDF-1α (A). The survival of the Jurkat T cells was measured with trypan blue exclusion and compared to a control treated only with 12.5nM SDF-1α. Jurkat T cells ($1x10^5$ cells) were treated with 5.6μM GST or 5.6μM GST-PmtA for 1 hour, and were not exposed to SDF-1α (B). The survival of the Jurkat T cells was measured with trypan blue exclusion an compared to an untreated control. (KMP030414).

3.2.3 The effect of PmtA on Cell Surface Receptors

PmtA's ability to block the chemotaxis of Jurkat T cells to of SDF-1α may lie in its interaction with the CXCR4 receptor. When SDF-1α binds CXCR4 internalizes quickly and traffics back to the plasma membrane, or degrades in the lysosome. In uniform concentrations of SDF-1α, the CXCR4 receptor internalizes and promptly degrades [126]. Improper internalization of the receptor interferes with controlled migration of the cell. IF PmtA interferes with internalization or surface expression of CXCR4 it may lead to uncontrolled cellular migration. Therefore PmtA's ability to block the CXCR4 receptor was examined.

Jurkat T cells were incubated with PmtA or GST and labeled with anti-CXCR4 antibody and a secondary FITC conjugated antibody were examined by flow cytometry. To determine if PmtA had effects on other receptors or if effects were specific to CXCR4, surface expression of CD3 was examined in parallel with CXCR4. Neither PmtA nor GST interfere with the detection of CXCR4 or CD3 on the surface of Jurkat T cells (Figure 3.6). However, PmtA could interact with CXCR4 in a way that does not interfere with the epitope region of the primary antibody, but does interfere with SDF-1α signal transduction.

To determine if PmtA blocks SDF-1α-mediate signal transduction, Jurkat T cells were pre-incubated with PmtA or GST and then directly exposed to SDF-1α, which causes the internalization of CXCR4. Cells incubated with GST or a vehicle control, and then SDF-1α, have a 40-50% decrease in surface fluorescent staining of CXCR4, while the surface fluorescence of cells incubated with GST-PmtA only decreases 20-25%

(Figure 3.7). This suggests that PmtA blocks the SDF-1α induced internalization of CXCR4. PmtA may modify CXCR4 surface expression, which can result in changes to the signaling cascade involved in chemotaxis. This was shown by both flow cytometery and fluorescence microscopy (Figure 3.7).

GST-PmtA and GST were incubated with Jurkat T cells at both 37°C (Figure 3.10) with 5% CO_2, and at 4°C (Figure3.11) to determine if GST and GST-PmtA interacted with cell surface receptors. A primary anti-GST tag antibody was used tag GST-PmtA and detected with a secondary antibody labeled with alexafluor647. It was determined that GST-PmtA could not be detected on the surface of the plasma membrane. From previous experiments GST-PmtA affects Jurkat T cells at concentrations ranging from 5.4μM to 14μM. Assuming that the interaction between GST-PmtA and CXCR4 has a K_d of $10^{-9\ M}$, which is typical of ligand-receptor interactions, the high concentration of GST-PmtA used would drive the koff rate to less than 10 seconds. Therefore it would be unlikely that the assay described here, that uses 5.4μM GST-PmtA, would be able to measure GST-PmtA on the surface of Jurkat T cells.

PmtA's ability to block the SDF-1α induced internalization of the CXCR4 receptor may cause downstream effects on the signal transduction cascade. SDF-1α is known to cause a very quick influx of calcium into the cell [126], which may be disturbed by the presence of PmtA. Attempts to measure this phenomena were confounded by the rapid dissipation of the calcium influx. The difference in the rate or amount of calcium influx between cells incubated with PmtA or GST could not be accurately assessed (data not shown).

SDF-1α is also known to cause the phosphorylation of MAP kinase ERK, which leads to transcriptional changes necessary for cells to migrate in the presences of SDF-1α [224]. Jurkat T cells were exposed to PmtA or GST, and subsequently exposed to SDF-1α. The phosphorylation of ERK was determined using flow cytometery. Neither incubation with GST or GST-PmtA affects the phosphorylation of ERK (Figure 3.12).

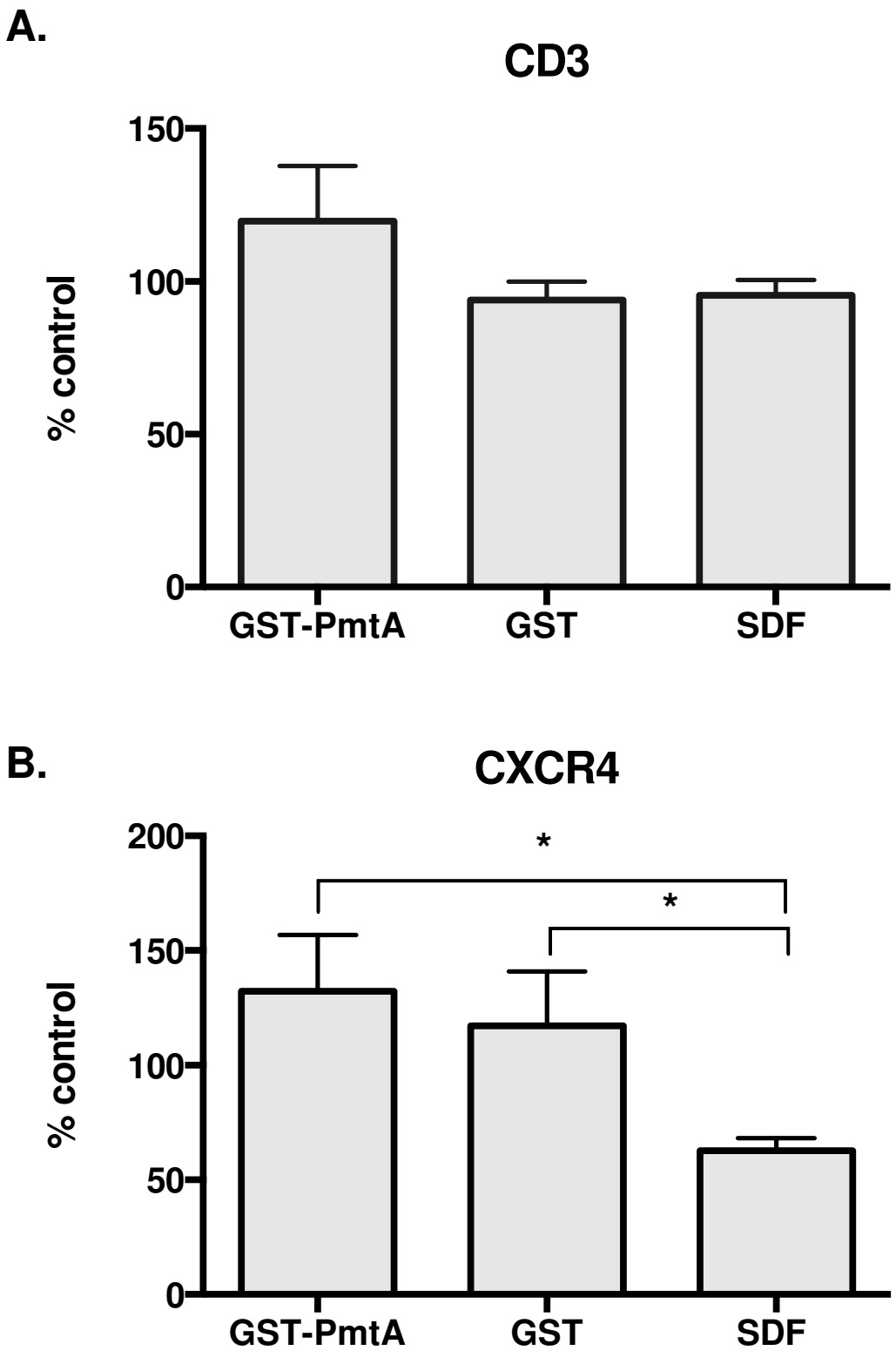
A.
CD3
150
100
50
0
% control
GST-PmtA
GST
SDF
B.
CXCR4
200
150
100
50
0
% control
*
*
GST-PmtA
GST
SDF

Figure 3.6

Figure 3.6: PmtA does not change expression of cell surface receptors CXCR4 and CD3. Jurkat T cells ($1x10^5$ cells) were treated with 5.6μM GST, 5.6μM GST-PmtA, or 0.75nM SDF-1α, and the surface expression of CXCR4 (A) and CD3 (B) was measured with flow cytometry. GST-PmtA did not affect expression of either surface receptor. Data presented as percent of an untreated control.

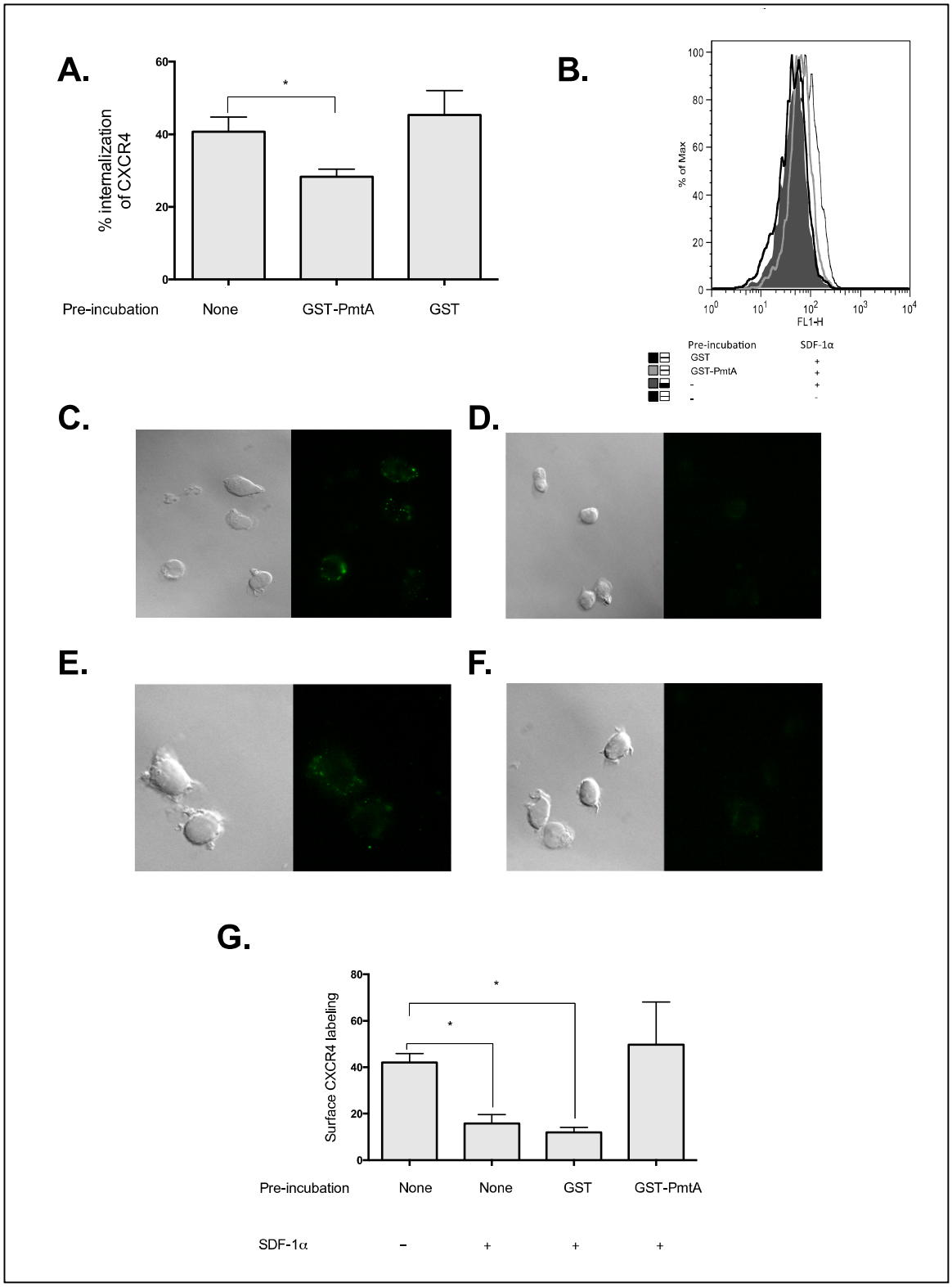
A.
% internalization of CXCR4
60
40
20
0
*
Pre-incubation
None
GST-PmtA
GST
B.
% of Max
100
80
60
40
20
0
10^0
10^1
10^2
10^3
10^4
FL1-H
Pre-incubation
SDF-1α
GST
+
GST-PmtA
+
-
+
-
-
C.
D.
E.
F.
G.
Surface CXCR4 labeling
80
60
40
20
0
*
*
Pre-incubation
None
None
GST
GST-PmtA
SDF-1α
–
+
+
+

Figure 3.7

Figure 3.7: PmtA Blocks SDF-1α induced internalization of CXCR4. A.) Jurkat T cells ($1x10^5$cells) were treated with 5.6μM GST, 5.6μM GST-PmtA for 50 minutes at 37°C and 5% CO_2 and then exposed to 0.75nM SDF-1α and the surface expression of CXCR4 was measured via flow cytometry. A.) Data was normalized to the amount of CXCR4 expression in Jurkat T cells that were not exposed to SDF-1α. Data is represented at mean of 3 independent experiments +/- SEM (*=$p<0.05$ one-tailed Student's T test). B.) Representative histogram from a single experiment. Jurkat T cells ($1x10^5$cells) were either left untreated (C and D), treated with 5.6μM GST-PmtA (E) or 5.6μM GST (F) for 50 minutes at 37°C and 5% CO_2. Cell shown in panels B-D were then exposed to 0.75nM SDF-1α and the surface expression of CXCR4 was visualized by fluorescent microscopy. G. Quantification of fluorescence from 3 separate images of each condition, and at least 5 replicates. (=$p<0.05$ two-tailed student's T test).

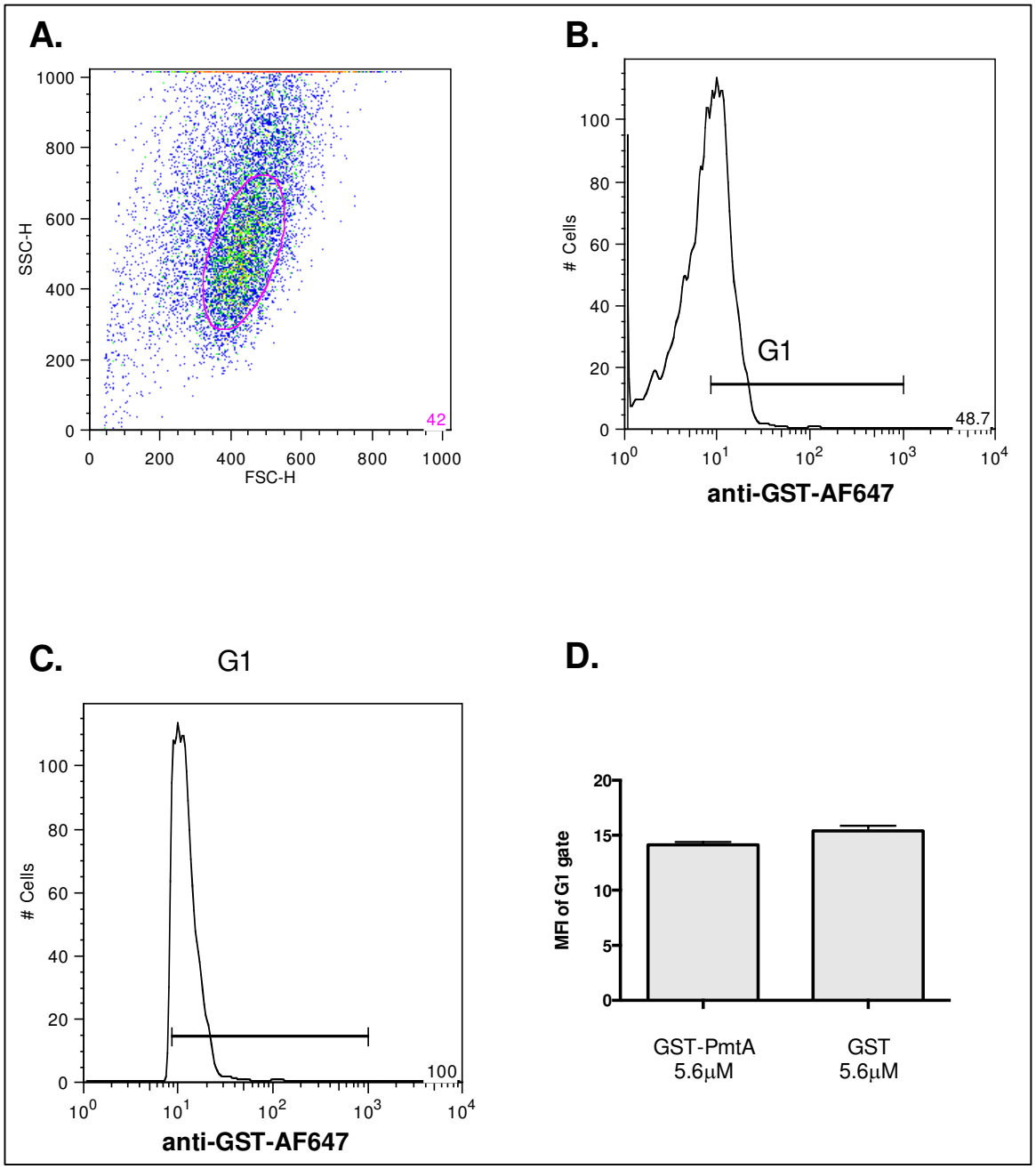
A.
SSC-H
FSC-H
42
B.
Cells
G1
48.7
anti-GST-AF647
C.
G1
Cells
100
anti-GST-AF647
D.
MFI of G1 gate
GST-PmtA
5.6µM
GST
5.6µM

Figure 3.8

Figure 3.8: PmtA was not found on the surface of Jurkat T cells incubated at 37°C. Jurkat T cells ($1x10^5$cells) were incubated with 5.6μM GST-PmtA or 5.6μM GST for 1 hour at 37°C. The cells were washed and probed with a primary anti-GST tag antibody, and a secondary anti-IgG antibody coupled to alexafluor647 (AF-647). Surface fluorescence was measured via flow cytometery (10,000 events). Cells were gated on forward and side scatter (A), and the fluorescence (FL4) of this gated population was analyzed (B). The geometric mean of fluorescence intensity of FL4H+ gate (C) was analyzed in with a students T test. Neither GST nor GST-PmtA were present on the surface of the Jurkat T cells. A-C were results of the negative untreated control. (KMP030314)

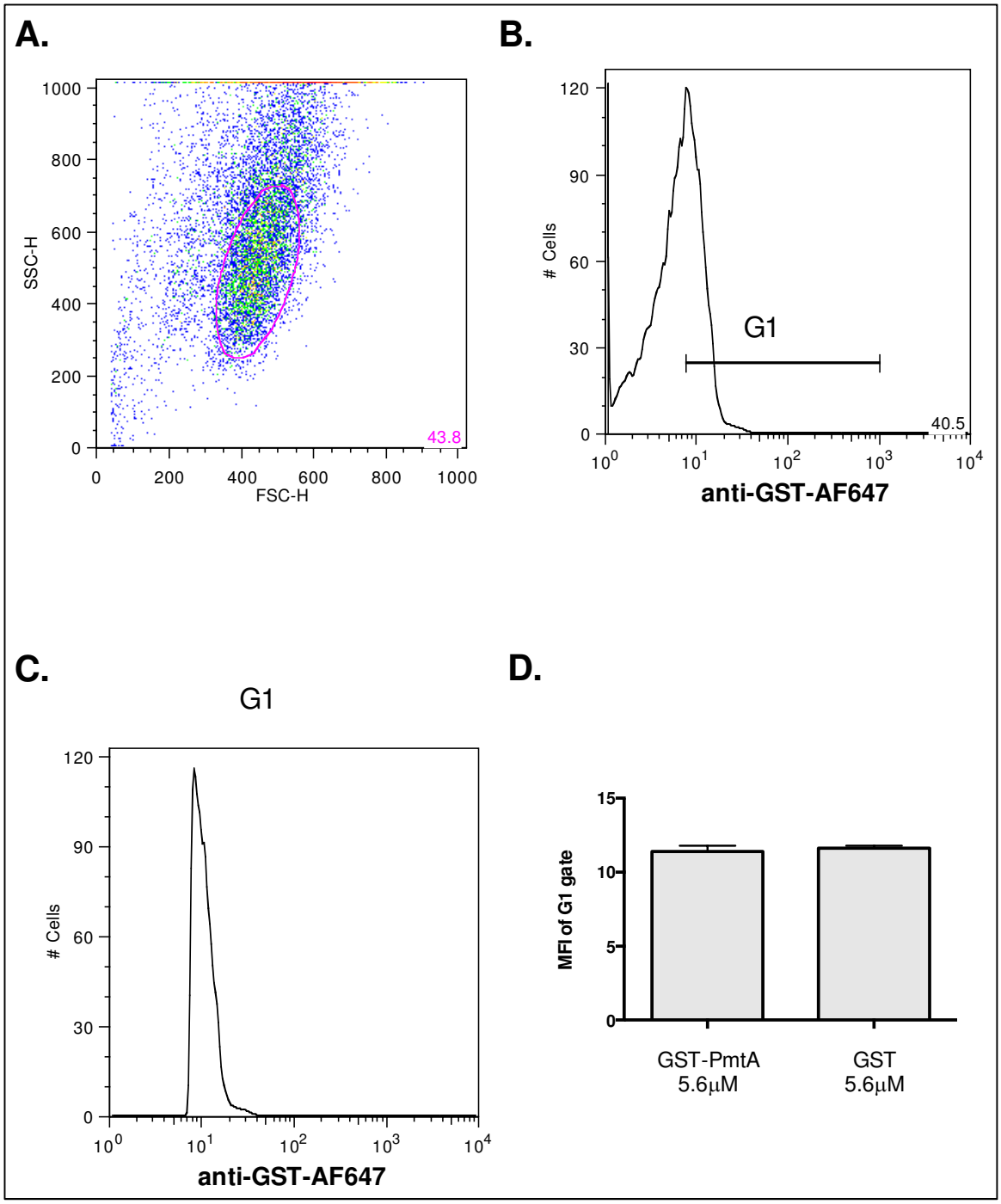
A.
SSC-H
FSC-H
43.8
B.
Cells
G1
40.5
anti-GST-AF647
C.
G1
Cells
anti-GST-AF647
D.
MFI of G1 gate
GST-PmtA
5.6µM
GST
5.6µM

Figure 3.9

Figure 3.9: PmtA was not found on the surface of Jurkat T cells incubated at 4°C. Jurkat T cells ($1x10^5$cells) were incubated with 5.6μM GST-PmtA or 5.6μM GST for 1 hour at 4°C. The cells were washed and probed with a primary anti-GST tag antibody, and a secondary anti-IgG antibody coupled to alexafluor647(AF-647). Surface fluorescence was measured via flow cytometery (10,000 events). Cells were gated on forward and side scatter (A), and the fluorescence (FL4) of this population was analyzed (B). The geometric mean of fluorescence intensity of G1 gate (C) was analyzed in with a students T test. Neither GST nor GST-PmtA were present on the surface of the Jurkat T cells. A-C were results of the negative untreated control. (KMP030514)

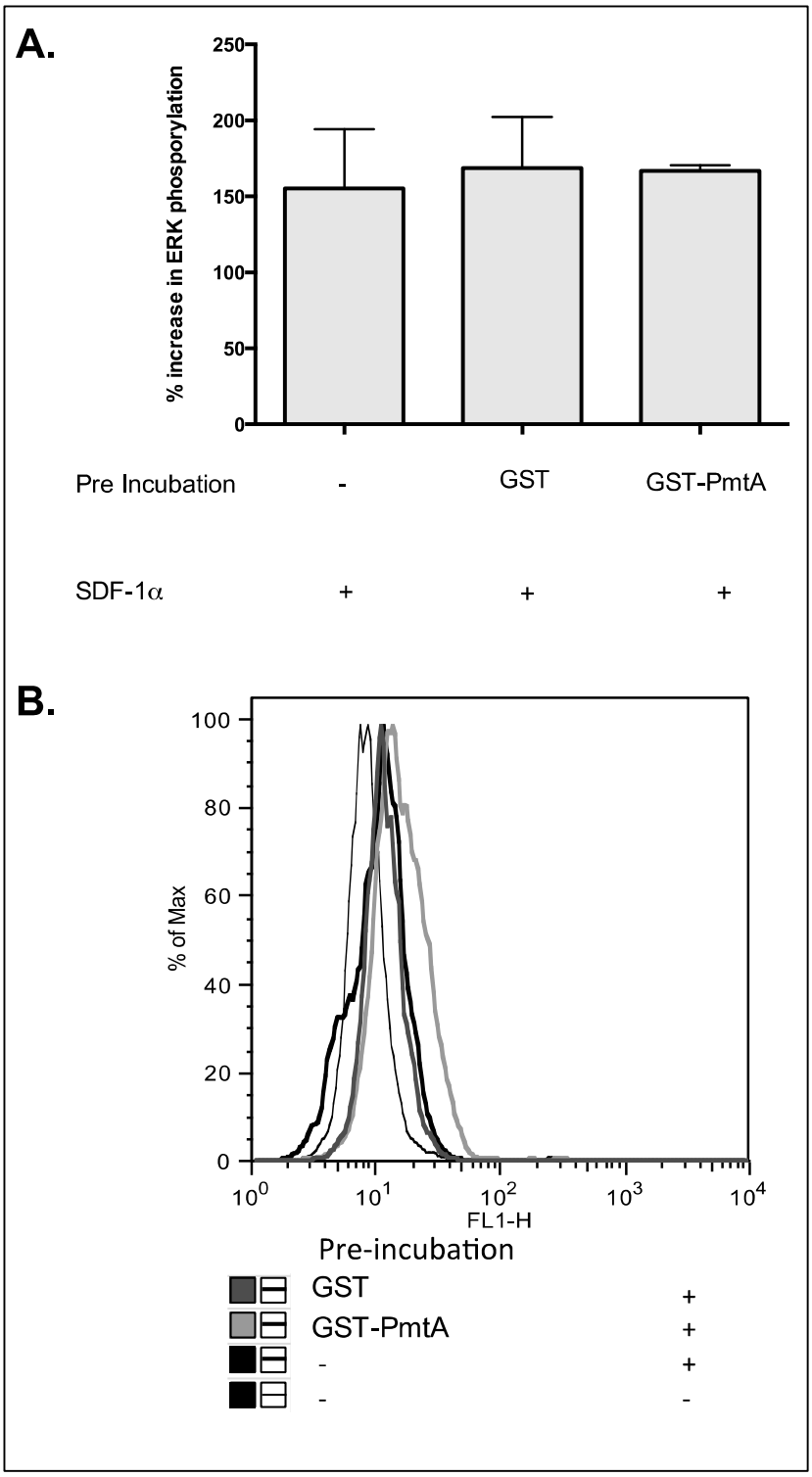
A.
% increase in ERK phosporylation
250
200
150
100
50
0
Pre Incubation
-
GST
GST-PmtA
SDF-1α
+
+
+
B.
% of Max
100
80
60
40
20
0
10^0
10^1
10^2
10^3
10^4
FL1-H
Pre-incubation
GST
+
GST-PmtA
+
-
+
-
-

Figure 3.10

Figure 3.10: PmtA does not affect the phosphorylation of ERK. Jurkat T cells ($1x10^5$ cells) were treated with 5.6μM GST, 5.6 μM GST-PmtA or left untreated for 50 min. The cells were then washed and stimulated with 25nM SDF-1α for 15min. Cells were subsequently fixed and permeablized. Phosphorylation of p42/44 ERK was measured with flow cytometery. Neither the GST or GST-PmtA treatments changed the levels of ERK phosphorylation. A) Data is shown as the percent increase in ERK phosphorylation compared to a control population that was not stimulated with SDF-1α and is the mean +/-SD of 3 separate experiments. B.) A histogram from a single experiment, representative of 3 separate experiments.

3.3 Discussion

This study suggests the immunomodulatory capacity of MT includes effects by both eukaryotic MT and bacterial MTs. Conventionally, MTs are classified as stress response proteins that expressed in response to high concentrations of essential and heavy metals. The ability of PmtA to disrupt mammalian cell movement suggests the study of bacterial MTs should encompass more than the ability to bind metals, similar to their eukaryotic counterparts.

Bacterial MT should be studied not only in the context of their immunomodulatory functions, but also as potential virulence factors for pathogens that express these proteins. PmtA's impact on mammalian cell movement may be advantageous to *P. aeruginosa* in infection. The pathogen *P. aeruginosa* causes many nosocomial infections by colonizing burn victims, patients on ventilators, and patients with catheters. *P. aeruginosa* lung infection often results in the death of people with the genetic disorder cystic fibrosis (CF). In CF patients, *P. aeruginosa* causes repeated acute infections, until it finally establishes a chronic lung infection that causes damage to lung epithelial cells [243]. In acute infections, resident progenitor epithelial cells constantly replace injured epithelial cells, but in chronic infections, resident progenitor cells cannot keep up with the rate of damage to these cells. In this case, replacement of epithelial cells depends on the migration of circulating progenitor epithelial cells to the site of damage, through CXCR4/SDF1-α signaling [236]. The disruption of CXCR4/SDF1-α signal transduction could weaken the immune response to the pathogen, and the repair

mechanisms critical to lung structural integrity. This could lead to a decrease in epithelial continuity and extensive damage to the lung.

In order for PmtA to disrupt the T cell migration during a lung infection there must be damage to the lung epithelium. PmtA, which could be either secreted from bacterial cells, or released as a result of damage to bacterial cells during infection, would have to breach the epithelial barrier to reach T cells located in the lamina propria. *P. aeruginosa* can attach to epithelial cells and destabilize the tight junctions, which would provide an exit for PmtA [166]. However it is more likely that PmtA can \ disrupt the migration of cells that are already in the lung, rather than be released from the lung and disrupt migration. A T cell mediated response to *P. aeruginosa* infection is necessary for the management of chronic infections [183]. Once T cells reach the site of infection, PmtA could disrupt the migration of the T cells and the ability of the immune response to combat infections. PMNs are another cell type that is very important for the clearance of *P. aeruginosa*. PMNs must be successfully trafficked into the lung in order to aid in the clearance of an infection. Future experiments should focus on the ability of PmtA to disrupt the migration of these cell types, as this could further dampen the immune response to *P. aeruginosa.*

The decrease of SDF-1α-induced internalization of CXCR4 after incubation of PmtA indicates that the protein interferes with the Jurkat T cell's desensitization to the SDF-1α signal. PmtA's interference with the CXCR4 internalization process indicates that the protein can alter migration patterns of immune cells by altering signal transduction at the receptor. As indicated by trypan blue exclusion studies, the presence of PmtA or GST does not change the survival of the Jurkat T cells. Additionally,

microscopic studies (data not shown) indicate that the morphology of the cells do not change with the addition of PmtA or GST.

The absence of PmtA on the surface of the cell at both 37°C and 4°C suggests that PmtA does not bind the receptor with high infinity. As previously discussed, the millimolar concentrations of GST-PmtA used would push the ligand-receptor interaction rate to less than 10 seconds, which would not be measureable. A better way to measure PmtA's ability to bind CXCR4 would be a competition-binding assay with SDF-1α. In this assay GST-PmtA would compete with SDF-1α for CXCR4 using either purified CXCR4 or whole Jurkat T cells both immobilized on a column. A known concentration of SDF-1α would be added to the immobilized receptor or cell and varying concentrations of GST-PmtA would be subsequently added. The column would then be washed and the elute collected. The concentration of SDF-1α in each elute could then be measured by ELISA. This would determine what concentration of GST-PmtA, if any, could displace SDF-1α from the receptor.

It is possible that PmtA would not be found on the surface of Jurkat T cells, and does not bind the CXCR4 receptor. PmtA could be internalized by the cell and affect the cell's ability to transduce intracellular signals. If the cell internalizes PmtA the thiol group present on the numerous cysteine residues of PmtA can oxidize and alter intracellular redox environment and, in turn, modify redox sensitive signaling. T cell migration depends on the uptake of H_2O_2. Activation of the Rho family GPTase Cdc42 requires the transport of H_2O_2 [244]. Mice that lack the ability to mediate the transport of H_2O_2 are deficient in trafficking of antigen primed T cells in response to SDF-1α [244].

The numerous thiol residues on PmtA could change the transport of ROS and impair the movement of Jurkat T cells.

Other cells, such as prostate cancer cells also rely on ROS to transmit intracellular signals after the binding of SDF-1α to the CXCR4 receptor. *In vitro* experiments with prostate cancer cells reveal that an increase in ROS results in an increase in migration. Additionally, the binding of SDF-1α to CXCR4 promotes intracellular ROS accumulation [245]. The addition of the antioxidant N-acetyl-cysteine (NAC) decreases the ability of prostrate cancer cells to migrate in response to SDF-1α *in vitro*. The main NADPH oxidase involved in the production of ROS upon SDF-1α binding to CXCR4 is NOX2. If NOX2 is blocked, cells do not migrate in response to SDF-1α [246]. This indicates that intracellular ROS produced upon the binding of SDF-1α to CXCR4 is necessary for cell migration. The cysteine residues present on PmtA suggest that it could work as an antioxidant. This may be a possible mechanism for the decrease in migration observed when cells are treated with GST-PmtA. The GST-PmtA could bind a receptor and become internalized, which could deplete the intracellular pool of ROS and decrease migration (Figure 3.11). This can be tested in the future by measuring the intracellular pool of ROS with the oxidant sensitive probe H_2DCFDA. Despite the ability of GST-PmtA to disrupt migration, it did not have an impact on ERK phosphorylation (Figure 3.10). This is consistent with the model that suggests PmtA works as an antioxidant since ERK phosphorylation in conjunction with SDF-1α binding to CXCR4 is and ROS independent process [247].

If PmtA is able to act as an antioxidant, it could have a global effect on ROS-reliant processes. For example, this study showed that the expression of CD3 on the surface of Jurkat T cells did not change with the addition of GST-PmtA. However, these studies did not address the effect of GST-PmtA on the activation of Jurkat T cells, which relies on ROS-mediated signals. In the future, GST-PmtA's ability to affect T cell activation should be studied.

Taken together, the results of this study suggest that *P. aeruginosa* PmtA could influence the course of an infection. Further study is needed to determine if the loss of migration due to the addition of PmtA is a global phenomena, or specific to CXCR4 signaling. The addition of PmtA may contribute to the redox sensitive signaling in immune cells. Overall these results suggest PmtA contributes to immune cell processes, which may make it a candidate for the development of a novel therapeutic intervention to *P. aeruginosa.*

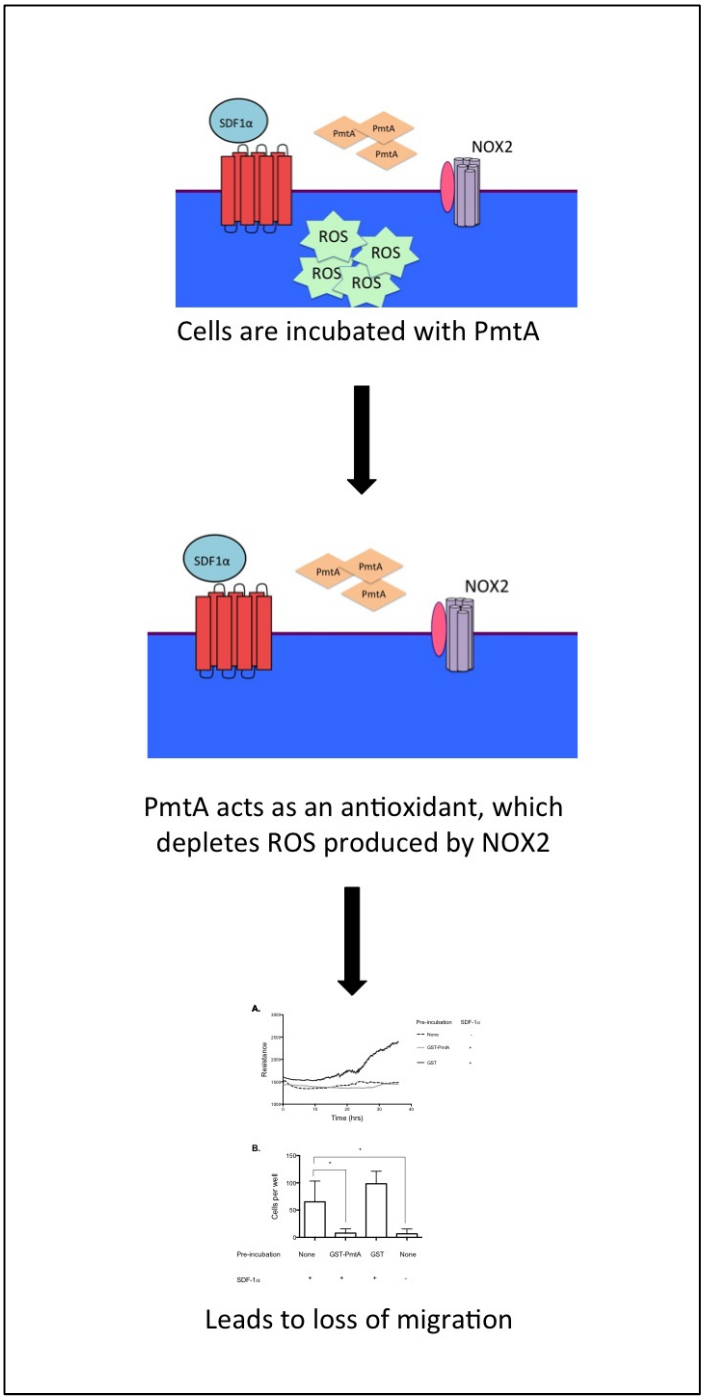
SDF1α
PmtA
PmtA
PmtA
NOX2
ROS
ROS
ROS
ROS
Cells are incubated with PmtA
SDF1α
PmtA
PmtA
PmtA
NOX2
PmtA acts as an antioxidant, which depletes ROS produced by NOX2
A.
Resistance
Time (hrs)
B.
Cells per well
Pre-incubation
None
GST-PmtA
GST
None
SDF-1α
Leads to loss of migration

Figure 3.11

Figure 3.11 Proposed model for PmtA induced inhibition of Jurkat T cell Chemotaxis. Based on information in previous studies, it can be proposed that PmtA is internalized by Jurkat T cells which allows it to deplete the pool of intracellular ROS produced upon the binding of SDF-1α to CXCR4. As seen in other studies, this would inhibit the migration of Jurkat T cells in response to SDF-1α.

CHAPTER 4: EXPRESSION OF PMTA INFLUENCES *P. aeruginosa* VIRULENCE

4.1 Introduction

Previous work presented in chapter 3 suggests that PmtA can modulate the immune system and thus the virulence of *P. aeruginosa*. *P. aeruginosa* expresses many known virulence factors, but the function of PmtA during *P. aeruginosa* infection has yet to be studied. If PmtA expression affects growth in the presence of stressors that are representative of the stressors present during infection it is reasonable to predict that PmtA may influence *P. aeruginosa* virulence *in vivo*. If PmtA is indeed a virulence factor, it could serve as a novel therapeutic target for an increasingly antibiotic-resistant human pathogen.

4.1.1 *P. aeruginosa*: An important infections agent

The opportunist pathogen, *P. aeruginosa* ranks among the top 5 organisms causing pulmonary, bloodstream, urinary tract, surgical site, and tissue infections [248]. The well-known nosocomial infection plagues patients on ventilators, those with catheters, or serious burns[249, 250]. This pathogen often colonizes the lungs of immunologically compromised people, such as those with cystic fibrosis (CF). For CF patients, *P. aeruginosa* causes massive chronic infections, and many times, death [251].

Conventional treatment of *P. aeruginosa* involves heavy doses of antibiotics. However, the pathogen can respond to antibiotic treatment through the expression of efflux pump systems that allow the bacteria to remove intracellular toxins like antibiotics [252, 253]. The ability of the pathogen to expel antibiotics and easily adapt to adverse environments has resulted in the increase in antibiotic-resistant strains of *P. aeruginosa* [254, 255]. The study of virulence factors that allow *P. aeruginosa* to colonize an immunologically compromised host can lead to the development of new innovative treatments.

4.1.2 Expression of Pseudomonas aeruginosa Virulence Factors

P. aeruginosa possesses a large bacterial genome that provides the pathogen with many metabolic options, and allows it to adapt to many environments [256, 257]. Constitutive transcription of the full genome would be metabolically inefficient. Bacteria use environmental cues to determine which portions of the genome to transcribe. One methods *P aeruginosa* uses to efficiently transcribe its genome is quorum sensing. therefore, the bacteria employ quorum sensing to transcribe the most useful genes for the current environment.

4.1.3 Quorum Sensing

Quorum sensing (QS) is a method of cell-to-cell signaling that involves freely diffusible molecules called autoinducers (AIs) [258-260]. As the cell density of *P. aeruginosa* increases, the AI concentration increases, which in turn modifies gene

expression. In a traditional luxI/LuxR QS system, LuxI synthesizes the AI that is detected by LuxR. The LuxI-AI complex activates transcription of target genes. One of the target genes of the LuxI-AI complex is the *luxI* gene, which in turn synthesizes more AI and creates a positive feedback loop. It is estimated that QS controls the expression of 10% of the *P. aeruginosa* genome. [261].

P. aeruginosa uses three QS systems, 2 LuxI/LuxR systems and 1 Pseudomonas quinolone signal (PQS) system [261]. In the LasI/LasR system, LasI synthesizes 3-ox-C12 homoserine lactone, which serves as an AI and is detected by LasR. The LasI-3-ox-C12 homoserine lactone complex increases the transcription of virulence genes as well as *lasI* [261-263]. The second LuxI/LuxR system, which uses RhlI/RhlR, works in the same manner but uses butanoyl homoserine lactone as its AI [264, 265]. It also controls the transcription of several virulence genes, such as those that control the production of pyocyanin [266]. The PQS system uses PsqA,B,C,D and H, which are detected by PqsR. Unlike the LuxI/LuxR-like systems, the expression of the PQS inducers are activated by LasR-AI complex and repressed by the RhlR-AI complex. The overlap of the QS systems allows for differential expression of virulence factors in diverse environmental conditions [261, 267-270]. In infection, *P. aeruginosa* uses QS to form a biofilm that allows the bacteria to persist in harsh conditions

4.1.4 Biofilm

When in a biofilm, a community of microbial cells attaches to a surface and secrete exopolysaccharide [271]. Microbial cells in a biofilm alter their metabolic activity, as well as their gene and protein expression. This metabolic shift allows the

bacteria to efficiently transcribe its genome and persist in its current environment. In a *P. aeruginosa* infection, biofilm formation contributes to the development of chronic infections, such as the infections that can occur in CF patients [272]. When in a biofilm *P. aeruginosa* produces the exopolysaccharide alginate, which serves as a barrier that protects the bacteria from immune cells, ROS, and antibiotics [271, 273].

The production of alginate converts *P. aeruginosa* to a mucoid phenotype, defined by the secretion of exopolysaccharides[274]. As the organism reaches a high density it converts to a mucoid producing strain is associated with a poor prognosis and is often observed in the infected lung of a CF patient post mortem [275]. Compared to non-mucoid strains, mucoid strains of *P. aeruginosa* are more difficult to clear and result in severe lung damage[276]. The mucoid matrix associated with the biofilm further protects the bacteria from phagocytosis by immune cells and increases resistance to antibiotics [277]. In murine models of chronic *P. aeruginosa* infection neutrophils surround the mucoid-producing biofilm, but phagocytose very few bacteria[278, 279]. This indicates that immune cells can do little to eliminate mucoid-producing strains of *P. aeruginosa*. In addition to alginate, *P. aeruginosa* in a biofim also expresses elastase and alkaline protease to prevent damage from host immune cells [280-283]. A therapy that blocks biofilm formation and mucoid conversation coupled with antibiotic therapy could increase the effectiveness of antibiotics against *P. aeruginosa*.

4.1.5 Type III Secretion System and Its Toxins

P. aeruginosa uses a Type III Secretion System (TTSS) to deliver 4 different effector toxins to host cells. The TTSS is essential to the pathogenesis of this organism, as neutralization of the TTSS prevents sepsis and improves survival of the host in animal models [284]. The TTSS delivers the toxins ExoS, ExoT, ExoU, and ExoY directly to host cells through a needle-like protrusion that extends through the host plasma membrane [285].

ExoS acts as GTPase-activating protein (GAP) with a Adenosine diphosphate (ADP)-ribosylating function [286]. GAP proteins regulate GTP binding proteins that control cell growth, differentiation and apoptosis. The N-terminus of ExoS is a Rho-specific GAP that interferes with G-protein signaling of host cells. The ExoS C -terminus can ADP-ribosylate host proteins and interfere with cell signaling transduction [287, 288]. ExoT also functions as a GAP and ADP-ribosylating protein. The ADP-ribosylating activity of ExoT depolymerizes the actin cytoskeleton [289]. ExoT injection causes cells to round, which can affect junctions between host cells as well as cell movement [290]. ExoU can irreversibly damage the tight junctions between epithelial cell membranes. The C-terminus of ExoU associates with plasma membrane phospholipids and the enzymatic activity of ExoU cleaves the phospholipids [291-294]. ExoU is essential to the virulence of *P. aeruginosa* in murine infection models and is present in 90% of all human infection [285]. The mechanisms of the second adeylate cyclase, ExoY are not as well characterized. Injection of ExoY elevates intracellular cAMP and disrupts the transcription of genes associated with actin cytoskeleton polymerization [285]. The disruption of the actin cytoskeletal polymerization by many of

these toxins leads to a decrease in the ability of the host to phagocytose bacterial cells, traffic to sites of infection and also increases cellular permeability [295].

P. aeruginosa also produces other proteins and metabolites that contribute to its virulence, but are not delivered through the TTSS, such as siderophores, elastase, alkaline proteases, hemolysins, cytotoxins, and pyocyanin [296]. The virulence factors expressed by *P. aeruginosa* affect a wide array of targets. QS allows the bacteria to efficiently express these virulence factors and adapt to certain conditions. The TTSS allows the bacteria to efficiently deliver toxins inside the host cells. Taken together, these characteristics give *P. aeruginosa* an enormous advantage in the colonization of an immune-compromised host and create challenges in the treatment of *P. aeruginosa*.

4.1.6 Pyocyanin

P. aeruginosa synthesizes a toxic blue heterocyclic phenazine from chorismic acid, called pyocyanin. The color of pyocyanin differs in reduced and oxidized states. Reduced pyocyanin is colorless, while the oxidized form turns blue [297]. In culture *P. aeruginosa* secretes pyocyanin into the medium during the stationary phase of bacterial growth [298]. (Figure 4.3). The highly diffusible pigment passes easily through host cell membranes where it changes to the redox environment of the cell and interferes with host cell respiration, electron transport, gene expression and immune function [297, 299, 300]. These effects on host cell metabolism and function allows the bacteria to manipulate the inflammatory environment and increase the survival and persistence of the pathogen.

Pyocyanin acts predominately as a redox sensitive molecule in *P. aeruginosa* lung infections. The ability of the metabolite to easily cross cell membranes allows it to

interact with NADPH of host cells. Pyocyanin oxidizes reduced NADPH and donates accepted electrons to oxygen to produce superoxide, which is converted to H_2O_2 [298]. H_2O_2 can then affect cell signaling and damage cellular components. Pyocyanin also allows H_2O_2 to persist in the environment, which further manipulates redox-sensitive signaling and damages cells. Pyocyanin inhibits the host cell expression of the antioxidant enzyme catalase that breaks down H_2O_2 [301]. This further increases H_2O_2-induced oxidative damage to the host cell, which aids in the persistence of the pathogen. The increase in intracellular ROS levels also results in a decrease of ATP synthesis and a decrease in GSH [297].

In the context of a biofilm, pyocyanin surrounds the *P. aeruginosa* biofilm and creates a redox-potential gradient. The reduced state protects bacteria in the biofilm from exogenous oxidant. The pyocyanin redox-potential gradient also enriches the environment with iron, which is essential to biofilm formation and stability [302].

Pyocyanin decreases the survival of neutrophils, an immune cell type essential to the elimination of *P. aeruginosa*. *In vitro*, incubation of neutrophils with concentrations of pyocyanin, comparable to the pyocyanin concentrations found in the sputum of CF patients, increases apoptosis of the cells, when compared to untreated counterparts [303]. Pyocyanin induced neutrophil apoptosis can be partially blocked by some antioxidants, which indicates exposure to pyocyanin induced oxidant causes neutrophil cell death. [303]. Neutrophils produce superoxide that usually dissipates quickly, forming the antimicrobial intermediate H_2O_2. Pyocyanin prolongs the production of superoxide, which increases the generation of H_2O_2 [303]. Exposure of neutrophils to pyocyanin elevates diacylglyceride levels, which induces NADPH-activity [304]. This leads to an

increase in superoxide and oxidant-induced damage to host cells, as pyocyanin also decrease the expression of host oxidant defenses [305].

During an *in vivo P. aeruginosa* infection, more neutrophils undergo apoptosis in mice infected with a wildtype strain of the bacteria than in mice infected with a strain of *P. aeruginosa* that lacks genes necessary for phenazine production and is thus pyocyanin-deficient. The mice infected with wildtype *P. aeruginosa* produced less neutrophil-dependent chemokines than those infected with the pyocyanin-deficient strains. This decrease is thought to be beneficial to the pathogen, [306] and indicates that pyocyanin inhibits the immune response to the pathogen and increase its virulence.

Pyocyanin also affects the ability of another professional antigen-presenting cell (APC) cell type to eliminate *P. aeruginosa* infection. Exposure of macrophages to pyocyanin decreases the ability of the macrophage to phagocytose bacteria and cell debris. Addition of antioxidants partially rescues the phagocytic capabilities of macrophages in the presence of pyocyanin [307]. The ability of pyocyanin to interfere profoundly with the functions of neutrophils and macrophages underscores the role played by that pyocyanin as a significant virulence factor.

Pyocyanin affects host cell gene expression through the induction of IL-8, ICAM1, CXCL1, CXCL2, and CXCL3 genes [308-310]. These genes are involved in directed cell migration and recruitment of immune cells to the sites of infection. In a lung infection, pyocyanin exposure also leads to the increase in the expression of five host mucin genes MUC5B, MUC20, MUC13, MUC2, and MUC5ac in cells that comprise the airway epithelium [308]. The expression of these genes allows for the

secretion of mucin, a glycol protein, by the airway mucosa [311]. Under normal conditions, mucin protects the airway epithelium from pathogens and debris, but the increase in expression of these results in genes-overproduction of mucin and airway obstruction [311]. The increase in mucin in the airway also leads to an increase in bacterial attachment to the epithelium [312]

4.1.7 Production of the PmtA deficient *P. aeruginosa* strain PW4670

The Manoil Laboratory at the University of Washington constructed a two-allele transposon library using *P. aeruginosa* PAO1 as the parent strain. The mutants from the primary transposon library carry either the ISlacZ/hah or the ISphoA/hah transposon. Eeach of these transposons carry a tetracycline resistance gene. The strains for the two-allele library were chosen from the primary library based on the insertion of the transposon into two sites of the same gene (where possible) the location of the insertion site in the middle of the gene, and in frame insertion of the transposon [313]. The two different insertion sites provide redundancy of the mutation, in which phenotypes can be verified with two distinct mutants. The PmtA gene is known as a probable metallothionein encoded by the ORF PA2140. There was only one transposon insertion site for this mutant and thus only one distinct mutant in the library known as strain PW4670. There is likely only one insertion site for transposon due to the small 240bp length of the ORF PA2140 (Figure 4.1).

After exposure to the transposon, bacteria were grown in the presence of tetracycline, as the bacteria should gain tetracycline resistance upon insertion of the transposon. Single colonies were isolated, grown up and the insertion of the transposon was confirmed using two different methods. The first was conventional DNA sequence,

known as Sanger sequencing, and the second was Tn-seq analysis. Tn-seq is a sensitive method to determine genetic interaction in mircoorganisms through massive parallel sequencing [314]. In Tn-seq an endonuclease site is incorporated into the end of the transposon and cuts 20bp downstream from the site [315]. Sequencing the DNA from the ends of the transposon, and the additional 20bp of flanking DNA is enough to determine the location of the transposon in the bacterial genome [316].

The Manoil laboratory confirmed the position of the ISphoA/hah transposon in PW4670 to be at base pair 108 of 240 through both Sanger sequence and Tn-Seq. The insertion of the transposon in the middle of the gene ensures that if any protein is still translated it is unlikely to have any biological affect. The insertion of the transposon was again confirmed with PCR (Figure 4.2).

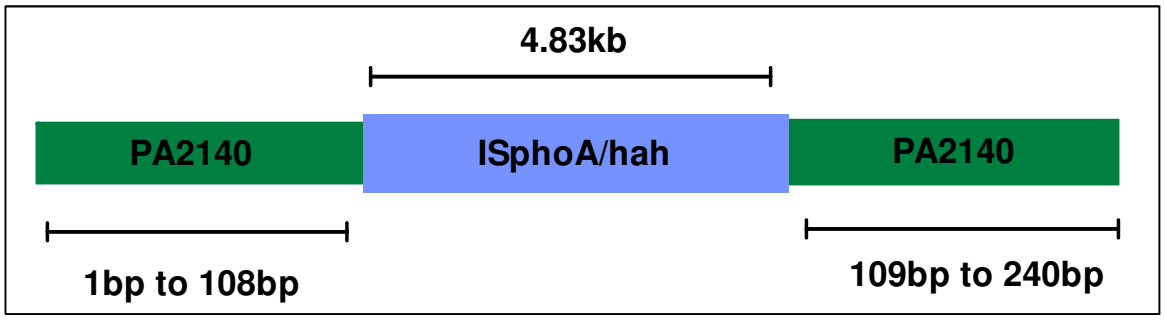

Figure 4.1: Position of the ISphoA/hah transposon in ORF PA22140. The 4.83kb transposon was incorporated into the PAO1 genome with the methods described after base pair 108. The incorporation of ISphoA/hah into the PA2140 ORF, responsible for the transcription of PmtA, is present in *P. aeruginosa* strain PW4670.

4.1.8 Hypothesis: The Absence of PmtA Expression in PW4670 will decrease the virulence of *P. aeruginosa*

The *P. aeruginosa* strain PW4670, derived from the PAO1 strain fails to express a fully functional PmtA protein due to the insertion of a transposon into the gene sequence. Strain PW4670 can be used to determine the function of PmtA in *P. aeruginosa* growth and infection. The absence of an PmtA is likely to alter *P. aeruginosa* resistance to metals stress and ROS, and alter the expression of oxidant sensitive virulence factors.

In the presence of oxidative stress eukaryotic cells upregulate expression of MT to protect the cell from the oxidative stress [106]. The cysteine residues on PmtA suggest that this protein can also act as an antioxidant in *P. aeruginosa.* If PmtA protects *P. aeruginosa* from oxidative stress it could enhance the survival of the bacteria in an infection. Professional phagocytic cells produce ROS to damage bacterial cells and eliminate an infection. The absence of a function PmtA protein could leave *P. aeruginosa* vulnerable to exogenous oxidative stress.

The absence of PmtA may also affect *P. aeruginosa*'s production of pyocyanin. In order to produce an oxidant to damage host cells *P. aeruginosa* must be able to protect itself through the production of antioxidants. Without the expression of PmtA, *P. aeruginosa* may decrease pyocyanin production to protect itself from oxidant, and thus decrease the virulence of the pathogen. If PmtA acts as an antioxidant, the absence of the protein could affect other aspects of bacterial growth, such as the formation of a

biofilm. This could leave the bacteria susceptible to phagocytosis by immune cells, may be inhibited. This would again suggest that PmtA is needed for full virulence of the pathogen.

The functions of PmtA in the growth of *P. aeruginosa* was studied through the comparison of the wildtype PAO1 strain to the PmtA deficient strain PW4670.

4.2 Results

4.2.1 Confirmation of Transposon Insertion

In order to elucidate the function of PmtA on *P. aeruginosa* a strain with a transposon inserted into the gene that encodes for PmtA was obtained from the Manoil Laboratory at the University of Washington. PW4670 was grown up in YTA broth streaked on YTA agar with 5μg/ml tetracycline. Single colonies were isolated and the presence of the transposon insertion was confirmed with PCR. The insertion of the transposon into the PmtA gene was confirmed using PCR with the appropriate primers suggested by the Manoil Laboratory (Table 4.1). PCR conditions were optimized with GoTaq mastermix. (Figure 4.2A). The PCR reaction that amplified wildtype PAO1 DNA with PmtA forward and reverse primers yielded an 833bp product, which indicates the PmtA gene is intact (Figure 4.2B Lane 1). The insertion of the transposon in PW4670 was confirmed by amplification of the PW4670 DNA with the PmtA reverse primer and the Hah-138 transposon specific primer. This reaction yielded a 375bp product, which confirms the insertion of the transposon is in the predicted portion of the gene (Figure 4.2B Lane 4). As expected, negative controls that amplified PAO1 DNA with PmtA

reverse and Hah-138 primers and PW4670 DNA amplification with PmtA forward and reverse primers did not yield PCR products (Figure 4.2B, Lanes 2 and 3).

Amplification Region	Primer name	Sequence 5' - 3'
PmtA Forward	54742R.f	GGTGTCGGTACCGGTGTTC
PmtA Reverse	54742R.r	GCAGTACAGGATTCCGCAGT
ISphoA/hah Transposon	Hah-138	CGGGTGCACTAATATCGCCCT

Table 4.1: Primers used for the confirmation of the ISphoA/hah Transposon Insertion. The Manoil laboratory at the University of Washington designed all three primers used to confirm the insertion of the ISphoA/hah transposon in the PmtA gene. A PCR reaction with PmtA Forward and PmtA Reverse Primers and wildtype PAO1 DNA as a template should yield an 833 bp product. The insertion of the 4.83Kb transposon in the PmtA gene to create strain PW4670 would not yield a product with the PmtA forward and reverse primers, but would yield a 375bp product with the PmtA reverse and Hah-138 primers.

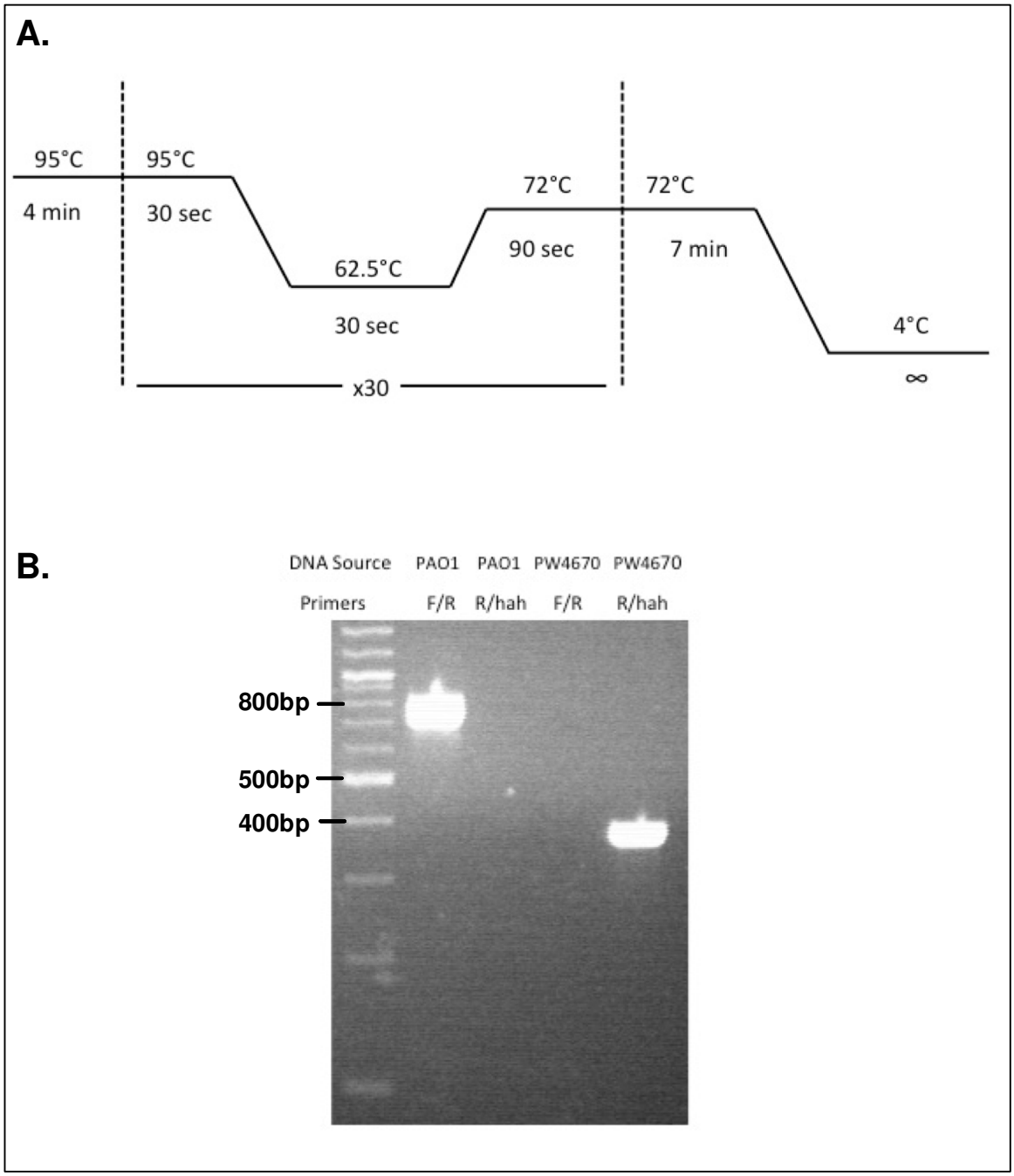
A.
95°C
4 min
95°C
30 sec
62.5°C
30 sec
72°C
90 sec
72°C
7 min
4°C
∞
x30
B.
DNA Source
Primers
PAO1
F/R
PAO1
R/hah
PW4670
F/R
PW4670
R/hah
800bp
500bp
400bp

Figure 4.2

Figure 4.2: PCR confirmation of Transposon Insertion into the PmtA Gene. A.) The PCR cycle was optimized for temperature, as well as DNA concentration. This PCR cycle was used to confirm the insertion of the IS*pho*A/hah transposon into the PmtA gene. B.) The optimized PCR reaction was run with combinations of the PmtA specific forward and reverse primers, as well as PmtA reverse and hah-138 primers, with DNA extracted from PAO1 and PW4670. The wildtype DNA yielded the predicted full 833bp product with the PmtA forward and PmtA reverse primers. PW4670 yielded a 375bp product, which indicates the insertion of the transposon in the PA2140 gene.

4.2.2 Growth Curves of PAO1 and PW4670

PAO1 and PW4670 were grown overnight at 37°C with vigorous shaking in YTA media or YTA media with tetracycline, respectively and transferred to fresh YTA media without antibiotics at a dilution of 1:100. The strains were incubated at 37°C with vigorous shaking for up to 1800 minutes. Bacterial growth was measured with absorbance readings at 600nm. No measurable difference between the growth of the two strains was observed. (Figure 4.3).

Although there was no measureable difference between PAO1 and PW4670 at OD600nm there was a visible difference in the appearance of the two strains. After 30 hours of growth, the media of the wild type PAO1 strain appeared green, while the PW4670 remained yellow (Figure 4.4A). Pyocyanin, a toxic secondary metabolite secreted by PAO1, creates the green color in the media.

4.2.3 Pyocyanin Production in PAO1 and PW4670

The toxic metabolite pyocyanin contributes to the overall virulence of *P. aeruginosa.* A deficiency of the PW4670 strain to produce pyocyanin would suggest that PmtA expression is necessary for the full virulence of the pathogen. In culture, expression of pyocyanin increases during stationary phase growth. The presence of pyocyanin in the cell-free supernatants of both PAO1 and PW4670 was measured at an absorbance of 691nm after 30 hours of growth and plotted as a ratio of 600nm to 691nm (Figure 4.5A). Cell-free supernatant from PAO1, collected from stationary phase cultures, consistently contained more pyocyanin than PW4670.

To confirm that the 691nm readings specifically measured pyocyanin in the supernatant and that the difference in 691nm absorbance readings was not due to the presence of pyocyanin in the colorless reduced state, pyocyanin was extracted from the supernatants after 30 hours of growth with a chloroform/HCl extraction [317, 318]. The absorbance at 691nm of both supernatants was recorded prior to the extraction (Figure 4.5,A-B). In the first portion of the extraction, chloroform was added to the PAO1 and PW4670 supernatants, which produced a blue product. When blue in color, the pH of pyocyanin in solution is 6 to 7, and the absorbance can be measured at 300nm (Figure 4.5, C-D). HCl was then added to the extractions, which lowers the pH of pyocyanin in solution to 1 to 2 and turns the pyocyanin pink. The absorbance was measured at 520nm (Figure 4.5, E-F). At all points in the extraction, the absorbance readings for PAO1 were higher than PW4670. This suggests the 691nm absorbance readings adequately measure the pyocyanin levels in the supernatant of both PAO1 and PW4670.

If PmtA acts as an antioxidant in the *P. aeruginosa* cell, the decrease in pyocyanin production may be because the bacteria lacks protection from oxidant without the expression of PmtA. The addition of an antioxidant in the media may rescue the pyocyanin expression in strain PW4670. The antioxidant glutathione at 10mM was added to the media of the PW4670 strain of *P. aeruginosa*, and pyocyanin production was measured overtime with absorbance readings of the cell-free supernatants at 691nm. The addition of glutathione rescued the pyocyanin production in strain PW4670 (Figure 4.6). The ability of another antioxidant, N-acetylcysteine (NAC), to rescue pyocyanin production in Pw4670 was also measured. Similar to glutathione, the addition of NAC increased pyocyanin expression in PW4670, after 30 hours of incubation (Figure 4.7).

The ability of these antioxidants to rescue pyocyanin production indicates that the genes necessary to produce pyocyanin are not interrupted in the mutant. It also suggests PmtA acts as an antioxidant, and the lack of this antioxidant decreases the expression of one of the pathogen's essential virulence factors.

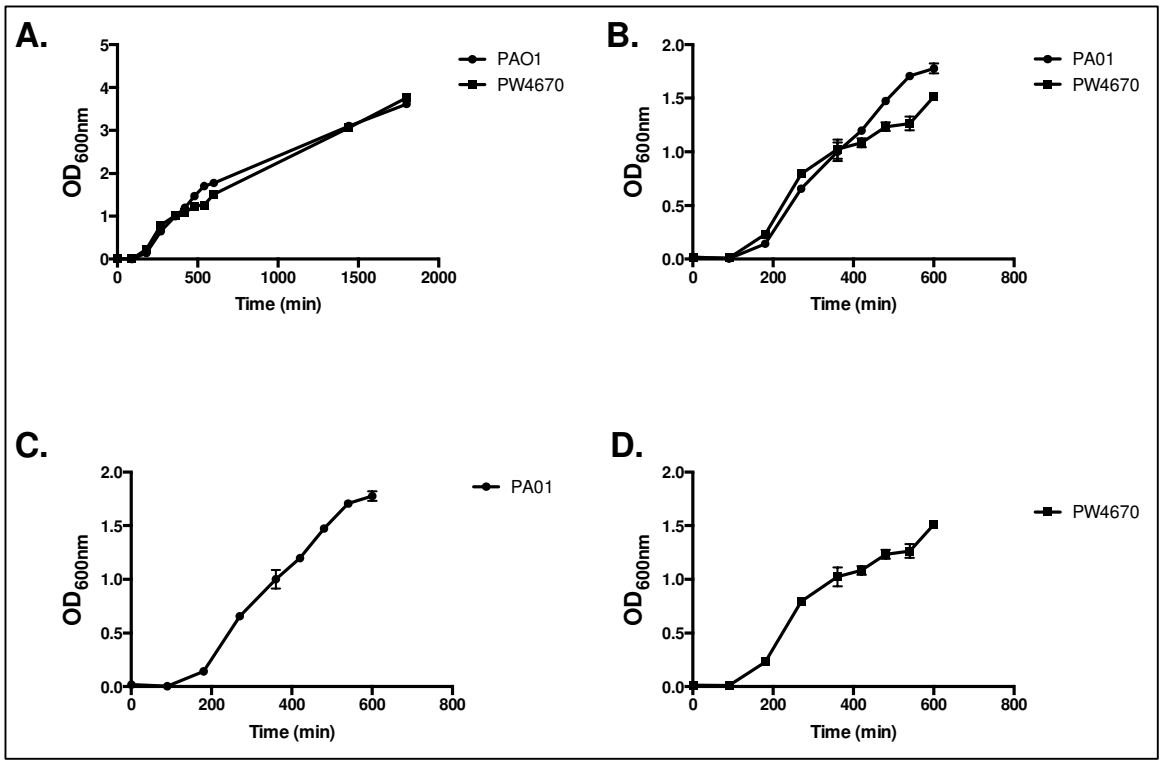

Figure 4.3: PAO1 and PW4670 strains of *P. aeruginosa* grow at similar rates

Both the wildtype PAO1 strain and PW4670 strains were grown overnight at 37°C with vigorous shaking by inoculating 5ml of YTA or YTA with tetracycline for PW4670 with a single colony from a streak plate. Fresh YTA (25ml) without antibiotics was then inoculated at a dilution of 1:100 with the overnight cultures and incubated at 37°C with vigorous shaking for 30 hours. Absorbance readings at 600nm were recorded every hour during log phase (B-D), and then again overnight, until the 30 hour time point (A). No difference in growth rate was observed between the strains.

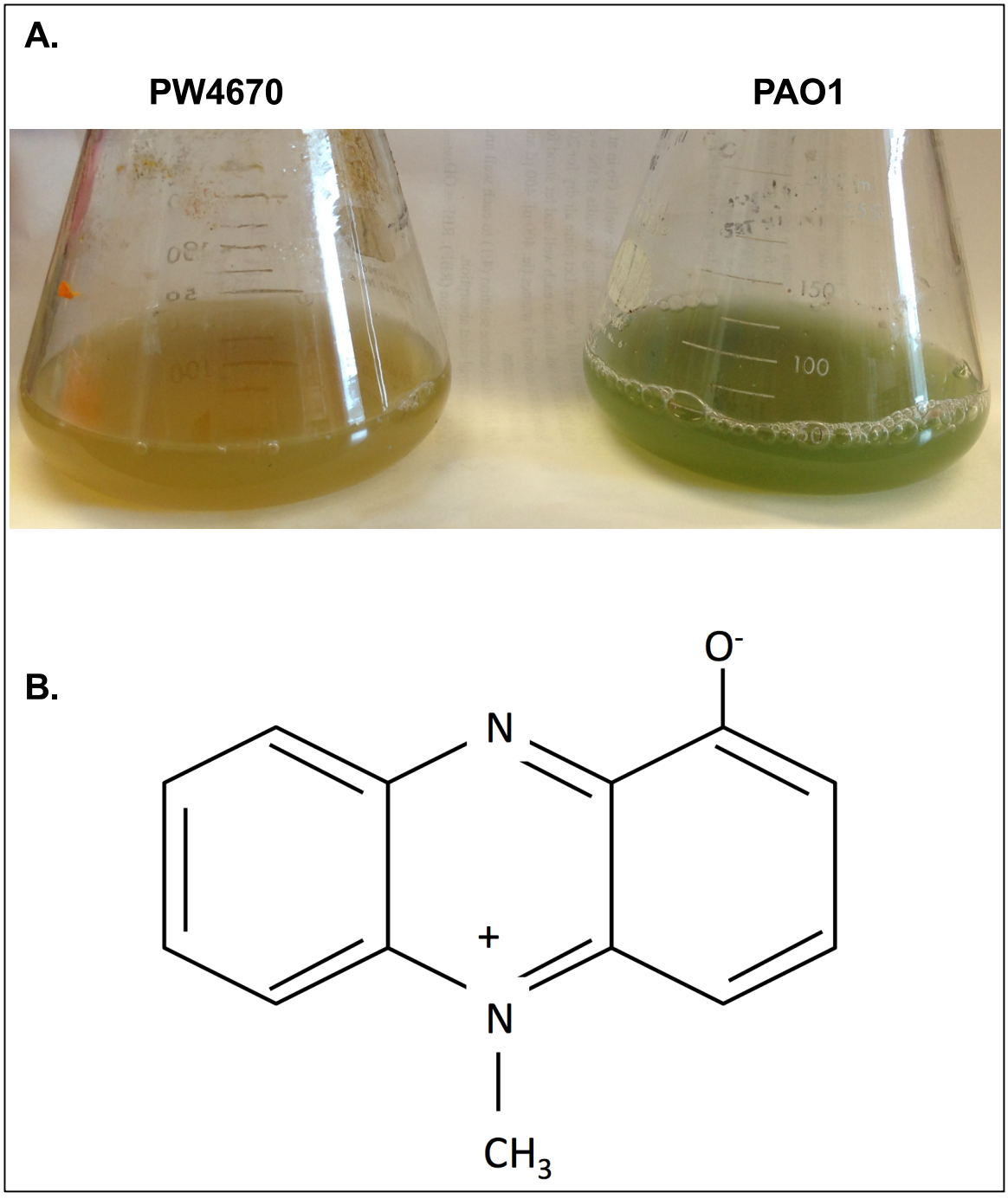

Figure 4.4

Figure 4.4: *P. aeruginosa* strain PW4670 fails to turn culture supernatant green, which indicates a lack of pyocyanin production.

Both the wildtype PAO1 strain and PW4670 strains were grown overnight at 37°C with vigorous shaking in either 5ml of YTA or YTA with tetracycline, respectively. Fresh YTA (50ml) without antibiotics was then inoculated at a dilution of 1:100 with the overnight cultures and incubated at 37°C with vigorous shaking for 30 hours. It was observed that after 30 hours the supernatant of PW4670 did not turn green while PAO1 supernatant was green (A). The green color in observed in the supernatant of many *P. aeruginosa* strains is due to the redox sensitive metabolite pyocyanin. (B) The structure of pyocyanin.

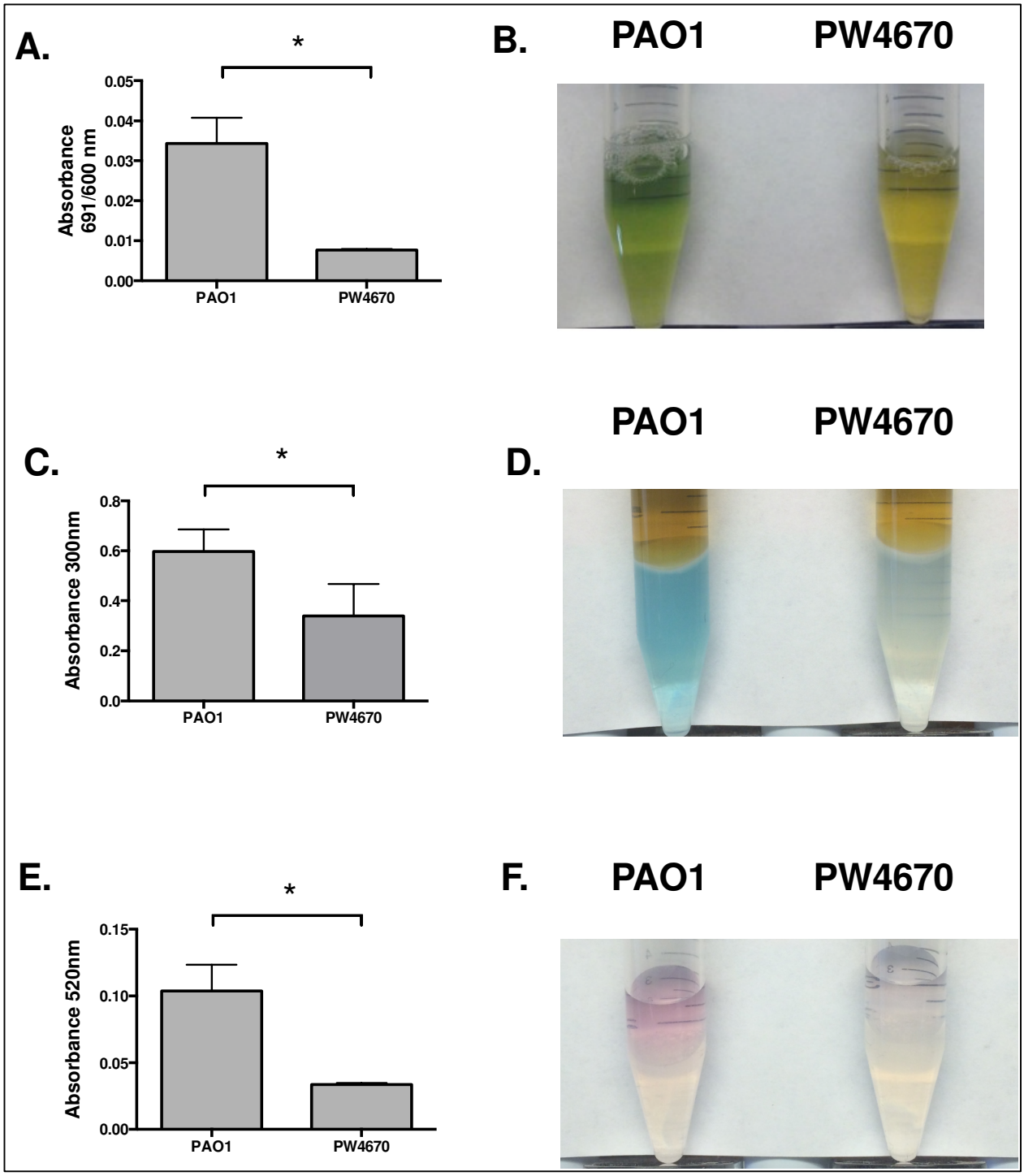
A.
*
Absorbance 691/600 nm
0.05
0.04
0.03
0.02
0.01
0.00
PAO1
PW4670
B.
PAO1
PW4670
C.
*
Absorbance 300nm
0.8
0.6
0.4
0.2
0.0
PAO1
PW4670
D.
PAO1
PW4670
E.
*
Absorbance 520nm
0.15
0.10
0.05
0.00
PAO1
PW4670
F.
PAO1
PW4670

Figure 4.5

Figure 4.5: The supernatant of *P. aeruginosa* strain PW4670 contains less pyocyanin than strain PAO1.

P. aeruginosa strains PW4670 and PAO1 were grown in YTA media for 30 hours at 37°C with vigorous shaking . At 30 hours, cell-free supernatant was collected through three consecutive centrifugations at 13,200rpm for 90s. In media, the absorbance of pyocyanin can be measured at 691nm (A-B). Pyocyanin was then extracted from the media supernatant with chloroform and HCL, using an established protocol. The supernatant was first vigorously vortexed with chloroform, which yielded a blue pyocyanin layer, that absorbs at 300nm (C-D). The blue pyocyanin layer was then exposed to HCl, which dropped the pH of the extract to ~2, and formed a pink layer that absorbs at 520nm (E-F). In all portions of the extraction, the pyocyanin levels of the wildtype PAO1 were higher than PW4670. *=$p<0.05$ according to a student's T test.

4.2.4 The Contribution of PmtA expression on *P. aeruginosa* Virulence

The lack of PmtA expression contributes to the decrease in pyocyanin expression, and may, therefore, contribute to the overall virulence of the pathogen. The murine alveolar macrophage cell line, MH-S, was exposed to dilutions of cell-free supernatants from 30-hour cultures of either PAO1 or PW4670. The cells that survived the after 30 minutes of exposure to PAO1 or PW4670 supernatants were counted and the cell number was compared to an untreated control to obtain the percent survival of each group. The PAO1 supernatant killed significantly more macrophages in all supernatant dilutions (Figure 4.8).

The virulence of the supernatant was further tested with a *Galleria mellonella* wax worm larvae model. In this model, larvae were injected with 5µl of cell-free supernatant from either PAO1 or PW4670 obtained after 30 hours of growth. The survival of the larvae was recorded after 24 hours. Three separate experiments were combined to increase the sample number, and an odds ratio was calculated. It was determined that death was 7.48 times more likely if the larvae were injected with PAO1 supernatant than PW4670 supernatant (Figure 4.9 A). This indicates that PAO1 supernatant is more likely to kill the larvae than PW4670 supernatant *in vivo.* The supernatants were dialyzed against PBS using a 3,000 to 6,000 Dalton dialysis membrane in order to dialyze out the pyocyanin but not small proteins such as PmtA. The dialyzed supernatants were than injected into the *G. mellonella* larvae and incubated at 25°C for 24 hours. After the supernatants were dialyzed, neither PAO1 nor PW4670 supernatant killed the larvae in 24 hours. This indicates that the lethal effects of the PAO1

supernatants can be attributed to a small molecule such as pyocyanin and not the PmtA in the media (4.9B).

4.2.5 The Contribution of PmtA expression on *P. aeruginosa* Biofilm Formation

The formation of a biofilm is crucial to the virulence of *P. aeruginosa*. Strains that form a biofilm secrete the exopolysaccharide alginate associated with the conversation to a mucoid-producing strain, and a poor prognosis for patients [274, 275]. The contribution of PmtA expression on the formation of a biofilm was determined a microtiter plate biofilm formation assay [187]. An inhibition in biofilm formation was observed in the PmtA-deficient strain, PW4670 compared to the wildtype PAO1 strain (Figure 4.10). The addition of the antioxidant, GSH, did not rescue biofilm formation, as it rescued pyocyanin expression (Figure 4.10). This indicates that the inhibition of biofilm formation in PW4670 is likely due to a mechanism unrelated to oxidative stress. The inhibition of biofilm formation may contribute to the overall virulence of *P. aeruginosa* strain PW4670.

4.2.6 Growth of PAO1 and PW4670 in the presence of Hydrogen Peroxide

The decrease in pyocyanin production PW4670, and its subsequent rescue with antioxidants suggests PmtA acts as an antioxidant much like its eukaryotic MT counterpart. To determine if PmtA expression protects *P. aeruginosa* from exogenous oxidant, both the wildtype PAO1 strain and the PmtA deficient PW4670 strain were grown to mid-log phase growth and subsequently exposed to 10mM H_2O_2. There was no

difference in the survival or subsequent growth between PW4670 and PAO1 upon treatment with H_2O_2. These results indicate that PmtA does not protect against exogenous H_2O_2, as was hypothesized (Figure 4.11).

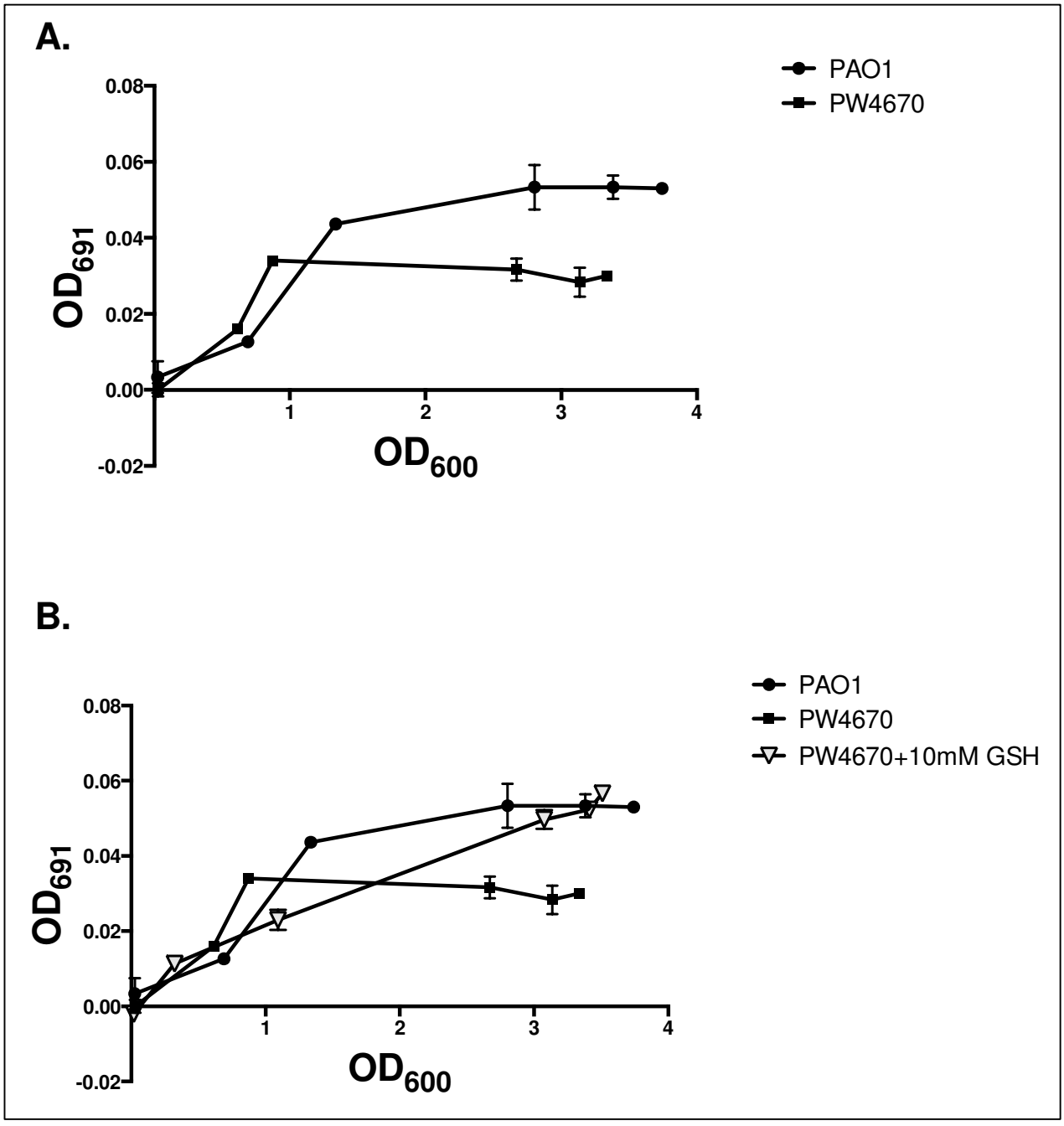
A.
PAO1
PW4670
0.08
0.06
0.04
0.02
0.00
-0.02
OD691
1
2
3
4
OD600
B.
PAO1
PW4670
PW4670+10mM GSH
0.08
0.06
0.04
0.02
0.00
-0.02
OD691
1
2
3
4
OD600

Figure 4.6

Figure 4.6: The Addition of the Antioxidant Glutathione Restores Production of Pyocyanin in *P. aeruginosa* strain PW4670. *P. aeruginosa* strains PAO1, PW4670 and PW4670 supplemented with 10mM glutathione (GSH) were grown in YTA media for 30 hours at 37°C with vigorous shaking. Over the 30 hour period, the growth of the bacteria (OD600) was compared to the production of pyocyanin in media (OD691). A.) The PAO1 produced more pyocyanin when compared to PW4670 B.) When PW4670 was supplemented with the antioxidant GSH, pyocyanin production was restored to near wild type levels after 30 hours of growth (B). These results are plotted as mean+/- SD and representative of three separate experiments.

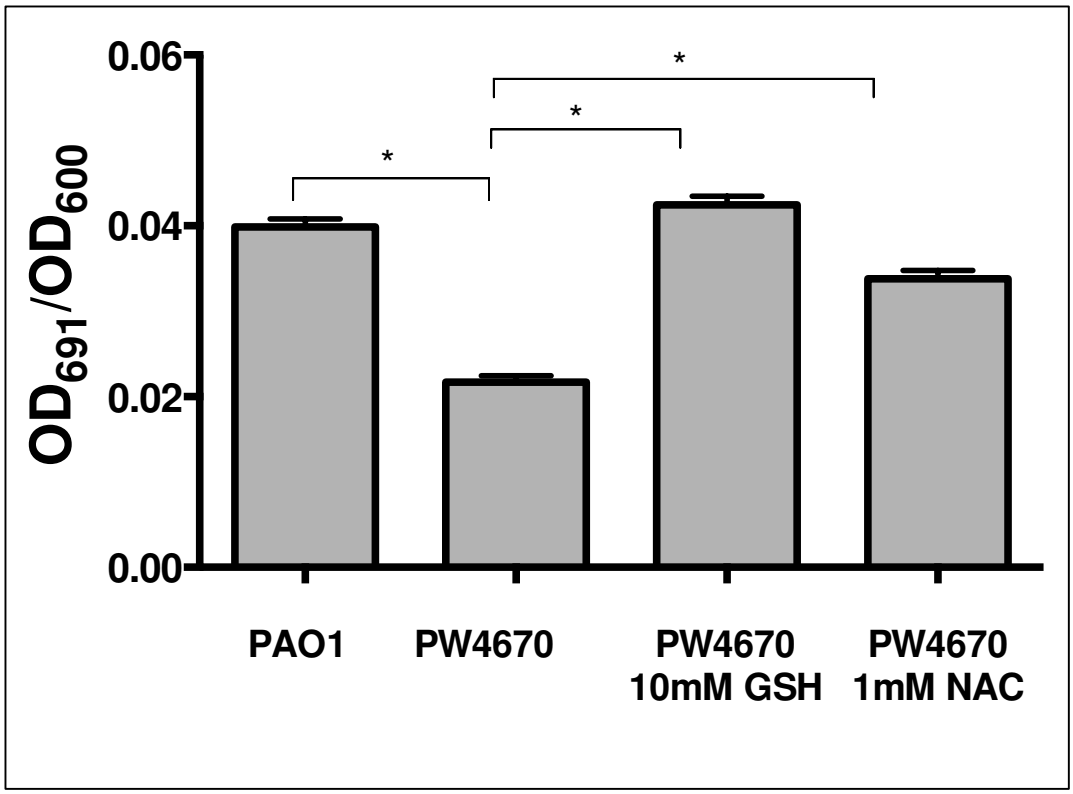

Figure 4.7: The Addition of the Antioxidants Glutathione and N-acetylcysteine Restores Production of Pyocyanin in *P. aeruginosa* strain PW4670. *P. aeruginosa* strains PAO1, PW4670 and PW4670 supplemented with 10mM glutathione (GSH) or 1mM N-acetylcysteine (NAC) were grown in YTA media for 30 hours at 37°C with vigorous shaking. Over the 30 hour period, the growth of the bacteria (OD_{600}) was compared to the production of pyocyanin in media (OD_{691}). The PAO1 produced more pyocyanin when compared to PW4670. The pyocyanin production of PW4670 was increased with the addition of GSH and NAC. These results are plotted as mean+/- SD and representative of three separate experiments. (*=$p<0.0001$) (ckm040114

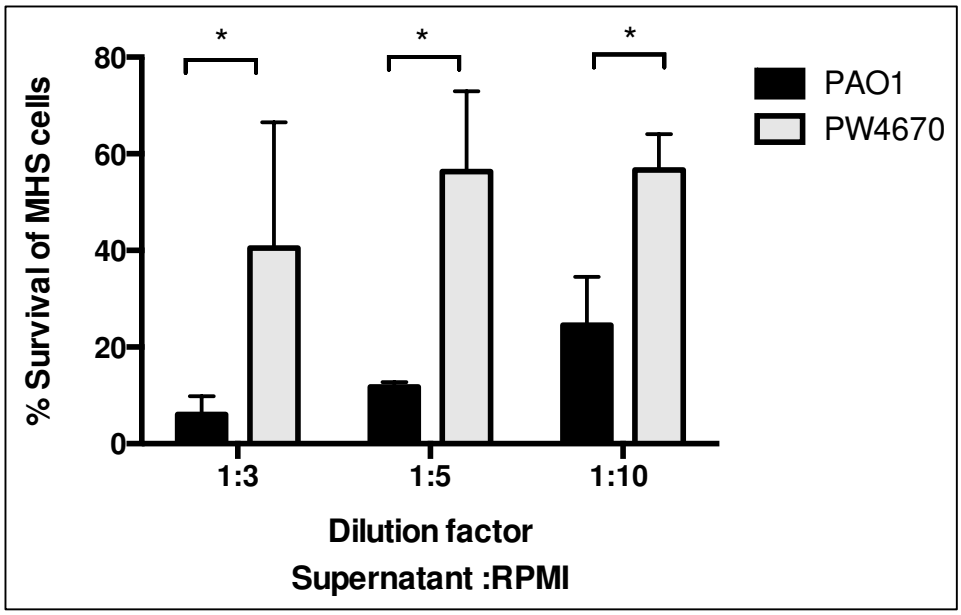

Figure 4.8: Supernatant from PAO1 cells decreases the survival of macrophage cells more than PW4670 supernatant.

P. aeruginosa strains PW4670 and PAO1 were grown in YTA media for 30 hours at 37°C with vigorous shaking. Bacterial cells from both strains were removed through centrifugation to obtain a cell free supernatant. The supernatants were diluted 1:3, 1:5, or 1:10 in supplemented RPMI media. The diluted supernatants were exposed to MHS cells that adhered to cell culture dishes for 24 hours. Survival of macrophage cells was determined with trypan blue exclusion. The survival of cells exposed to bacterial supernatants was compared the number of control cells exposed to the same dilution of YTA:RPMI to determine the percent survival. This experiment was done in triplicate and is representative of three separate experiments. Statistical significance was calculated with a two-tailed student's T test *$p<0.05$. (kmp012414)

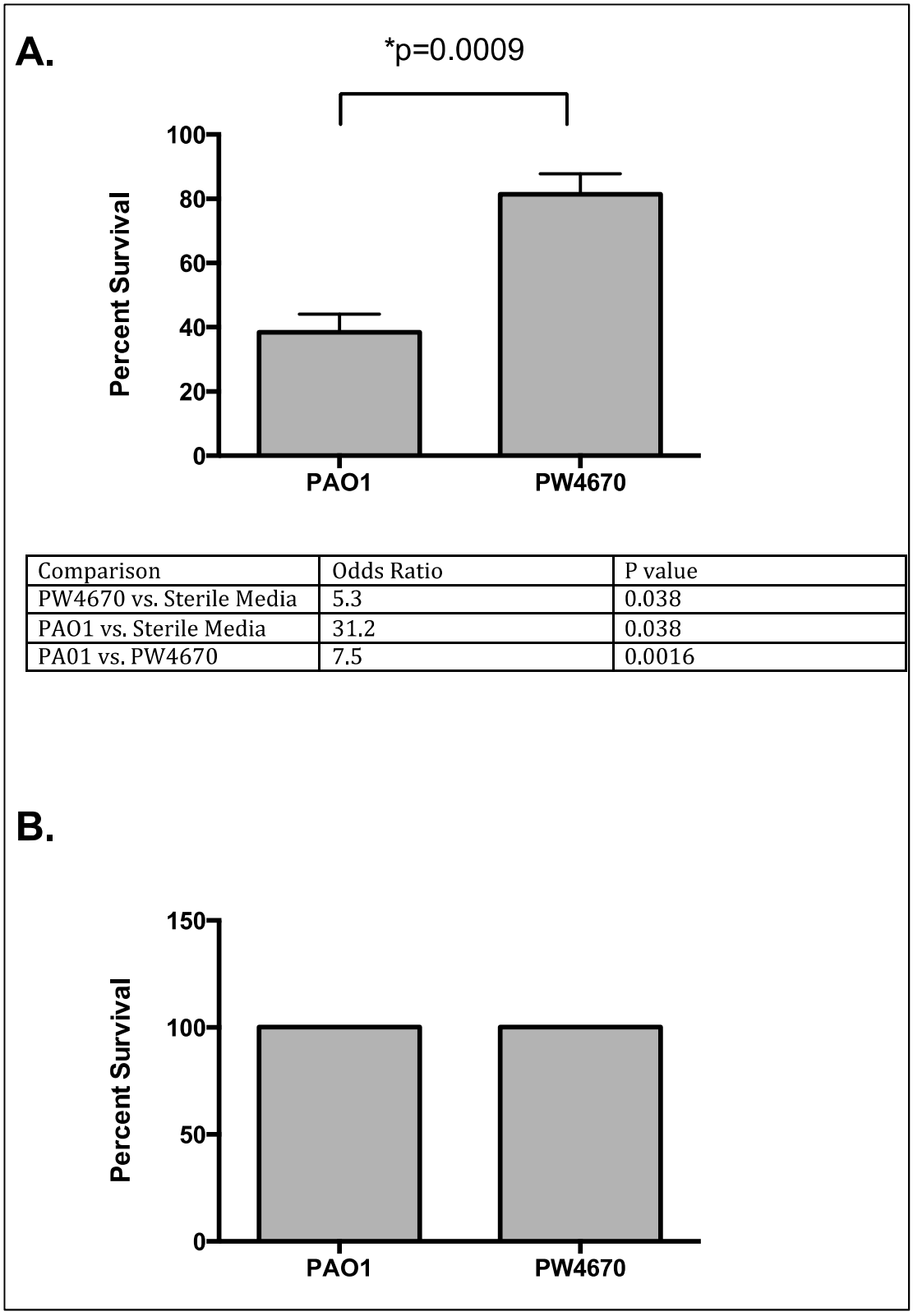

Comparison	Odds Ratio	P value
PW4670 vs. Sterile Media	5.3	0.038
PAO1 vs. Sterile Media	31.2	0.038
PA01 vs. PW4670	7.5	0.0016

Figure 4.9

Figure 4.9: Supernatant from PAO1 is more lethal than PW4670 in a *G. mellonella* model. *P. aeruginosa* strain PAO1 and PW4670 were grown in YTA media for 30 hours. Cell-free supernatant was obtained through centrifugation and injected into *G. melonella* larvae. Death over the worms was recorded at 24 hours. The data is depicted as an odds ratio, where 1 (dotted line) indicates no effect. An odds ratio of three separate experiments with 9 worms per group was calculated and compared to a control injected with sterile YTA media (A) The average odds of death with the injection of PW4670 supernatant compared to the control was 5.3 with an average p value of p=0.32, which does not indicate significance. The average odds of death with PAO1 supernatant injection compared to the control was 31.2, with an average p value of p=0.038, which indicates significance. The three separate experiments were combined to increase the sample size and the PAO1 group was compared to the PW4670 injected group (B). This comparison yielded an odds ratio of 7.48, which indicates death was 7.48 times more likely in the PA01 injected group than the PW4670 group. The p value for this comparison was *p=0.0016, which indicates that this difference was significant. (kmp032714, 040114, 040214) B. Supernatants were dialyzed with 3,000-6,000 molecular weight cut off dialysis membrane overnight and then injected into larvae the next morning. After 24 hours of incubation neither the PAO1 or PW4670 dialyzed supernatants killed any of the larvae.

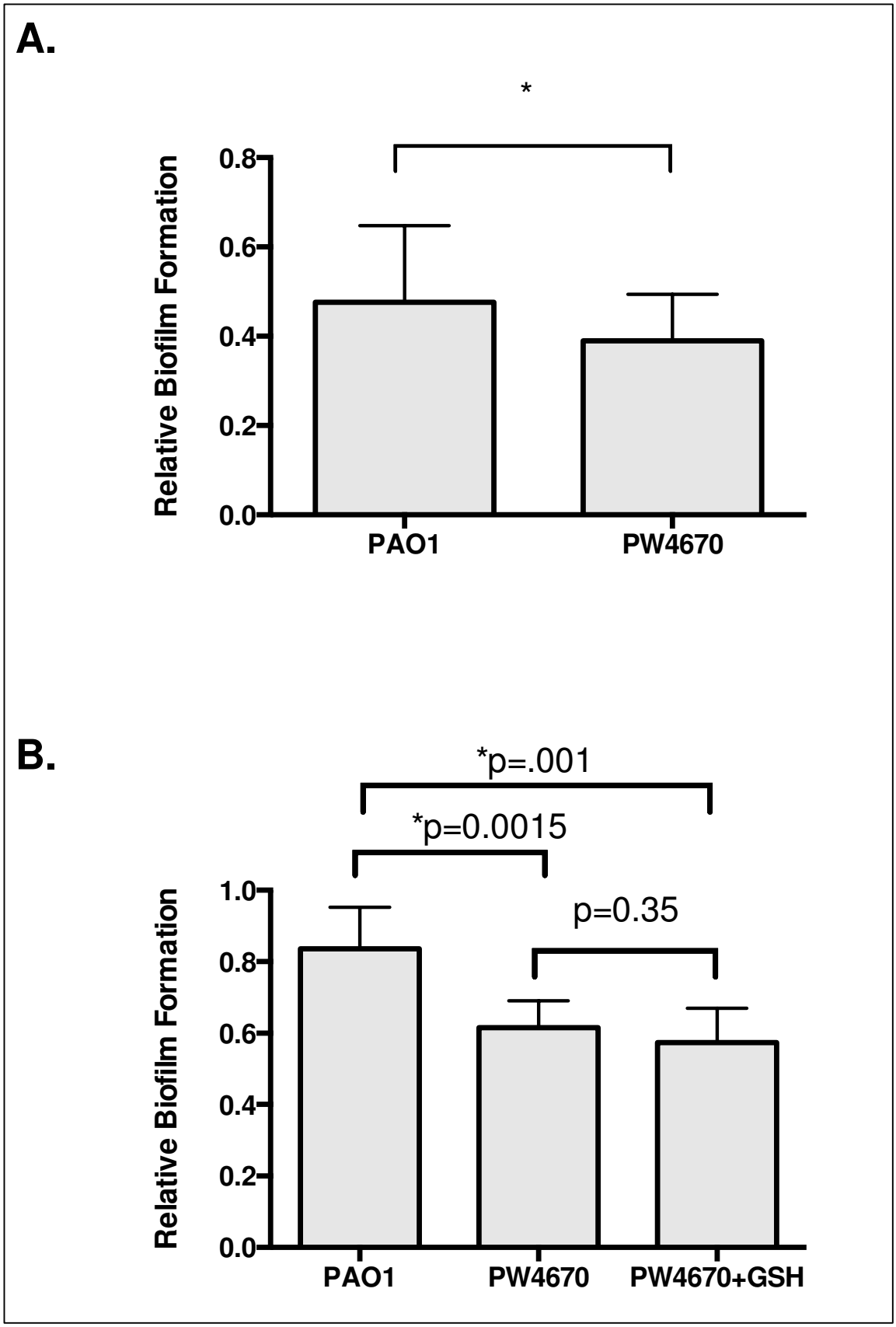
A.
*
Relative Biofilm Formation
0.8
0.6
0.4
0.2
0.0
PAO1
PW4670
B.
*p=.001
*p=0.0015
p=0.35
Relative Biofilm Formation
1.0
0.8
0.6
0.4
0.2
0.0
PAO1
PW4670
PW4670+GSH

Figure 4.10: The absence of PmtA affects Biofilm Formation

P. aeruginosa strains PW4670 and PAO1 overnight cultures were transferred to fresh YTA media in a 96 well plate, at a dilution of 1:10. The plate was incubated in 37°C without shaking to allow the formation of a biofilm. After 24 hours of growth, the growth yield of each well was measured with an absorbance reading at 595nm. The media was aspirated from the wells and the remaining biofilm was fixed to the sides of the well. The biofilm was then stained with 0.1% crystal violet for 40 minutes and subsequently removed from the wells. Ethanol:acetone (4:1) was added to precipitate the crystal violet from the biofilm and the colorimetric change produced by the crystal violet stain was measured through an absorbance reading at 595nm. The absorbance reading after the addition of crystal violet was divided by the growth yield absorbance readings to calculate the relative biofilm formation. These results are the results for 3 separate experiments and 50 data points per strain. Calculations of relative biofilm formation over 1.0 were excluded. The data, plotted as mean +/- SD. *p=0.0007 according to a Two-tailed Student's T test. B.) GSH at 10mM was added to the YTA media in the plate to determine if the addition of an antioxidant would rescue the biofilm formation. GSH did not increase biofilm formation in the microtiter plate assay. Calculations of relative biofilm formation over 1.0 were excluded from analysis. The data is plotted as mean +/- SD, and p values were calculated using a two-tailed student's T test. Data is representative of 3 separate experiments. (avt030214, 030714, kmp032514) (avt032714, 040114, 040414)

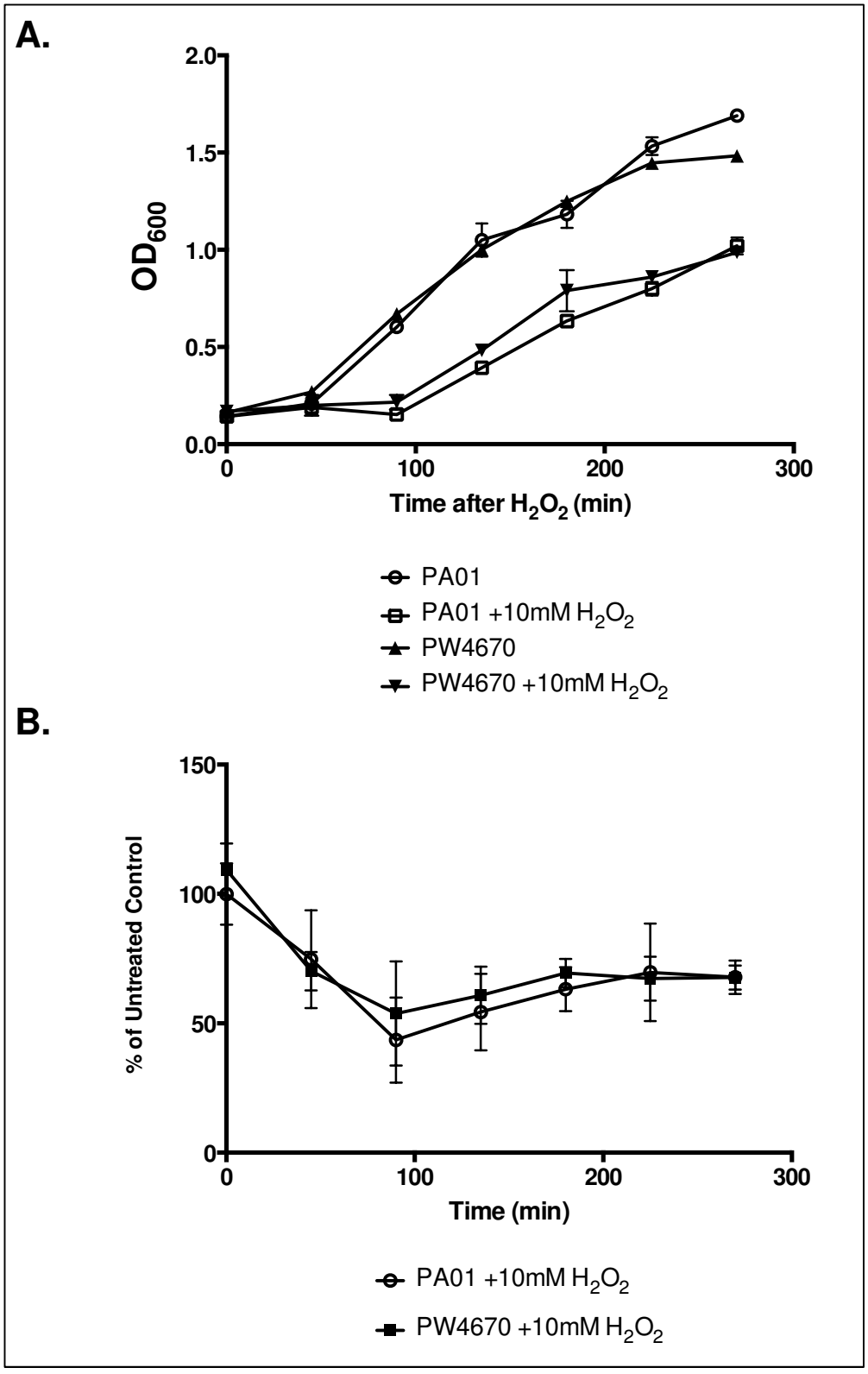
A.
2.0
1.5
1.0
0.5
0.0
OD600
0
100
200
300
Time after H2O2 (min)
PA01
PA01 +10mM H2O2
PW4670
PW4670 +10mM H2O2
B.
150
100
50
0
% of Untreated Control
0
100
200
300
Time (min)
PA01 +10mM H2O2
PW4670 +10mM H2O2

Figure 4.11

Figure 4.11: Expression of PmtA does not affect the growth of *P. aeruginosa* upon exposure to hydrogen peroxide. Both the wildtype PAO1 strain and PW4670 strains were grown overnight at 37°C with vigorous shaking by inoculating 5ml of YTA or YTA with tetracycline for PW4670 with a single colony from a streak plate. Fresh YTA (50ml) without antibiotics was then inoculated with a 1:100 dilution of the overnight culture and grown for ~3 hours until the bacteria entered mid-log phase growth. Each 50ml culture was then split into to 25ml cultures, and one culture of each strain was exposed to 10mM H_2O_2. Absorbance readings at 600nm were taken for ~4 hours after the addition of H_2O_2 and growth curves were plotted (A). The growth of the two strains after the addition of H_2O_2 was compared to the untreated control flasks to calculate the percent of untreated control (B). The percent of untreated control is plotted as the mean+/- SD from the means of three separate experiments. The expression of PmtA did not alter the bacteria's resistance to the oxidant H_2O_2.

4.3 Discussion

The expression of many virulence factors by the human pathogen *P. aeruginosa* vastly complicates the treatment of these infections. In order to effectively treat the multi-drug resistant bacteria, an understanding of the functions of each virulence factor expressed by *P. aeruginosa* is extremely important. The functions of the metallothionein PmtA expressed by *P. aeruginosa* in the context of virulence have not been previously studied. The similarities of PmtA to its immunomodulatory mammalian MT counterpart suggest that PmtA can affect the redox environment in infection, and as a consequence affect *P. aeruginosa* virulence.

In this study, we have shown that a deficiency in the expression of PmtA results in a dramatic phenotypic difference in the production of the redox-active virulence factor pyocyanin. Expression of pyocyanin is associated with the death of PMNs and macrophages, which are the dominant immune cell types present in the immune response to *P. aeruginosa* infection [181, 279, 319-321]. The *in vitro* decrease in pyocyanin expression in the PmtA-deficient strain PW4670 suggests that this strain could be less able to kill immune cells and less able to establish a persistent infection than its parent strain counterpart. Incubation of supernatants from the parent strain PAO1 and the PmtA-deficient PW4670 with MH-S alveolar macrophage cell line and subsequent measurement of survival shows that the supernatant from PAO1 can kill immune cells more efficiently than supernatants from PW4670 culture. Resident alveolar macrophage cells are the first immune cells to encounter *P. aeruginosa* in a lung infection. These cells are responsible for the production and release of cytokines and chemokines upon

contact with MAMPs. They are essential to the host defense as they recruit other immune cells to the site of infection [176-178]. In this study we show that *P. aeruginosa* strain that lacks the expression of a functional PmtA protein is less likely to kill these critical immune cells *in vitro*. This suggests that the strain that lacks PmtA, PW4670, would be less likely to interfere with the immune response from alveolar macrophage cells, and therefore less likely than its parent strain, PAO1, to perpetuate an infection.

In vivo studies used the *Galleria mellonella* moth larvae as a host to study the pathogenicity of the PAO1 and PW4670 supernatants. The *G. mellonella* model was used because the innate immune system of insects is highly homologous to that of mammals [322]. The *G. mellonella* larvae show a high degree of resistance to microbial infections through both cellular and humoral defenses [322, 323]. This model therefore provides an accurate prediction of virulence prior to mammalian studies. The studies done using this model indicate that the supernatant from PAO1 was more likely to kill the larvae than the supernatant from PW4670. The supernatants from both PAO1 and PW4670 were also dialyzed using a 3,000 to 6,000 Dalton molecular weight cut off dialysis membrane. This size membrane would allow the pyocyanin to be filtered out of the supernatant, but retain slightly larger proteins, particularly PmtA. When the supernatants were dialyzed, the PAO1 supernatant was no more likely to kill the larvae than the PW4670 supernatant. This indicates that the pyocyanin is more likely to be the lethal factor in the PAO1 supernatant than the PmtA protein. In the future, the lethal dose 50 (LD50) of both PW4670 and PAO1 should be calculated in the larvae model to determine if the difference in the by

products of the supernatant translates to a difference in virulence. It is likely that the PW4670 will be less virulent than PAO1 since mammalian models have shown that pyocyanin expression is necessary for the full virulence of *P. aeruginosa* [306].

A decrease in the production of the redox-active metabolite pyocyanin affects the redox environment of the bacteria in a host. Pyocyanin oxidizes NADPH and donates electrons to oxygen molecules to create ROS and prolong the persistence of harmful oxidants produced by PMNs and macrophages. Though the ROS produced by immune cells are intended to kill the bacteria, oxidants are not specific to the bacteria and can potentially harm the host cells as well. Additionally, pyocyanin decreases the expression of host defenses to ROS, such as the expression of catalases, which increases the likelihood of ROS-induced host cell death. Our experiments suggest that PmtA expression is necessary for the production of pyocyanin, and therefore the lack of this MT would lessen the ability of the bacteria to manipulate the ROS response of the host. This would be a disadvantage to the bacteria, and again suggests that the PmtA-deficient strain PW4670 is less able to cause an infection than its parents strain PAO1.

In addition, the prolonged persistence of the oxidant may be advantageous to the bacteria. *P. aeruginosa* expresses and efflux pump that serves to expel antibiotics from inside the bacterial cell to protect the cell from the effects of the antibiotic. The negative regulator MexR controls the expression of the efflux pump [324]. In the absence of oxidant, MexR binds to the promoter region of the *mexAB-oprM* operon that encodes for the expression of the pump, and represses transcription. In the presence of oxidant, two cysteine residues on MexR form a disulfide bond and the repressor no longer binds the promoter region. This allows for transcription and expression of the efflux pump [325].

A decrease in extracellular oxidant as a result of the decrease in pyocyanin production may not push the formation of the MexR disulfide bond, and limit the expression of the efflux pump. This may make the bacteria more susceptible to antibiotics. In the absence of the oxidant pyocyanin, or in low levels of pyocyanin, the oxidant-sensitive signaling of MexR, may not become dysregulated, and leave the bacteria susceptible to the antibiotics.

The absence of a functional PmtA protein also affects biofilm formation of *P. aeruginosa*. In a biofilm, microbial cells alter their metabolic activity allowing the bacteria to adapt to new environments. In a *P. aeruginosa* lung infection, the formation of a biofilm increases the likelihood that the patient will develop chronic *P. aeruginosa* infections [272]. Inhibition of biofilm formation is associated with a decrease in virulence in *P. aeruginosa* [326]. Since many of the metabolic shifts associated with biofilm formation are controlled through QS, it is also possible that the absence of a fully functional PmtA protein disrupts QS. The few antibiotics that are able to kill *P. aeruginosa* must penetrate the biofilm in order to affect the growth of the pathogen. The conversion of to a mucoid-producing strain of bacteria, which usually happens upon biofilm formation and is regulated by QS, makes it extremely difficult for the antibiotic to reach the bacteria.

It will be necessary in the future to complement the PW4670 strain in order to determine that the pyocyanin and biofilm-deficient phenotypes measured here can be contributed to the absence of PmtA. The gene that encodes the PmtA protein may lie in an operon, which could complicate complementation. If the gene is in an operon, the production of these other genes present in the operon should be

confirmed through PCR or western blot analysis. The complementation of PW4670 with PmtA is necessary to attribute the observed phenotypes to PmtA and not the other genes present in the operon.

The data collected in this study may be promising in the future treatment of *P. aeruginosa.* A treatment of *P. aeruginosa* that combines a decrease in pyocyanin production and biofilm production with antibiotics may represent a new type of therapeutic intervention. The decrease in pyocyanin not only inhibits the ability of the pathogen to evade the immune response, but may also change redox-sensitive transcription elements in the bacteria that are responsible for the expression of the efflux pump. PmtA represents a novel target to decrease the expression of pyocyanin and subsequently affect the pathogen's susceptibility to antibiotic intervention. The disruption the expression of a single protein, PmtA, may be an easier mechanism than the disruption of the several genes involved in the production of many different stages of pyocyanin expression. This type of therapy that combines the targeting of a virulence factor with the administration of antibiotics may represent a new, innovative option in the treatment of the deadly human pathogen *P. aeruginosa.*

CHAPTER 5: CONCLUSIONS AND FUTURE DIRECTIONS

MTs represent a family of low molecular weight, cysteine rich proteins that use cysteine residues to associate with heavy metals [1]. MTs are evolutionarily conserved and are present in a diverse and extensive set of organisms [327]. The mammalian MT, specifically MT-I and MT-II, is the most extensively studied MT. Among the many functions of this MT is the ability of the MT to influence the functions of immune cells, including proliferation, migration, and antibody response.

The interactions of MTs from other organisms with the mammalian immune system have not been studied until now. A prokaryotic MT, known as PmtA, from the human pathogen *P. aeruginosa* may interact with immune cells during infection. This studied aimed to determine if PmtA possesses similar immunomodulatory to mammalian MT, in particular PmtA's influence over cell migration and overall virulence of the pathogen.

The effect of PmtA on Jurkat T cell chemotaxis was determined through the use of GST-PmtA purified from *E. coli*. The Jurkat T cell model was used in order to compare the chemotactic effect of mammalian MT to that of PmtA, since it had been previously established that mammalian MT causes chemotaxis of this cell type [130]. This cell type also lacks the TLR-4 receptor that responds to LPS, therefore any residual LPS from the purification of GST-PmtA would not affect the results of the study. Chemotaxis was measured *in vitro* with the conventional Boyden chamber assay as well as the innovative, real-time, automated ECIS/Taxis assay [135, 140]. Although GST-PmtA did not cause chemotaxis of Jurkat T cells, GST-PmtA did block the migration of

cells in response to a known chemoattractant, SDF-1α. GST-PmtA also disrupted the desensitization by internalization of the receptor SDF-1α receptor CXCR4. This indicates that that PmtA does indeed influence the migration of immune cell *in vitro*.

The influence of PmtA on *P. aeruginosa* growth and virulence was determined with a comparison of a wildtype PAO1 strain and strain PW4670, in which a transposon interrupts the gene responsible for the transcription of PmtA. A comparison of the strains showed that pyocyanin production in strain PW4670 was severely inhibited. The production of pyocyanin in PW4670 could be rescued with the addition of the anti-oxidant glutathione. This suggests that PmtA acts as an antioxidant in *P. aeruginosa* and the absence of this antioxidant decreases the ability of the organism to produce its redox-sensitive virulence factor, pyocyanin. This work is the first demonstration that the expression of an MT could affect the virulence of the human pathogen *P. aeruginosa.*

The capacity of PmtA to modulate the actions of immune cells and influence the expression of a virulence factor in a human pathogen leads to many new avenues of research. PmtA modulates chemotaxis of immune cells differently from MT, in that it does not induce chemotaxis, but does block chemotaxis. Recent studies out of our lab suggest that mammalian MT can also block chemotaxis of Jurkat T cells (not yet published). It is therefore reasonable to hypothesize that PmtA may influence the functions of immune cells in other ways. For example, mammalian MTs are known to increase the proliferation of T and B cells [56]. If PmtA increases the proliferation of both T and B cells it could be advantageous to the host in elimination of the infection by increasing the number of effector cells at the site of infection. In contrast, it could cause the recruitment and proliferation of too many inflammatory cells to the site of infection

and cause damage to host tissues. Proliferation of both B and T cells as a result of PmtA exposure could also result in immune dysregulation through polyclonal activation. Both of these scenarios would suggest that PmtA could act as a immune modulator and influence the course of infection.

Since PmtA was not found on the outside of Jurkat T cell (Figure 3.10, 3.11), PmtA could be taken up by Jurkat T cells and affect cell signaling through interaction with intracellular components. In addition, if PmtA can be found intracellularly, it could influence the redox status of the cell and alter redox-sensitive signaling. Since it is known that H_2O_2 uptake is essential to the activation of Rho family GTPase and subsequent actin polymerization and migration in T cells, [244] a PmtA-induced change in the redox status of the cell is likely to affect a cell's ability to migrate in response to chemokines. In this case, PmtA may not be a specific inhibitor of cell movement, but a global inhibitor that can exert an inhibitory chemotactic effect on more than one chemokine-receptor axis or more than one immune cell type. In order to determine if PmtA can affect the over all redox-status of the cell it will be necessary to measure the intracellular ROS in presence of PmtA with the redox sensitive probe H_2DCFDA. It would also be interesting to study PmtA's ability to affect the movement of Jurkat T cells and other cell types in response to other chemokines. This will determine if PmtA specifically exhibits a response on CXCR4 or if the response is a global response.

The ability of PmtA to effect the migration of immune cells coupled with the fact that its expression is necessary for the production of the virulence factor pyocyanin suggests that PmtA contributes to the overall virulence of *P. aeruginosa*. Infection models can be used to determine if there is a difference in host survival between

organisms inoculated with wildtype strain PAO1 or PmtA-deficient strain PW4670. A simple infection model uses *Galleria mellonella* larvae injected with various concentrations of both strains of *P. aeruginosa*. In this model the survival of the larvae over time is recorded. It will also be necessary to determine if there is a difference in virulence in a more complex mouse-model of infection. In this model mice could be inoculated intranasally and the survival of mice inoculated with either PAO1 or PW4670 would be recorded. Additionally, bacterial burden in the lungs or in the broncho-alveolar fluid can be measured. Histological staining of the lungs of mice infected would also determine if there is a difference in immune cell infiltration into the site of infection when a mouse is infected with either PAO1 or PW4670.

The decrease in pyocyanin production as a result of the absence of PmtA may make the bacteria more susceptible to antibiotic therapy than its wildtype counterpart. Through adaptations of the previously mention infection models, it could be determined if PmtA-deficient bacteria are more susceptible to antibiotic treatment. Additionally, blocking the function of PmtA, with an PmtA-specific siRNA, coupled with antibiotic therapy could also influence the effectiveness of antibiotic intervention. An PmtA-specific antibody may not be effective as it would have to traverse the peptidoglycan layer of *P. aeruginosa.* It may be easier to disrupt a single gene, rather than the several genes involved pyocyanin production and biofilm production.

A continuation of the study of the functions of PmtA in context of infection could be vital to future treatments of *P. aeruginosa* infection. If the addition of an PmtA-specific siRNA blocks the function of this protein *in vivo*, it could represent a novel therapeutic intervention. As more and more pathogens begin to acquire resistance to

antibiotics, new therapies must be developed so humans do no succumb to once-treatable infections. Targeting of virulence factors and resistance mechanism, such as the *P. aeruginosa* efflux pump, to weaken bacteria is a potential new avenue to combat the ever-growing problem of bacterial resistance to antibiotics. If targeting PmtA decreases the production of pyocyanin or changes the over redox-environment at the site of infection, it could decrease the virulence of the bacteria and allow antibiotics to penetrate the bacteria. The implication of targeting a bacterial MT in the management of a bacterial infection represents potential novel and innovative approach to the treatment of antibiotic resistant human pathogens.

CHAPTER 6: REFERENCES

1. Kagi, J.H. and A. Schaffer, *Biochemistry of metallothionein.* Biochemistry, 1988. **27**(23): p. 8509-15.
2. Heesen, C., et al., *Endocrine and cytokine responses to acute psychological stress in multiple sclerosis.* Brain Behav Immun, 2002. **16**(3): p. 282-7.
3. Gilgun-Sherki, Y., E. Melamed, and D. Offen, *The role of oxidative stress in the pathogenesis of multiple sclerosis: the need for effective antioxidant therapy.* J Neurol, 2004. **251**(3): p. 261-8.
4. Nazli, A., et al., *Epithelia under metabolic stress perceive commensal bacteria as a threat.* Am J Pathol, 2004. **164**(3): p. 947-57.
5. Mawdsley, J.E. and D.S. Rampton, *Psychological stress in IBD: new insights into pathogenic and therapeutic implications.* Gut, 2005. **54**(10): p. 1481-91.
6. Dominguez, C., et al., *Oxidative stress at onset and in early stages of type 1 diabetes in children and adolescents.* Diabetes Care, 1998. **21**(10): p. 1736-42.
7. Steptoe, A. and M. Kivimaki, *Stress and cardiovascular disease.* Nat Rev Cardiol, 2012. **9**(6): p. 360-70.
8. Fleshner, M., *Stress-evoked sterile inflammation, danger associated molecular patterns (DAMPs), microbial associated molecular patterns (MAMPs) and the inflammasome.* Brain Behav Immun, 2013. **27**(1): p. 1-7.
9. Hemingway, H., et al., *Social and psychosocial influences on inflammatory markers and vascular function in civil servants (the Whitehall II study).* Am J Cardiol, 2003. **92**(8): p. 984-7.
10. Kiecolt-Glaser, J.K., et al., *Chronic stress and age-related increases in the proinflammatory cytokine IL-6.* Proc Natl Acad Sci U S A, 2003. **100**(15): p. 9090-5.
11. Glaser, R., et al., *Stress-induced modulation of the immune response to recombinant hepatitis B vaccine.* Psychosom Med, 1992. **54**(1): p. 22-9.
12. Morag, M., et al., *Psychological variables as predictors of rubella antibody titers and fatigue--a prospective, double blind study.* J Psychiatr Res, 1999. **33**(5): p. 389-95.
13. Bailey, M.T., et al., *Exposure to a social stressor alters the structure of the intestinal microbiota: implications for stressor-induced immunomodulation.* Brain Behav Immun, 2011. **25**(3): p. 397-407.
14. Konstantinos, A.P. and J.F. Sheridan, *Stress and influenza viral infection: modulation of proinflammatory cytokine responses in the lung.* Respir Physiol, 2001. **128**(1): p. 71-7.
15. Thannickal, V.J. and B.L. Fanburg, *Reactive oxygen species in cell signaling.* Am J Physiol Lung Cell Mol Physiol, 2000. **279**(6): p. L1005-28.
16. Borghesi, L.A. and M.A. Lynes, *Stress proteins as agents of immunological change: some lessons from metallothionein.* Cell Stress Chaperones, 1996. **1**(2): p. 99-108.

17. Poljsak, B. and I. Milisav, *Clinical implications of cellular stress responses.* Bosn J Basic Med Sci, 2012. **12**(2): p. 122-6.
18. Robert, J., *Evolution of heat shock protein and immunity.* Dev Comp Immunol, 2003. **27**(6-7): p. 449-64.
19. Kampinga, H.H., et al., *Guidelines for the nomenclature of the human heat shock proteins.* Cell Stress Chaperones, 2009. **14**(1): p. 105-11.
20. Welch, W.J. and J.P. Suhan, *Morphological study of the mammalian stress response: characterization of changes in cytoplasmic organelles, cytoskeleton, and nucleoli, and appearance of intranuclear actin filaments in rat fibroblasts after heat-shock treatment.* J Cell Biol, 1985. **101**(4): p. 1198-211.
21. Koga, T., et al., *T cells against a bacterial heat shock protein recognize stressed macrophages.* Science, 1989. **245**(4922): p. 1112-5.
22. Nieland, T.J., et al., *Isolation of an immunodominant viral peptide that is endogenously bound to the stress protein GP96/GRP94.* Proc Natl Acad Sci U S A, 1996. **93**(12): p. 6135-9.
23. Srivastava, P.K., et al., *Heat shock proteins come of age: primitive functions acquire new roles in an adaptive world.* Immunity, 1998. **8**(6): p. 657-65.
24. Wells, A.D., et al., *Hsp72-mediated augmentation of MHC class I surface expression and endogenous antigen presentation.* Int Immunol, 1998. **10**(5): p. 609-17.
25. Tamura, Y., et al., *Immunotherapy of tumors with autologous tumor-derived heat shock protein preparations.* Science, 1997. **278**(5335): p. 117-20.
26. Udono, H. and P.K. Srivastava, *Heat shock protein 70-associated peptides elicit specific cancer immunity.* J Exp Med, 1993. **178**(4): p. 1391-6.
27. Suto, R. and P.K. Srivastava, *A mechanism for the specific immunogenicity of heat shock protein-chaperoned peptides.* Science, 1995. **269**(5230): p. 1585-8.
28. Srivastava, P., *Interaction of heat shock proteins with peptides and antigen presenting cells: chaperoning of the innate and adaptive immune responses.* Annu Rev Immunol, 2002. **20**: p. 395-425.
29. Lehner, T., et al., *Heat shock proteins generate beta-chemokines which function as innate adjuvants enhancing adaptive immunity.* Eur J Immunol, 2000. **30**(2): p. 594-603.
30. Wang, Y., et al., *Stimulation of Th1-polarizing cytokines, C-C chemokines, maturation of dendritic cells, and adjuvant function by the peptide binding fragment of heat shock protein 70.* J Immunol, 2002. **169**(5): p. 2422-9.
31. Furey, W.F., et al., *Crystal structure of Cd,Zn metallothionein.* Science, 1986. **231**(4739): p. 704-10.
32. Ejnik, J., et al., *Interprotein metal ion exchange between cadmium-carbonic anhydrase and apo- or zinc-metallothionein.* J Biol Inorg Chem, 1999. **4**(6): p. 784-90.
33. Zeng, J., et al., *Thionein (apometallothionein) can modulate DNA binding and transcription activation by zinc finger containing factor Sp1.* FEBS Lett, 1991. **279**(2): p. 310-2.
34. Daston, G.P., et al., *Altered Zn status by alpha-hederin in the pregnant rat and its relationship to adverse developmental outcome.* Reprod Toxicol, 1994. **8**(1): p. 15-24.

35. Kang, Y.J., *Metallothionein redox cycle and function.* Exp Biol Med (Maywood), 2006. **231**(9): p. 1459-67.
36. Theocharis, S.E., A.P. Margeli, and A. Koutselinis, *Metallothionein: a multifunctional protein from toxicity to cancer.* Int J Biol Markers, 2003. **18**(3): p. 162-9.
37. Chatham, W.W., et al., *Degradation of human articular cartilage by neutrophils in synovial fluid.* Arthritis Rheum, 1993. **36**(1): p. 51-8.
38. Kitsis, E. and G. Weissmann, *The role of the neutrophil in rheumatoid arthritis.* Clin Orthop Relat Res, 1991(265): p. 63-72.
39. Kinne, R.W., et al., *Macrophages in rheumatoid arthritis.* Arthritis Res, 2000. **2**(3): p. 189-202.
40. Taysi, S., et al., *Lipid peroxidation, some extracellular antioxidants, and antioxidant enzymes in serum of patients with rheumatoid arthritis.* Rheumatology International, 2002. **21**(5): p. 200-204.
41. Kumagai, T., et al., *A lipid peroxidation-derived inflammatory mediator: identification of 4-hydroxy-2-nonenal as a potential inducer of cyclooxygenase-2 in macrophages.* J Biol Chem, 2004. **279**(46): p. 48389-96.
42. Youn, J., et al., *Metallothionein suppresses collagen-induced arthritis via induction of TGF-beta and down-regulation of proinflammatory mediators.* Clin Exp Immunol, 2002. **129**(2): p. 232-9.
43. Blindauer, C.A., *Metallothioneins with unusual residues: histidines as modulators of zinc affinity and reactivity.* J Inorg Biochem, 2008. **102**(3): p. 507-21.
44. Blindauer, C.A., *Bacterial metallothioneins: past, present, and questions for the future.* J Biol Inorg Chem, 2011. **16**(7): p. 1011-24.
45. Stadtman, E.R., *Oxidation of free amino acids and amino acid residues in proteins by radiolysis and by metal-catalyzed reactions.* Annu Rev Biochem, 1993. **62**: p. 797-821.
46. Karin, M., et al., *Human metallothionein genes are clustered on chromosome 16.* Proc Natl Acad Sci U S A, 1984. **81**(17): p. 5494-8.
47. Cox, D.R. and R.D. Palmiter, *The metallothionein-I gene maps to mouse chromosome 8: implications for human Menkes' disease.* Hum Genet, 1983. **64**(1): p. 61-4.
48. Takahashi, S., *Molecular functions of metallothionein and its role in hematological malignancies.* J Hematol Oncol, 2012. **5**: p. 41.
49. Emeny, R.T., et al., *Manipulations of metallothionein gene dose accelerate the response to Listeria monocytogenes.* Chem Biol Interact, 2009. **181**(2): p. 243-53.
50. Palmiter, R.D., et al., *MT-III, a brain-specific member of the metallothionein gene family.* Proc Natl Acad Sci U S A, 1992. **89**(14): p. 6333-7.
51. Quaife, C.J., et al., *Induction of a new metallothionein isoform (MT-IV) occurs during differentiation of stratified squamous epithelia.* Biochemistry, 1994. **33**(23): p. 7250-9.
52. Savino, W., et al., *Thymic hormone-containing cells. V. Immunohistological detection of metallothionein within the cells bearing thymulin (a zinc-*

containing hormone) in human and mouse thymuses. J Histochem Cytochem, 1984. **32**(9): p. 942-6.
53. Borghesi, L.A., et al., *Interactions of metallothionein with murine lymphocytes: plasma membrane binding and proliferation.* Toxicology, 1996. **108**(1-2): p. 129-40.
54. Canpolat, E. and M.A. Lynes, *In vivo manipulation of endogenous metallothionein with a monoclonal antibody enhances a T-dependent humoral immune response.* Toxicol Sci, 2001. **62**(1): p. 61-70.
55. Youn, J., et al., *Immunomodulatory activities of extracellular metallothionein. II. Effects on macrophage functions.* J Toxicol Environ Health, 1995. **45**(4): p. 397-413.
56. Lynes, M.A., J.S. Garvey, and D.A. Lawrence, *Extracellular metallothionein effects on lymphocyte activities.* Mol Immunol, 1990. **27**(3): p. 211-9.
57. Lynes, M.A., et al., *Immunomodulatory activities of extracellular metallothionein. I. Metallothionein effects on antibody production.* Toxicology, 1993. **85**(2-3): p. 161-77.
58. Apel, K. and H. Hirt, *Reactive oxygen species: metabolism, oxidative stress, and signal transduction.* Annu Rev Plant Biol, 2004. **55**: p. 373-99.
59. Halliwell, B. and O.I. Aruoma, *DNA damage by oxygen-derived species. Its mechanism and measurement in mammalian systems.* FEBS Lett, 1991. **281**(1-2): p. 9-19.
60. Halliwell, B. and S. Chirico, *Lipid peroxidation: its mechanism, measurement, and significance.* Am J Clin Nutr, 1993. **57**(5 Suppl): p. 715S-724S; discussion 724S-725S.
61. Cerielo, A., et al., *Hyperglycemia counterbalances the antihypertensive effect of glutathione in diabetic patients: evidence linking hypertension and glycemia through the oxidative stress in diabetes mellitus.* J Diabetes Complications, 1997. **11**(4): p. 250-5.
62. Dincer, Y., et al., *Effect of oxidative stress on glutathione pathway in red blood cells from patients with insulin-dependent diabetes mellitus.* Metabolism, 2002. **51**(10): p. 1360-2.
63. Signorelli, S.S., et al., *Oxidative stress and endothelial damage in patients with asymptomatic carotid atherosclerosis.* Clin Exp Med, 2001. **1**(1): p. 9-12.
64. Pedersen-Lane, J.H., R.B. Zurier, and D.A. Lawrence, *Analysis of the thiol status of peripheral blood leukocytes in rheumatoid arthritis patients.* J Leukoc Biol, 2007. **81**(4): p. 934-41.
65. Seven, A., et al., *Lipid, protein, DNA oxidation and antioxidant status in rheumatoid arthritis.* Clin Biochem, 2008. **41**(7-8): p. 538-43.
66. Lang, A.E., *The progression of Parkinson disease: a hypothesis.* Neurology, 2007. **68**(12): p. 948-52.
67. Spina, M.B. and G. Cohen, *Dopamine turnover and glutathione oxidation: implications for Parkinson disease.* Proc Natl Acad Sci U S A, 1989. **86**(4): p. 1398-400.
68. Barranco, S.C., et al., *Relationship between colorectal cancer glutathione levels and patient survival: early results.* Dis Colon Rectum, 2000. **43**(8): p. 1133-40.

69. Pastore, A., et al., *Analysis of glutathione: implication in redox and detoxification.* Clin Chim Acta, 2003. **333**(1): p. 19-39.
70. Zitka, O., et al., *Redox status expressed as GSH:GSSG ratio as a marker for oxidative stress in paediatric tumour patients.* Oncol Lett, 2012. **4**(6): p. 1247-1253.
71. Groemping, Y. and K. Rittinger, *Activation and assembly of the NADPH oxidase: a structural perspective.* Biochem J, 2005. **386**(Pt 3): p. 401-16.
72. Rhee, S.G., *Cell signaling. H2O2, a necessary evil for cell signaling.* Science, 2006. **312**(5782): p. 1882-3.
73. Segal, A.W. and A. Abo, *The biochemical basis of the NADPH oxidase of phagocytes.* Trends Biochem Sci, 1993. **18**(2): p. 43-7.
74. de Oliveira-Junior, E.B., et al., *The human NADPH oxidase: primary and secondary defects impairing the respiratory burst function and the microbicidal ability of phagocytes.* Scand J Immunol, 2011. **73**(5): p. 420-7.
75. Roos, D., R. van Bruggen, and C. Meischl, *Oxidative killing of microbes by neutrophils.* Microbes Infect, 2003. **5**(14): p. 1307-15.
76. Babior, B.M., J.T. Curnutte, and B.S. Kipnes, *Pyridine nucleotide-dependent superoxide production by a cell-free system from human granulocytes.* J Clin Invest, 1975. **56**(4): p. 1035-42.
77. Berendes, H., R.A. Bridges, and R.A. Good, *A fatal granulomatosus of childhood: the clinical study of a new syndrome.* Minn Med, 1957. **40**(5): p. 309-12.
78. Segal, A.W. and O.T. Jones, *Novel cytochrome b system in phagocytic vacuoles of human granulocytes.* Nature, 1978. **276**(5687): p. 515-7.
79. Segal, A.W., et al., *Absence of a newly described cytochrome b from neutrophils of patients with chronic granulomatous disease.* Lancet, 1978. **2**(8087): p. 446-9.
80. Quie, P.G., et al., *In vitro bactericidal capacity of human polymorphonuclear leukocytes: diminished activity in chronic granulomatous disease of childhood.* J Clin Invest, 1967. **46**(4): p. 668-79.
81. Holmes, B., A.R. Page, and R.A. Good, *Studies of the metabolic activity of leukocytes from patients with a genetic abnormality of phagocytic function.* J Clin Invest, 1967. **46**(9): p. 1422-32.
82. Baehner, R.L. and D.G. Nathan, *Leukocyte oxidase: defective activity in chronic granulomatous disease.* Science, 1967. **155**(3764): p. 835-6.
83. Robinson, J.M., *Phagocytic leukocytes and reactive oxygen species.* Histochem Cell Biol, 2009. **131**(4): p. 465-9.
84. Phillips, D.C., et al., *Aberrant reactive oxygen and nitrogen species generation in rheumatoid arthritis (RA): causes and consequences for immune function, cell survival, and therapeutic intervention.* Antioxid Redox Signal, 2010. **12**(6): p. 743-85.
85. Babior, B.M., R.S. Kipnes, and J.T. Curnutte, *Biological defense mechanisms. The production by leukocytes of superoxide, a potential bactericidal agent.* J Clin Invest, 1973. **52**(3): p. 741-4.

86. Winterbourn, C.C. and D. Metodiewa, *The reaction of superoxide with reduced glutathione.* Archives of Biochemistry and Biophysics, 1994. **314**(2): p. 284-90.
87. Babior, B.M., J.T. Curnutte, and R.S. Kipnes, *Biological defense mechanisms. Evidence for the participation of superoxide in bacterial killing by xanthine oxidase.* J Lab Clin Med, 1975. **85**(2): p. 235-44.
88. Klebanoff, S.J., *Role of the superoxide anion in the myeloperoxidase-mediated antimicrobial system.* J Biol Chem, 1974. **249**(12): p. 3724-8.
89. Rosen, H. and S.J. Klebanoff, *Bactericidal activity of a superoxide anion-generating system. A model for the polymorphonuclear leukocyte.* J Exp Med, 1979. **149**(1): p. 27-39.
90. Robinson, J.M., *Reactive oxygen species in phagocytic leukocytes.* Histochem Cell Biol, 2008. **130**(2): p. 281-97.
91. Winterbourn, C.C. and M.B. Hampton, *Thiol chemistry and specificity in redox signaling.* Free Radic Biol Med, 2008. **45**(5): p. 549-61.
92. Denu, J.M. and K.G. Tanner, *Specific and reversible inactivation of protein tyrosine phosphatases by hydrogen peroxide: evidence for a sulfenic acid intermediate and implications for redox regulation.* Biochemistry, 1998. **37**(16): p. 5633-42.
93. Groen, A., et al., *Differential oxidation of protein-tyrosine phosphatases.* J Biol Chem, 2005. **280**(11): p. 10298-304.
94. Lee, S.R., et al., *Reversible inactivation of the tumor suppressor PTEN by H2O2.* J Biol Chem, 2002. **277**(23): p. 20336-42.
95. Meng, T.C., T. Fukada, and N.K. Tonks, *Reversible oxidation and inactivation of protein tyrosine phosphatases in vivo.* Mol Cell, 2002. **9**(2): p. 387-99.
96. Ross, S.H., et al., *Differential redox regulation within the PTP superfamily.* Cell Signal, 2007. **19**(7): p. 1521-30.
97. Cantin, A.M., P. Larivee, and R.O. Begin, *Extracellular glutathione suppresses human lung fibroblast proliferation.* Am J Respir Cell Mol Biol, 1990. **3**(1): p. 79-85.
98. Das, S.K., A.C. White, and B.L. Fanburg, *Modulation of transforming growth factor-beta 1 antiproliferative effects on endothelial cells by cysteine, cystine, and N-acetylcysteine.* J Clin Invest, 1992. **90**(5): p. 1649-56.
99. Jakob, U., et al., *Chaperone activity with a redox switch.* Cell, 1999. **96**(3): p. 341-52.
100. Jakob, U., M. Eser, and J.C. Bardwell, *Redox switch of hsp33 has a novel zinc-binding motif.* J Biol Chem, 2000. **275**(49): p. 38302-10.
101. Gallogly, M.M. and J.J. Mieyal, *Mechanisms of reversible protein glutathionylation in redox signaling and oxidative stress.* Curr Opin Pharmacol, 2007. **7**(4): p. 381-91.
102. Berndt, C., C.H. Lillig, and A. Holmgren, *Thiol-based mechanisms of the thioredoxin and glutaredoxin systems: implications for diseases in the cardiovascular system.* Am J Physiol Heart Circ Physiol, 2007. **292**(3): p. H1227-36.
103. Choi, H., et al., *Structural basis of the redox switch in the OxyR transcription factor.* Cell, 2001. **105**(1): p. 103-13.

104. Zheng, M., F. Aslund, and G. Storz, *Activation of the OxyR transcription factor by reversible disulfide bond formation.* Science, 1998. **279**(5357): p. 1718-21.
105. Aslund, F., et al., *Regulation of the OxyR transcription factor by hydrogen peroxide and the cellular thiol-disulfide status.* Proc Natl Acad Sci U S A, 1999. **96**(11): p. 6161-5.
106. Banerjee, D., S. Onosaka, and M.G. Cherian, *Immunohistochemical localization of metallothionein in cell nucleus and cytoplasm of rat liver and kidney.* Toxicology, 1982. **24**(2): p. 95-105.
107. Maret, W., *The function of zinc metallothionein: a link between cellular zinc and redox state.* J Nutr, 2000. **130**(5S Suppl): p. 1455S-8S.
108. Maret, W. and A. Krezel, *Cellular zinc and redox buffering capacity of metallothionein/thionein in health and disease.* Mol Med, 2007. **13**(7-8): p. 371-5.
109. Tarpey, M.M., D.A. Wink, and M.B. Grisham, *Methods for detection of reactive metabolites of oxygen and nitrogen: in vitro and in vivo considerations.* Am J Physiol Regul Integr Comp Physiol, 2004. **286**(3): p. R431-44.
110. Jones, D.P., *Redox potential of GSH/GSSG couple: assay and biological significance.* Methods Enzymol, 2002. **348**: p. 93-112.
111. Marnett, L.J., *Lipid peroxidation-DNA damage by malondialdehyde.* Mutat Res, 1999. **424**(1-2): p. 83-95.
112. Bass, D.A., et al., *Flow cytometric studies of oxidative product formation by neutrophils: a graded response to membrane stimulation.* J Immunol, 1983. **130**(4): p. 1910-7.
113. Moser, B., et al., *Chemokines: multiple levels of leukocyte migration control.* Trends Immunol, 2004. **25**(2): p. 75-84.
114. Maghazachi, A.A., *Intracellular signaling events at the leading edge of migrating cells.* Int J Biochem Cell Biol, 2000. **32**(9): p. 931-43.
115. Murphy, K., et al., *Janeway's immunobiology*. 8th ed. 2012, New York: Garland Science. xix, 868 p.
116. Nickoloff, B.J., et al., *Cellular localization of interleukin-8 and its inducer, tumor necrosis factor-alpha in psoriasis.* Am J Pathol, 1991. **138**(1): p. 129-40.
117. Seitz, M., et al., *Enhanced production of neutrophil-activating peptide-1/interleukin-8 in rheumatoid arthritis.* J Clin Invest, 1991. **87**(2): p. 463-9.
118. Mahida, Y.R., et al., *Enhanced synthesis of neutrophil-activating peptide-1/interleukin-8 in active ulcerative colitis.* Clin Sci (Lond), 1992. **82**(3): p. 273-5.
119. DiMango, E., et al., *Activation of NF-kappaB by adherent Pseudomonas aeruginosa in normal and cystic fibrosis respiratory epithelial cells.* J Clin Invest, 1998. **101**(11): p. 2598-605.
120. DiMango, E., et al., *Diverse Pseudomonas aeruginosa gene products stimulate respiratory epithelial cells to produce interleukin-8.* J Clin Invest, 1995. **96**(5): p. 2204-10.
121. Tsai, W.C., et al., *CXC chemokine receptor CXCR2 is essential for protective innate host response in murine Pseudomonas aeruginosa pneumonia.* Infect Immun, 2000. **68**(7): p. 4289-96.

122. Oppenheim, J.J. and D. Yang, *Alarmins: chemotactic activators of immune responses.* Curr Opin Immunol, 2005. **17**(4): p. 359-65.
123. Zlotnik, A. and O. Yoshie, *The chemokine superfamily revisited.* Immunity, 2012. **36**(5): p. 705-16.
124. Chen, S.C., et al., *Ectopic expression of the murine chemokines CCL21a and CCL21b induces the formation of lymph node-like structures in pancreas, but not skin, of transgenic mice.* J Immunol, 2002. **168**(3): p. 1001-8.
125. Charmoy, M., et al., *Neutrophil-derived CCL3 is essential for the rapid recruitment of dendritic cells to the site of Leishmania major inoculation in resistant mice.* PLoS Pathog, 2010. **6**(2): p. e1000755.
126. Busillo, J.M. and J.L. Benovic, *Regulation of CXCR4 signaling.* Biochim Biophys Acta, 2007. **1768**(4): p. 952-63.
127. Wong, M.M. and E.N. Fish, *Chemokines: attractive mediators of the immune response.* Semin Immunol, 2003. **15**(1): p. 5-14.
128. Kolaczkowska, E. and P. Kubes, *Neutrophil recruitment and function in health and inflammation.* Nat Rev Immunol, 2013. **13**(3): p. 159-75.
129. Hauser, A.E., et al., *Chemotactic responsiveness toward ligands for CXCR3 and CXCR4 is regulated on plasma blasts during the time course of a memory immune response.* J Immunol, 2002. **169**(3): p. 1277-82.
130. Yin, X., D.A. Knecht, and M.A. Lynes, *Metallothionein mediates leukocyte chemotaxis.* BMC Immunol, 2005. **6**: p. 21.
131. Boyden, S., *The chemotactic effect of mixtures of antibody and antigen on polymorphonuclear leucocytes.* J Exp Med, 1962. **115**: p. 453-66.
132. Lauffenburger, D.A., R.T. Tranquillo, and S.H. Zigmond, *Concentration gradients of chemotactic factors in chemotaxis assays.* Methods Enzymol, 1988. **162**: p. 85-101.
133. Nelson, R.D., P.G. Quie, and R.L. Simmons, *Chemotaxis under agarose: a new and simple method for measuring chemotaxis and spontaneous migration of human polymorphonuclear leukocytes and monocytes.* J Immunol, 1975. **115**(6): p. 1650-6.
134. Newton-Nash, D.K., et al., *Assessment of chemokinetic behavior of inflammatory lung macrophages in a linear under-agarose assay.* J Leukoc Biol, 1990. **48**(4): p. 297-305.
135. Pietrosimone, K.M., et al., *In vitro assays of chemotaxis as a window into mechanisms of toxicant-induced immunomodulation.* Curr Protoc Toxicol, 2013. **58**: p. 18 17 1-18 17 24.
136. Giaever, I. and C.R. Keese, *Monitoring fibroblast behavior in tissue culture with an applied electric field.* Proc Natl Acad Sci U S A, 1984. **81**(12): p. 3761-4.
137. Keese C, G.I., *A Whole Cell Biosensor bsed on Cell-Substrate Interactions.* IEEE Engineering in Medicine and Biology Society, 1990. **12**(3): p. 0500-0501.
138. Hadjout, N., et al., *Automated real-time measurement of chemotactic cell motility.* Biotechniques, 2001. **31**(5): p. 1130-8.
139. Hadjout, N., et al., *Automated real-time measurements of leukocyte chemotaxis.* J Immunol Methods, 2007. **320**(1-2): p. 70-80.
140. Pietrosimone, K.M., et al., *Measurement of Cellular Chemotaxis with ECIS/Taxis.* J Vis Exp, 2012(62).

141. Segal, G. and E.Z. Ron, *Regulation of heat-shock response in bacteria.* Ann N Y Acad Sci, 1998. **851**: p. 147-51.
142. Segal, G. and E.Z. Ron, *Heat shock activation of the groESL operon of Agrobacterium tumefaciens and the regulatory roles of the inverted repeat.* J Bacteriol, 1996. **178**(12): p. 3634-40.
143. Susin, M.F., et al., *GroES/GroEL and DnaK/DnaJ have distinct roles in stress responses and during cell cycle progression in Caulobacter crescentus.* J Bacteriol, 2006. **188**(23): p. 8044-53.
144. Olafson, R.W., K. Abel, and R.G. Sim, *Prokaryotic metallothionein: preliminary characterization of a blue-green alga heavy metal-binding protein.* Biochem Biophys Res Commun, 1979. **89**(1): p. 36-43.
145. Olafson, R.W. and R.G. Sim, *An electrochemical approach to quantitation and characterization of metallothioneins.* Anal Biochem, 1979. **100**(2): p. 343-51.
146. Olafson, R.W., R.G. Sim, and A. Kearns, *Physiological and chemical characterization of invertebrate metallothionein-like proteins.* Experientia Suppl, 1979. **34**: p. 197-204.
147. Blindauer, C.A. and P.J. Sadler, *How to hide zinc in a small protein.* Acc Chem Res, 2005. **38**(1): p. 62-9.
148. Olafson, R.W., W.D. McCubbin, and C.M. Kay, *Primary- and secondary-structural analysis of a unique prokaryotic metallothionein from a Synechococcus sp. cyanobacterium.* Biochem J, 1988. **251**(3): p. 691-9.
149. Higham, D.P., P.J. Sadler, and M.D. Scawen, *Cadmium-Resistant Pseudomonas putida Synthesizes Novel Cadmium Proteins.* Science, 1984. **225**(4666): p. 1043-6.
150. Williams, R.J. and J.J. Frausto Da Silva, *Evolution was chemically constrained.* J Theor Biol, 2003. **220**(3): p. 323-43.
151. Shi, J., et al., *Cyanobacterial metallothionein gene expressed in Escherichia coli. Metal-binding properties of the expressed protein.* FEBS Lett, 1992. **303**(2-3): p. 159-63.
152. Gold, B., et al., *Identification of a copper-binding metallothionein in pathogenic mycobacteria.* Nat Chem Biol, 2008. **4**(10): p. 609-16.
153. Wolschendorf, F., et al., *Copper resistance is essential for virulence of Mycobacterium tuberculosis.* Proc Natl Acad Sci U S A, 2011. **108**(4): p. 1621-6.
154. Daniels, M.J., et al., *Coordination of Zn2+ (and Cd2+) by prokaryotic metallothionein. Involvement of his-imidazole.* J Biol Chem, 1998. **273**(36): p. 22957-61.
155. Jiang, L.J., W. Maret, and B.L. Vallee, *The glutathione redox couple modulates zinc transfer from metallothionein to zinc-depleted sorbitol dehydrogenase.* Proc Natl Acad Sci U S A, 1998. **95**(7): p. 3483-8.
156. Morby, A.P., et al., *SmtB is a metal-dependent repressor of the cyanobacterial metallothionein gene smtA: identification of a Zn inhibited DNA-protein complex.* Nucleic Acids Res, 1993. **21**(4): p. 921-5.
157. Linnane, S.J., et al., *Total sputum nitrate plus nitrite is raised during acute pulmonary infection in cystic fibrosis.* Am J Respir Crit Care Med, 1998. **158**(1): p. 207-12.

158. Woese, C.R., et al., *The Phylogeny of Purple Bacteria - the Gamma-Subdivision.* Systematic and Applied Microbiology, 1985. **6**(1): p. 25-33.
159. Selifonov, S.A., J.E. Gurst, and L.P. Wackett, *Regioselective dioxygenation of ortho-trifluoromethylbenzoate by Pseudomonas aeruginosa 142: evidence for 1,2-dioxygenation as a mechanism in ortho-halobenzoate dehalogenation.* Biochem Biophys Res Commun, 1995. **213**(3): p. 759-67.
160. Van Delden, C. and B.H. Iglewski, *Cell-to-cell signaling and Pseudomonas aeruginosa infections.* Emerg Infect Dis, 1998. **4**(4): p. 551-60.
161. Forman, H.J. and M. Torres, *Redox signaling in macrophages.* Mol Aspects Med, 2001. **22**(4-5): p. 189-216.
162. Morissette, C., et al., *Lung phagocyte bactericidal function in strains of mice resistant and susceptible to Pseudomonas aeruginosa.* Infect Immun, 1996. **64**(12): p. 4984-92.
163. Sadikot, R.T., et al., *p47phox deficiency impairs NF-kappa B activation and host defense in Pseudomonas pneumonia.* J Immunol, 2004. **172**(3): p. 1801-8.
164. Day, B.J., et al., *Role for cystic fibrosis transmembrane conductance regulator protein in a glutathione response to bronchopulmonary pseudomonas infection.* Infect Immun, 2004. **72**(4): p. 2045-51.
165. Ahmad, I.M., B.E. Britigan, and M.Y. Abdalla, *Oxidation of thiols and modification of redox-sensitive signaling in human lung epithelial cells exposed to Pseudomonas pyocyanin.* J Toxicol Environ Health A, 2011. **74**(1): p. 43-51.
166. Singh, P.K., et al., *Production of beta-defensins by human airway epithelia.* Proc Natl Acad Sci U S A, 1998. **95**(25): p. 14961-6.
167. Taggart, C.C., et al., *Inactivation of human beta-defensins 2 and 3 by elastolytic cathepsins.* J Immunol, 2003. **171**(2): p. 931-7.
168. Hajjar, A.M., et al., *Human Toll-like receptor 4 recognizes host-specific LPS modifications.* Nat Immunol, 2002. **3**(4): p. 354-9.
169. Takeuchi, O., et al., *Cutting edge: role of Toll-like receptor 1 in mediating immune response to microbial lipoproteins.* J Immunol, 2002. **169**(1): p. 10-4.
170. Brightbill, H.D., et al., *Host defense mechanisms triggered by microbial lipoproteins through toll-like receptors.* Science, 1999. **285**(5428): p. 732-6.
171. Hayashi, T., et al., *Enhancement of innate immunity against Mycobacterium avium infection by immunostimulatory DNA is mediated by indoleamine 2,3-dioxygenase.* Infect Immun, 2001. **69**(10): p. 6156-64.
172. Muzio, M., et al., *Toll-like receptor family and signalling pathway.* Biochem Soc Trans, 2000. **28**(5): p. 563-6.
173. Muir, A., et al., *Toll-like receptors in normal and cystic fibrosis airway epithelial cells.* Am J Respir Cell Mol Biol, 2004. **30**(6): p. 777-83.
174. Ratner, A.J., et al., *Cystic fibrosis pathogens activate Ca2+-dependent mitogen-activated protein kinase signaling pathways in airway epithelial cells.* J Biol Chem, 2001. **276**(22): p. 19267-75.
175. Koh, A.Y., et al., *Inescapable need for neutrophils as mediators of cellular innate immunity to acute Pseudomonas aeruginosa pneumonia.* Infect Immun, 2009. **77**(12): p. 5300-10.
176. Aderem, A. and R.J. Ulevitch, *Toll-like receptors in the induction of the innate immune response.* Nature, 2000. **406**(6797): p. 782-7.

177. Thoma-Uszynski, S., et al., *Induction of direct antimicrobial activity through mammalian toll-like receptors.* Science, 2001. **291**(5508): p. 1544-7.
178. Sauer, H., M. Wartenberg, and J. Hescheler, *Reactive oxygen species as intracellular messengers during cell growth and differentiation.* Cell Physiol Biochem, 2001. **11**(4): p. 173-86.
179. Speert, D.P., et al., *Functional characterization of macrophage receptors for in vitro phagocytosis of unopsonized Pseudomonas aeruginosa.* J Clin Invest, 1988. **82**(3): p. 872-9.
180. Kooguchi, K., et al., *Role of alveolar macrophages in initiation and regulation of inflammation in Pseudomonas aeruginosa pneumonia.* Infect Immun, 1998. **66**(7): p. 3164-9.
181. Cheung, D.O., K. Halsey, and D.P. Speert, *Role of pulmonary alveolar macrophages in defense of the lung against Pseudomonas aeruginosa.* Infect Immun, 2000. **68**(8): p. 4585-92.
182. Dunkley, M.L., R.L. Clancy, and A.W. Cripps, *A role for CD4+ T cells from orally immunized rats in enhanced clearance of Pseudomonas aeruginosa from the lung.* Immunology, 1994. **83**(3): p. 362-9.
183. Moser, C., et al., *Early immune response in susceptible and resistant mice strains with chronic Pseudomonas aeruginosa lung infection determines the type of T-helper cell response.* APMIS, 1999. **107**(12): p. 1093-100.
184. Moser, C., et al., *Improved outcome of chronic Pseudomonas aeruginosa lung infection is associated with induction of a Th1-dominated cytokine response.* Clin Exp Immunol, 2002. **127**(2): p. 206-13.
185. Reszka, K.J., et al., *Oxidation of pyocyanin, a cytotoxic product from Pseudomonas aeruginosa, by microperoxidase 11 and hydrogen peroxide.* Free Radic Biol Med, 2004. **36**(11): p. 1448-59.
186. Ayers, F.C., et al., *Fluorometric quantitation of cellular and nonprotein thiols.* Anal Biochem, 1986. **154**(1): p. 186-93.
187. O'Toole, G.A., *Microtiter dish biofilm formation assay.* J Vis Exp, 2011(47).
188. Blindauer, C.A., et al., *Multiple bacteria encode metallothioneins and SmtA-like zinc fingers.* Mol Microbiol, 2002. **45**(5): p. 1421-32.
189. Fredriksson, R., et al., *The G-protein-coupled receptors in the human genome form five main families. Phylogenetic analysis, paralogon groups, and fingerprints.* Mol Pharmacol, 2003. **63**(6): p. 1256-72.
190. Kobilka, B.K., *G protein coupled receptor structure and activation.* Biochim Biophys Acta, 2007. **1768**(4): p. 794-807.
191. Ji, T.H., M. Grossmann, and I. Ji, *G protein-coupled receptors. I. Diversity of receptor-ligand interactions.* J Biol Chem, 1998. **273**(28): p. 17299-302.
192. Pin, J.P., T. Galvez, and L. Prezeau, *Evolution, structure, and activation mechanism of family 3/C G-protein-coupled receptors.* Pharmacol Ther, 2003. **98**(3): p. 325-54.
193. Lodish H, B.A., Zipursky SL, et al., *Molecular Cell BIology* 4ed. 2000, New York: W. H Freeman.
194. Aksamit, R.R., P.S. Backlund, Jr., and G.L. Cantoni, *Cholera toxin inhibits chemotaxis by a cAMP-independent mechanism.* Proc Natl Acad Sci U S A, 1985. **82**(22): p. 7475-9.

195. Backlund, P.S., Jr., et al., *Pertussis toxin inhibition of chemotaxis and the ADP-ribosylation of a membrane protein in a human-mouse hybrid cell line.* Proc Natl Acad Sci U S A, 1985. **82**(9): p. 2637-41.
196. Becker, E.L., et al., *The inhibition of neutrophil granule enzyme secretion and chemotaxis by pertussis toxin.* J Cell Biol, 1985. **100**(5): p. 1641-6.
197. Spangrude, G.J., et al., *Inhibition of lymphocyte and neutrophil chemotaxis by pertussis toxin.* J Immunol, 1985. **135**(6): p. 4135-43.
198. Becker, O.M., et al., *G protein-coupled receptors: in silico drug discovery in 3D.* Proc Natl Acad Sci U S A, 2004. **101**(31): p. 11304-9.
199. Shirozu, M., et al., *Structure and chromosomal localization of the human stromal cell-derived factor 1 (SDF1) gene.* Genomics, 1995. **28**(3): p. 495-500.
200. De La Luz Sierra, M., et al., *Differential processing of stromal-derived factor-1alpha and stromal-derived factor-1beta explains functional diversity.* Blood, 2004. **103**(7): p. 2452-9.
201. Pablos, J.L., et al., *Stromal-cell derived factor is expressed by dendritic cells and endothelium in human skin.* Am J Pathol, 1999. **155**(5): p. 1577-86.
202. Ratajczak, M.Z., et al., *The pleiotropic effects of the SDF-1-CXCR4 axis in organogenesis, regeneration and tumorigenesis.* Leukemia, 2006. **20**(11): p. 1915-24.
203. Suratt, B.T., et al., *Role of the CXCR4/SDF-1 chemokine axis in circulating neutrophil homeostasis.* Blood, 2004. **104**(2): p. 565-71.
204. Ma, Q., et al., *Impaired B-lymphopoiesis, myelopoiesis, and derailed cerebellar neuron migration in CXCR4- and SDF-1-deficient mice.* Proc Natl Acad Sci U S A, 1998. **95**(16): p. 9448-53.
205. Nagasawa, T., et al., *Defects of B-cell lymphopoiesis and bone-marrow myelopoiesis in mice lacking the CXC chemokine PBSF/SDF-1.* Nature, 1996. **382**(6592): p. 635-8.
206. Zou, Y.R., et al., *Function of the chemokine receptor CXCR4 in haematopoiesis and in cerebellar development.* Nature, 1998. **393**(6685): p. 595-9.
207. Sanchez-Martin, L., et al., *The chemokine CXCL12 regulates monocyte-macrophage differentiation and RUNX3 expression.* Blood, 2011. **117**(1): p. 88-97.
208. Bleul, C.C., et al., *The HIV coreceptors CXCR4 and CCR5 are differentially expressed and regulated on human T lymphocytes.* Proc Natl Acad Sci U S A, 1997. **94**(5): p. 1925-30.
209. Zhou, N., et al., *Structural and functional characterization of human CXCR4 as a chemokine receptor and HIV-1 co-receptor by mutagenesis and molecular modeling studies.* J Biol Chem, 2001. **276**(46): p. 42826-33.
210. Haribabu, B., et al., *Regulation of human chemokine receptors CXCR4. Role of phosphorylation in desensitization and internalization.* J Biol Chem, 1997. **272**(45): p. 28726-31.
211. Tarasova, N.I., R.H. Stauber, and C.J. Michejda, *Spontaneous and ligand-induced trafficking of CXC-chemokine receptor 4.* J Biol Chem, 1998. **273**(26): p. 15883-6.

212. Cristillo, A.D., et al., *Up-regulation of HIV coreceptor CXCR4 expression in human T lymphocytes is mediated in part by a cAMP-responsive element.* FASEB J, 2002. **16**(3): p. 354-64.
213. Vinante, F., et al., *CD30 triggering by agonistic antibodies regulates CXCR4 expression and CXCL12 chemotactic activity in the cell line L540.* Blood, 2002. **99**(1): p. 52-60.
214. Cristillo, A.D. and B.E. Bierer, *Regulation of CXCR4 expression in human T lymphocytes by calcium and calcineurin.* Mol Immunol, 2003. **40**(8): p. 539-53.
215. Wu, Q., et al., *Extracellular calcium increases CXCR4 expression on bone marrow-derived cells and enhances pro-angiogenesis therapy.* J Cell Mol Med, 2009. **13**(9B): p. 3764-73.
216. Kury, P., et al., *Cyclic AMP and tumor necrosis factor-alpha regulate CXCR4 gene expression in Schwann cells.* Mol Cell Neurosci, 2003. **24**(1): p. 1-9.
217. De Paoli, P., *The immunological effects of interleukin 2 therapy in HIV+ patients.* Arch Immunol Ther Exp (Warsz), 2000. **48**(4): p. 243-9.
218. Wang, J., et al., *IL-4 and a glucocorticoid up-regulate CXCR4 expression on human CD4+ T lymphocytes and enhance HIV-1 replication.* J Leukoc Biol, 1998. **64**(5): p. 642-9.
219. Chen, S., et al., *Transforming growth factor-beta1 increases CXCR4 expression, stromal-derived factor-1alpha-stimulated signalling and human immunodeficiency virus-1 entry in human monocyte-derived macrophages.* Immunology, 2005. **114**(4): p. 565-74.
220. Liles, W.C., et al., *Mobilization of hematopoietic progenitor cells in healthy volunteers by AMD3100, a CXCR4 antagonist.* Blood, 2003. **102**(8): p. 2728-30.
221. Broxmeyer, H.E., et al., *Rapid mobilization of murine and human hematopoietic stem and progenitor cells with AMD3100, a CXCR4 antagonist.* J Exp Med, 2005. **201**(8): p. 1307-18.
222. Furze, R.C. and S.M. Rankin, *The role of the bone marrow in neutrophil clearance under homeostatic conditions in the mouse.* FASEB J, 2008. **22**(9): p. 3111-9.
223. Eash, K.J., et al., *CXCR2 and CXCR4 antagonistically regulate neutrophil trafficking from murine bone marrow.* J Clin Invest, 2010. **120**(7): p. 2423-31.
224. Ottoson, N.C., et al., *Cutting edge: T cell migration regulated by CXCR4 chemokine receptor signaling to ZAP-70 tyrosine kinase.* J Immunol, 2001. **167**(4): p. 1857-61.
225. Fernandis, A.Z., R.P. Cherla, and R.K. Ganju, *Differential regulation of CXCR4-mediated T-cell chemotaxis and mitogen-activated protein kinase activation by the membrane tyrosine phosphatase, CD45.* J Biol Chem, 2003. **278**(11): p. 9536-43.
226. Andreotti, A.H., et al., *T-cell signaling regulated by the Tec family kinase, Itk.* Cold Spring Harb Perspect Biol, 2010. **2**(7): p. a002287.
227. Fischer, A.M., et al., *Regulation of CXC chemokine receptor 4-mediated migration by the Tec family tyrosine kinase ITK.* J Biol Chem, 2004. **279**(28): p. 29816-20.

228. Princen, K., et al., *Inhibition of human immunodeficiency virus replication by a dual CCR5/CXCR4 antagonist.* J Virol, 2004. **78**(23): p. 12996-3006.
229. Verani, A., et al., *CXCR4 is a functional coreceptor for infection of human macrophages by CXCR4-dependent primary HIV-1 isolates.* J Immunol, 1998. **161**(5): p. 2084-8.
230. Roussos, E.T., J.S. Condeelis, and A. Patsialou, *Chemotaxis in cancer.* Nat Rev Cancer, 2011. **11**(8): p. 573-87.
231. Shim, H., S. Oishi, and N. Fujii, *Chemokine receptor CXCR4 as a therapeutic target for neuroectodermal tumors.* Semin Cancer Biol, 2009. **19**(2): p. 123-34.
232. Friedl, P. and B. Weigelin, *Interstitial leukocyte migration and immune function.* Nat Immunol, 2008. **9**(9): p. 960-9.
233. Murakami, T., et al., *Expression of CXC chemokine receptor-4 enhances the pulmonary metastatic potential of murine B16 melanoma cells.* Cancer Res, 2002. **62**(24): p. 7328-34.
234. Huang, E.H., et al., *A CXCR4 antagonist CTCE-9908 inhibits primary tumor growth and metastasis of breast cancer.* J Surg Res, 2009. **155**(2): p. 231-6.
235. Robledo, M.M., et al., *Expression of functional chemokine receptors CXCR3 and CXCR4 on human melanoma cells.* J Biol Chem, 2001. **276**(48): p. 45098-105.
236. Gomperts, B.N., et al., *Circulating progenitor epithelial cells traffic via CXCR4/CXCL12 in response to airway injury.* J Immunol, 2006. **176**(3): p. 1916-27.
237. Blindauer, C.A., et al., *A metallothionein containing a zinc finger within a four-metal cluster protects a bacterium from zinc toxicity.* Proc Natl Acad Sci U S A, 2001. **98**(17): p. 9593-8.
238. Poltorak, A., et al., *Defective LPS signaling in C3H/HeJ and C57BL/10ScCr mice: mutations in Tlr4 gene.* Science, 1998. **282**(5396): p. 2085-8.
239. Goujon, M., et al., *A new bioinformatics analysis tools framework at EMBL-EBI.* Nucleic Acids Res, 2010. **38**(Web Server issue): p. W695-9.
240. Larkin, M.A., et al., *Clustal W and Clustal X version 2.0.* Bioinformatics, 2007. **23**(21): p. 2947-8.
241. McWilliam, H., et al., *Analysis Tool Web Services from the EMBL-EBI.* Nucleic Acids Res, 2013. **41**(Web Server issue): p. W597-600.
242. Altschul, S.F., et al., *Basic local alignment search tool.* J Mol Biol, 1990. **215**(3): p. 403-10.
243. Hong, K.U., et al., *Basal cells are a multipotent progenitor capable of renewing the bronchial epithelium.* Am J Pathol, 2004. **164**(2): p. 577-88.
244. Hara-Chikuma, M., et al., *Chemokine-dependent T cell migration requires aquaporin-3-mediated hydrogen peroxide uptake.* J Exp Med, 2012. **209**(10): p. 1743-52.
245. Chetram, M.A., A.S. Don-Salu-Hewage, and C.V. Hinton, *ROS enhances CXCR4-mediated functions through inactivation of PTEN in prostate cancer cells.* Biochem Biophys Res Commun, 2011. **410**(2): p. 195-200.
246. Jones, K.J., et al., *Cysteine (C)-X-C Receptor 4 Regulates NADPH Oxidase-2 During Oxidative Stress in Prostate Cancer Cells.* Cancer Microenviron, 2013.

247. Lee, R.L., J. Westendorf, and M.R. Gold, *Differential role of reactive oxygen species in the activation of mitogen-activated protein kinases and Akt by key receptors on B-lymphocytes: CD40, the B cell antigen receptor, and CXCR4.* J Cell Commun Signal, 2007. **1**(1): p. 33-43.
248. Trautmann, M., P.M. Lepper, and M. Haller, *Ecology of Pseudomonas aeruginosa in the intensive care unit and the evolving role of water outlets as a reservoir of the organism.* Am J Infect Control, 2005. **33**(5 Suppl 1): p. S41-9.
249. Rosenberger, L.H., D.J. Lapar, and R.G. Sawyer, *Infections caused by multidrug resistant organisms are not associated with overall, all-cause mortality in the surgical intensive care unit: the 20,000 foot view.* J Am Coll Surg, 2012. **214**(5): p. 747-55.
250. Pena, C., et al., *Prospective multicenter study of the impact of carbapenem resistance on mortality in Pseudomonas aeruginosa bloodstream infections.* Antimicrob Agents Chemother, 2012. **56**(3): p. 1265-72.
251. Frederiksen, B., C. Koch, and N. Hoiby, *Changing epidemiology of Pseudomonas aeruginosa infection in Danish cystic fibrosis patients (1974-1995).* Pediatr Pulmonol, 1999. **28**(3): p. 159-66.
252. Chuanchuen, R., C.T. Narasaki, and H.P. Schweizer, *The MexJK efflux pump of Pseudomonas aeruginosa requires OprM for antibiotic efflux but not for efflux of triclosan.* Journal of Bacteriology, 2002. **184**(18): p. 5036-5044.
253. Aendekerk, S., et al., *The MexGHI-OpmD multidrug efflux pump controls growth, antibiotic susceptibility and virulence in Pseudomonas aeruginosa via 4-quinolone-dependent cell-to-cell communication.* Microbiology-Sgm, 2005. **151**: p. 1113-1125.
254. Hauser, A.R., et al., *Type III protein secretion is associated with poor clinical outcomes in patients with ventilator-associated pneumonia caused by Pseudomonas aeruginosa.* Crit Care Med, 2002. **30**(3): p. 521-8.
255. Talbot, G.H., et al., *Bad bugs need drugs: an update on the development pipeline from the Antimicrobial Availability Task Force of the Infectious Diseases Society of America.* Clin Infect Dis, 2006. **42**(5): p. 657-68.
256. Davies, D.G., et al., *The involvement of cell-to-cell signals in the development of a bacterial biofilm.* Science, 1998. **280**(5361): p. 295-8.
257. Passador, L., et al., *Expression of Pseudomonas aeruginosa virulence genes requires cell-to-cell communication.* Science, 1993. **260**(5111): p. 1127-30.
258. Fuqua, C. and E.P. Greenberg, *Listening in on bacteria: acyl-homoserine lactone signalling.* Nat Rev Mol Cell Biol, 2002. **3**(9): p. 685-95.
259. Smith, R.S., et al., *The Pseudomonas aeruginosa quorum-sensing molecule N-(3-oxododecanoyl)homoserine lactone contributes to virulence and induces inflammation in vivo.* J Bacteriol, 2002. **184**(4): p. 1132-9.
260. Smith, R.S. and B.H. Iglewski, *Pseudomonas aeruginosa quorum sensing as a potential antimicrobial target.* J Clin Invest, 2003. **112**(10): p. 1460-5.
261. Rutherford, S.T. and B.L. Bassler, *Bacterial quorum sensing: its role in virulence and possibilities for its control.* Cold Spring Harb Perspect Med, 2012. **2**(11).
262. Parsek, M.R., et al., *Acyl homoserine-lactone quorum-sensing signal generation.* Proc Natl Acad Sci U S A, 1999. **96**(8): p. 4360-5.

263. Val, D.L. and J.E. Cronan, Jr., *In vivo evidence that S-adenosylmethionine and fatty acid synthesis intermediates are the substrates for the LuxI family of autoinducer synthases.* J Bacteriol, 1998. **180**(10): p. 2644-51.
264. Pesci, E.C., et al., *Regulation of las and rhl quorum sensing in Pseudomonas aeruginosa.* J Bacteriol, 1997. **179**(10): p. 3127-32.
265. Latifi, A., et al., *A hierarchical quorum-sensing cascade in Pseudomonas aeruginosa links the transcriptional activators LasR and RhlR (VsmR) to expression of the stationary-phase sigma factor RpoS.* Mol Microbiol, 1996. **21**(6): p. 1137-46.
266. Brint, J.M. and D.E. Ohman, *Synthesis of multiple exoproducts in Pseudomonas aeruginosa is under the control of RhlR-RhlI, another set of regulators in strain PAO1 with homology to the autoinducer-responsive LuxR-LuxI family.* J Bacteriol, 1995. **177**(24): p. 7155-63.
267. Xiao, G., J. He, and L.G. Rahme, *Mutation analysis of the Pseudomonas aeruginosa mvfR and pqsABCDE gene promoters demonstrates complex quorum-sensing circuitry.* Microbiology, 2006. **152**(Pt 6): p. 1679-86.
268. Xiao, G., et al., *MvfR, a key Pseudomonas aeruginosa pathogenicity LTTR-class regulatory protein, has dual ligands.* Mol Microbiol, 2006. **62**(6): p. 1689-99.
269. Deziel, E., et al., *Analysis of Pseudomonas aeruginosa 4-hydroxy-2-alkylquinolines (HAQs) reveals a role for 4-hydroxy-2-heptylquinoline in cell-to-cell communication.* Proc Natl Acad Sci U S A, 2004. **101**(5): p. 1339-44.
270. Gallagher, L.A., et al., *Functions required for extracellular quinolone signaling by Pseudomonas aeruginosa.* J Bacteriol, 2002. **184**(23): p. 6472-80.
271. Gacesa, P., *Bacterial alginate biosynthesis--recent progress and future prospects.* Microbiology, 1998. **144 (Pt 5)**: p. 1133-43.
272. Shirtliff, M.E., J.T. Mader, and A.K. Camper, *Molecular interactions in biofilms.* Chem Biol, 2002. **9**(8): p. 859-71.
273. Hentzer, M., et al., *Alginate overproduction affects Pseudomonas aeruginosa biofilm structure and function.* J Bacteriol, 2001. **183**(18): p. 5395-401.
274. Govan, J.R., et al., *Isolation of a mucoid alginate-producing Pseudomonas aeruginosa strain from the equine guttural pouch.* J Clin Microbiol, 1992. **30**(3): p. 595-9.
275. Lam, J., et al., *Production of mucoid microcolonies by Pseudomonas aeruginosa within infected lungs in cystic fibrosis.* Infect Immun, 1980. **28**(2): p. 546-56.
276. Song, Z., et al., *Pseudomonas aeruginosa alginate is refractory to Th1 immune response and impedes host immune clearance in a mouse model of acute lung infection.* J Med Microbiol, 2003. **52**(Pt 9): p. 731-40.
277. Pritt, B., L. O'Brien, and W. Winn, *Mucoid Pseudomonas in cystic fibrosis.* Am J Clin Pathol, 2007. **128**(1): p. 32-4.
278. Bjarnsholt, T., et al., *Pseudomonas aeruginosa biofilms in the respiratory tract of cystic fibrosis patients.* Pediatr Pulmonol, 2009. **44**(6): p. 547-58.
279. Kolpen, M., et al., *Polymorphonuclear leucocytes consume oxygen in sputum from chronic Pseudomonas aeruginosa pneumonia in cystic fibrosis.* Thorax. **65**(1): p. 57-62.
280. Mull, J.D. and W.S. Callahan, *The role of the elastase of Pseudomonas aeruginosa in experimental infection.* Exp Mol Pathol, 1965. **4**(6): p. 567-75.

281. Weber, B., et al., *Interaction of pseudomonas exoproducts with phagocytic cells.* Can J Microbiol, 1982. **28**(6): p. 679-85.
282. Oliver, A.M. and D.M. Weir, *Inhibition of bacterial binding to mouse macrophages by Pseudomonas alginate.* J Clin Lab Immunol, 1983. **10**(4): p. 221-4.
283. Konig, B., S.S. Pedersen, and W. Konig, *Effect of Pseudomonas aeruginosa alginate on Escherichia coli- and Staphylococcus aureus-induced inflammatory mediator release from human cells.* Int Arch Allergy Immunol, 1993. **100**(2): p. 144-50.
284. Shime, N., et al., *Therapeutic administration of anti-PcrV F(ab')(2) in sepsis associated with Pseudomonas aeruginosa.* J Immunol, 2001. **167**(10): p. 5880-6.
285. Engel, J. and P. Balachandran, *Role of Pseudomonas aeruginosa type III effectors in disease.* Curr Opin Microbiol, 2009. **12**(1): p. 61-6.
286. Epelman, S., et al., *Different domains of Pseudomonas aeruginosa exoenzyme S activate distinct TLRs.* J Immunol, 2004. **173**(3): p. 2031-40.
287. Barbieri, A.M., et al., *ADP-ribosylation of Rab5 by ExoS of Pseudomonas aeruginosa affects endocytosis.* Infect Immun, 2001. **69**(9): p. 5329-34.
288. Coburn, J. and D.M. Gill, *ADP-ribosylation of p21ras and related proteins by Pseudomonas aeruginosa exoenzyme S.* Infect Immun, 1991. **59**(11): p. 4259-62.
289. Deng, Q., J. Sun, and J.T. Barbieri, *Uncoupling Crk signal transduction by Pseudomonas exoenzyme T.* J Biol Chem, 2005. **280**(43): p. 35953-60.
290. Krall, R., et al., *Pseudomonas aeruginosa ExoT is a Rho GTPase-activating protein.* Infect Immun, 2000. **68**(10): p. 6066-8.
291. Rabin, S.D., et al., *A C-terminal domain targets the Pseudomonas aeruginosa cytotoxin ExoU to the plasma membrane of host cells.* Infect Immun, 2006. **74**(5): p. 2552-61.
292. Sato, H. and D.W. Frank, *ExoU is a potent intracellular phospholipase.* Mol Microbiol, 2004. **53**(5): p. 1279-90.
293. Stirling, F.R., et al., *Eukaryotic localization, activation and ubiquitinylation of a bacterial type III secreted toxin.* Cell Microbiol, 2006. **8**(8): p. 1294-309.
294. Viboud, G.I. and J.B. Bliska, *Yersinia outer proteins: role in modulation of host cell signaling responses and pathogenesis.* Annu Rev Microbiol, 2005. **59**: p. 69-89.
295. Hauser, A.R., *The type III secretion system of Pseudomonas aeruginosa: infection by injection.* Nat Rev Microbiol, 2009. **7**(9): p. 654-65.
296. Xiao, R. and W.S. Kisaalita, *Iron acquisition from transferrin and lactoferrin by Pseudomonas aeruginosa pyoverdin.* Microbiology, 1997. **143 (Pt 7)**: p. 2509-15.
297. Rada, B. and T.L. Leto, *Pyocyanin effects on respiratory epithelium: relevance in Pseudomonas aeruginosa airway infections.* Trends Microbiol, 2013. **21**(2): p. 73-81.
298. Pierson, L.S., 3rd and E.A. Pierson, *Metabolism and function of phenazines in bacteria: impacts on the behavior of bacteria in the environment and*

biotechnological processes. Appl Microbiol Biotechnol, 2010. **86**(6): p. 1659-70.
299. Rada, B., et al., *The Pseudomonas toxin pyocyanin inhibits the dual oxidase-based antimicrobial system as it imposes oxidative stress on airway epithelial cells.* J Immunol, 2008. **181**(7): p. 4883-93.
300. Mahajan-Miklos, S., et al., *Molecular mechanisms of bacterial virulence elucidated using a Pseudomonas aeruginosa-Caenorhabditis elegans pathogenesis model.* Cell, 1999. **96**(1): p. 47-56.
301. O'Malley, Y.Q., et al., *The Pseudomonas secretory product pyocyanin inhibits catalase activity in human lung epithelial cells.* Am J Physiol Lung Cell Mol Physiol, 2003. **285**(5): p. L1077-86.
302. Koley, D., et al., *Discovery of a biofilm electrocline using real-time 3D metabolite analysis.* Proc Natl Acad Sci U S A, 2011. **108**(50): p. 19996-20001.
303. Usher, L.R., et al., *Induction of neutrophil apoptosis by the Pseudomonas aeruginosa exotoxin pyocyanin: a potential mechanism of persistent infection.* J Immunol, 2002. **168**(4): p. 1861-8.
304. Park, J.W. and B.M. Babior, *Effects of diacylglycerol on the activation and kinetics of the respiratory burst oxidase in a cell-free system from human neutrophils: evidence that diacylglycerol may regulate nucleotide uptake by a GTP-binding protein.* Arch Biochem Biophys, 1993. **306**(1): p. 119-24.
305. Muller, M. and T.C. Sorrell, *Modulation of neutrophil superoxide response and intracellular diacylglyceride levels by the bacterial pigment pyocyanin.* Infect Immun, 1997. **65**(6): p. 2483-7.
306. Allen, L., et al., *Pyocyanin production by Pseudomonas aeruginosa induces neutrophil apoptosis and impairs neutrophil-mediated host defenses in vivo.* J Immunol, 2005. **174**(6): p. 3643-9.
307. Bianchi, S.M., et al., *Impairment of apoptotic cell engulfment by pyocyanin, a toxic metabolite of Pseudomonas aeruginosa.* Am J Respir Crit Care Med, 2008. **177**(1): p. 35-43.
308. Rada, B., et al., *Reactive oxygen species mediate inflammatory cytokine release and EGFR-dependent mucin secretion in airway epithelial cells exposed to Pseudomonas pyocyanin.* Mucosal Immunol, 2011. **4**(2): p. 158-71.
309. Look, D.C., et al., *Pyocyanin and its precursor phenazine-1-carboxylic acid increase IL-8 and intercellular adhesion molecule-1 expression in human airway epithelial cells by oxidant-dependent mechanisms.* J Immunol, 2005. **175**(6): p. 4017-23.
310. Denning, G.M., et al., *Pseudomonas pyocyanin increases interleukin-8 expression by human airway epithelial cells.* Infect Immun, 1998. **66**(12): p. 5777-84.
311. Jeffery, P.K. and D. Li, *Airway mucosa: secretory cells, mucus and mucin genes.* Eur Respir J, 1997. **10**(7): p. 1655-62.
312. Devaraj, N., et al., *Differential binding of Pseudomonas aeruginosa to normal and cystic fibrosis tracheobronchial mucins.* Glycobiology, 1994. **4**(3): p. 307-16.
313. Held, K., et al., *Sequence-verified two-allele transposon mutant library for Pseudomonas aeruginosa PAO1.* J Bacteriol, 2012. **194**(23): p. 6387-9.

314. van Opijnen, T., K.L. Bodi, and A. Camilli, *Tn-seq: high-throughput parallel sequencing for fitness and genetic interaction studies in microorganisms.* Nat Methods, 2009. **6**(10): p. 767-72.
315. Morgan, R.D., et al., *The MmeI family: type II restriction-modification enzymes that employ single-strand modification for host protection.* Nucleic Acids Res, 2009. **37**(15): p. 5208-21.
316. van Opijnen, T. and A. Camilli, *Transposon insertion sequencing: a new tool for systems-level analysis of microorganisms.* Nat Rev Microbiol, 2013. **11**(7): p. 435-42.
317. Hassett, D.J., et al., *Response of Pseudomonas aeruginosa to pyocyanin: mechanisms of resistance, antioxidant defenses, and demonstration of a manganese-cofactored superoxide dismutase.* Infect Immun, 1992. **60**(2): p. 328-36.
318. Luong, P.M., et al., *Emergence of the P2 phenotype in Pseudomonas aeruginosa PAO1 strains involves various mutations in mexT or mexF.* J Bacteriol, 2014. **196**(2): p. 504-13.
319. Cifani, N., et al., *Reactive-oxygen-species-mediated P. aeruginosa killing is functional in human cystic fibrosis macrophages.* PLoS One, 2013. **8**(8): p. e71717.
320. Hayes, E., et al., *The cystic fibrosis neutrophil: a specialized yet potentially defective cell.* Arch Immunol Ther Exp (Warsz), 2011. **59**(2): p. 97-112.
321. Jensen, P.O., et al., *The immune system vs. Pseudomonas aeruginosa biofilms.* FEMS Immunol Med Microbiol, 2010. **59**(3): p. 292-305.
322. Hoffmann, J.A., *Innate immunity of insects.* Curr Opin Immunol, 1995. **7**(1): p. 4-10.
323. Seed, K.D. and J.J. Dennis, *Development of Galleria mellonella as an alternative infection model for the Burkholderia cepacia complex.* Infect Immun, 2008. **76**(3): p. 1267-75.
324. Poole, K., et al., *Expression of the multidrug resistance operon mexA-mexB-oprM in Pseudomonas aeruginosa: mexR encodes a regulator of operon expression.* Antimicrob Agents Chemother, 1996. **40**(9): p. 2021-8.
325. Chen, H., et al., *The Pseudomonas aeruginosa multidrug efflux regulator MexR uses an oxidation-sensing mechanism.* Proc Natl Acad Sci U S A, 2008. **105**(36): p. 13586-91.
326. Christiaen, S.E.A., Matthijs, N., Zhang, X.H., Nelis, .H.J, Bossier, P., Coenye, T., *Bacteria that inhibit quorum sensing decrease biofilm formation and virulence in Pseudomonas aeruginosa PAO1.* Pathogens and Disease, 2014.
327. Klaassen, C.D., J. Liu, and S. Choudhuri, *Metallothionein: an intracellular protein to protect against cadmium toxicity.* Annu Rev Pharmacol Toxicol, 1999. **39**: p. 267-94.